THE GEOLOGICAL SOCIETY OF AMERICA®

Mantle and geological evidence for a Late Jurassic–Cretaceous suture spanning North America

Karin Sigloch[1,†] and Mitchell G. Mihalynuk[2]
[1]*Department of Earth Sciences, University of Oxford, South Parks Road, Oxford OX1 3AN, UK*
[2]*British Columbia Geological Survey, P.O. Box Stn Prov Govt, Victoria, BC, V8W 9N3, Canada*

ABSTRACT

Crustal blocks accreted to North America form two major belts that are separated by a tract of collapsed Jurassic–Cretaceous basins extending from Alaska to Mexico. Evidence of oceanic lithosphere that once underlay these basins is rare at Earth's surface. Most of the lithosphere was subducted, which accounts for the general difficulty of reconstructing oceanic regions from surface evidence. However, this seafloor was not destroyed; it remains in the mantle beneath North America and is visible to seismic tomography, revealing configurations of arc-trench positions back to the breakup of Pangea. The double uncertainty of where trenches ran and how subducting lithosphere deformed while sinking in the mantle is surmountable, owing to the presence of a special-case slab geometry. Wall-like, linear slab belts exceeding 10,000 km in length appear to trace out intra-oceanic subduction zones that were stationary over tens of millions of years, and beneath which lithosphere sank almost vertically. This hypothesis sets up an absolute lower-mantle reference frame. Combined with a complete Atlantic spreading record that positions paleo–North America in this reference frame, the slab geometries permit detailed predictions of where and when ocean basins at the leading edge of westward-drifting North America were subducted, how intra-oceanic subduction zones were overridden, and how their associated arcs and basement terranes were sutured to the continent. An unconventional paleogeography is predicted in which mid- to late Mesozoic arcs grew in a long-lived archipelago located 2000–4000 km west of Pangean North America (while also consistent with the conventional view of a continental arc in early Mesozoic times). The Farallon Ocean subducted beneath the outboard (western) edge of the archipelago, whereas North America converged on the archipelago by westward subduction of an intervening, major ocean, the Mezcalera-Angayucham Ocean.

The most conspicuous geologic prediction is that of an oceanic suture that must run along the entire western margin of North America. It formed diachronously between ca. 155 Ma and ca. 50 Ma, analogous to diachronous suturing of southwest Pacific arcs to the northward-migrating Australian continent today. We proceed to demonstrate that this suture prediction fits the spatio-temporal evidence for the collapse of at least 11 Middle Jurassic to Late Cretaceous basins wedged between the Intermontane and Insular-Guerrero superterranes, about half of which are known to contain mantle rocks. These relatively late suturing ages run counter to the Middle Jurassic or older timing required and asserted by the prevailing, Andean-analogue model for the North American Cordillera. We show that the arguments against late suturing are controvertible, and we present multiple lines of direct evidence for late suturing, consistent with geophysical observations. We refer to our close integration of surface and subsurface evidence from geology and geophysics as "tomotectonic analysis." This type of analysis provides a stringent test for currently accepted tectonic models and offers a blueprint for similar, continental-scale investigations in other accretionary orogens.

1. INTRODUCTION

Subduction of ocean basins leaves two kinds of records. At the surface, it builds accretionary orogens from crustal slivers that grew or fused above subduction zones, for example, arcs, accretionary wedges, and ophiolites. In the mantle, subducted oceanic lithosphere loses its rigidity and becomes part of a viscously deforming slab that sinks toward Earth's core under the pull of gravity. A sinking slab remains visible to seismic tomography because it is cooler than ambient mantle, and seismic waves propagate through it at slightly faster velocities. Joint sampling of the subsurface by thousands to millions of crossing wave paths, generated by hundreds or thousands of earthquakes, enables computation of three-dimensional (3-D) tomographic images of the whole-mantle structure. Some high-velocity domains connect upward to active subduction zones, providing a direct verification of slab origin as cold, dense, and seismically fast oceanic lithosphere (e.g., for North America, see Grand et al., 1997).

It should be possible to reconcile the subsurface record of subduction, as imaged by geophysics, with the geological record of accretionary orogens—an integration we refer to as "tomotectonic" analysis. For Jurassic–Cretaceous North America, the prevailing interpretation of the land and marine surface records is that of eastward subduction of a single large oceanic plate, the Farallon plate, beneath the western continental margin since at least 180 Ma (Hamilton, 1969; Ernst, 1970; Burchfiel and Davis, 1972, 1975; Monger et al., 1972; Monger and Price, 1979). This scenario is analogous to today's Nazca plate subducting beneath the Andean margin of South America. It has been challenged by a minority of geologists who instead argued that Mesozoic North America overrode and accreted a huge archipelago of intra-oceanic trenches and their arc terranes (Moores, 1970, 1998; Schweickert and Cowan, 1975; Ingersoll and Schweickert, 1986; Ingersoll, 2008; Dickinson, 2004, 2008), which implies eastward and westward subduction of more than one plate. The controversy was revived by Johnston (2001, 2008) and Hildebrand (2009, 2012), who focused on westward subduction beneath a ribbon continent that included peri-cratonic terranes.

Magnetic isochrons on the Pacific plate leave no doubt that the Farallon plate existed and grew to the (north-)east of the Pacific plate since 180+ Ma (Engebretson et al., 1985; Atwater, 1989; Seton et al., 2012). Quantitative plate reconstructions (e.g., Engebretson et al., 1985;

†karin.sigloch@earth.ox.ac.uk

GSA Bulletin; November/December 2017; v. 129; no. 11/12; p. 1489–1520; doi: 10.1130/B31529.1; 7 figures; 2 tables; Data Repository item 2017185; published online 30 June 2017.

Seton et al., 2012) are based on these data, but because isochrons reflect seafloor spreading rather than subduction, they cannot resolve the ambiguity of Andean- versus archipelago-style paleogeography. This is illustrated by Figure 1, where preserved constraints on the Farallon-Pacific spreading ridge are consistent with either a margin-hugging Farallon trench (Fig. 1A) or an intra-oceanic Farallon trench far outboard in the proto–Pacific basin (Fig. 1B), which would have been overridden and "accreted" to the west coast late in its life. This ambiguity was clearly pointed out by early workers in marine geophysics (Engebretson et al., 1985; Atwater, 1970, 1989), but they adopted the Andean-type trench configuration that has since prevailed in the geologic community (Fig. 1A).

The model of unchanging Farallon-beneath-continent subduction has the appeal of continuity and simplicity. The Farallon plate subducts eastward into the continental Cascadia trench today (Fig. 1C), and there was also eastward subduction beneath the southwest coast of the United States prior to ca. 170 Ma, which built the so-called "native Triassic–Jurassic arc" on cratonic basement (e.g., Asmerom et al., 1990; Dickinson, 2008; Barth et al., 2011; Saleeby and Dunne, 2015), also called "Nazas arc" in Mexico (Dickinson and Lawton, 2001). By equating the eastward-spreading Farallon plate, which existed since at least 180 Ma, with the eastward subducting plate that generated the native arc, the Andean-analogue model interpolates that Farallon subduction beneath the continent would also have operated at all intermediate times. For the Canadian segment of the Cordillera since ~175 m.y., this scenario was espoused by van der Heyden (1992) and many followers, and recently reasserted in a review by Monger (2014). For the U.S. segment, Andean-style subduction has been asserted in a large body of literature (e.g., Hamilton, 1969; Burchfiel et al., 1992; Barth et al., 2011) for the time since birth of the Sierra Nevada batholith ca. 210 Ma, or even earlier (e.g., Saleeby and Dunne, 2015). Some workers have included episodes of back-arc basin development (e.g., Dickinson, 1976); others have envisaged enhanced retro-arc basin development via oblique subduction (e.g., Saleeby, 1981, 1983; McClelland et al., 1992) or eastward subduction punctuated by periods of largely transcurrent motion (Ernst, 2011).

The challenge for Andean-style models is to explain a long sequence of Cretaceous arc terrane accretions to the west coast from Mexico to Alaska, most notably a microcontinent composed of the Insular (Peninsular-Alexander-Wrangellia) and Guerrero superterranes (for brief terrane descriptions, see Table 1). Such models need to argue that these accretions happened earlier, because the vast Cretaceous Farallon plate in Figure 1A was devoid of active arcs. The terrane accretions are naturally accounted for by archipelago models, where the Farallon plate was much smaller and the "NEGOTIABLE" region in Figure 1B was populated by intra-oceanic arc terranes in the style of today's southwest Pacific Ocean.

These conflicting scenarios were first evaluated against the distribution and depth extent of subducted lithosphere by Sigloch and Mihalynuk (2013); through tomotectonic analysis, we found strong support for an archipelago paleogeography. Voluminous and very deep slab material observed at the longitudes of the Farallon trench position of Figure 1B argues for intra-oceanic Farallon subduction, unless slabs moved laterally over large and strongly variable distances after subduction. If convective displacements in the mantle were perfectly understood, it would be straightforward to infer paleo-trench locations from slab geometries alone, but

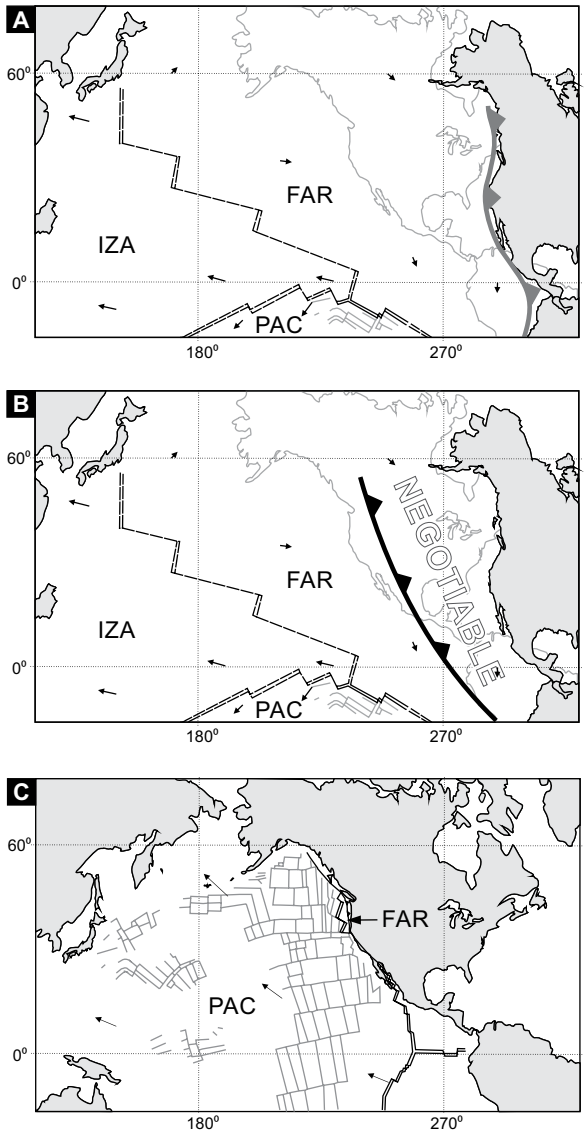

Figure 1. Evolution of the northern Pacific basin as constrained by seafloor magnetic isochron data, modified from Engebretson et al. (1985). (A) Early Cretaceous (140 Ma) reconstruction of continents and oceanic plates, in a fixed hotspot (i.e., lower-mantle) reference frame. Unfilled gray coastlines show present-day positions of the Americas for reference. On the nascent Pacific plate (PAC), west-northwest–striking isochrons record the existence of a spreading ridge and hence of the adjacent Farallon plate (FAR). The existence of the Izanagi (IZA) plate is similarly recorded by ENE-striking isochrons on PAC. Blank areas of seafloor have since subducted. Eastward-dipping trench (gray barbs) along the American west coast marks the eastern edge of the Farallon plate, as implied by the standard "Andean-analogue" model. Paleolocation of North America (and of its subsequent westward drift) is constrained by the fully preserved isochron record of the central Atlantic. (B) Same as in A, but with a more westerly, intra-oceanic Farallon trench (black barbs). Isochron data are equally compatible with this scenario. The area labeled "NEGOTIABLE" remains unconstrained by marine surface observations and hosted the "archipelago" of island arcs that we interpret from observed geometries of subducted seafloor. (C) Pacific basin at present day (0 Ma), showing all PAC-FAR and PAC-IZA isochrons preserved on the PAC plate. Those already formed in A and B are now located around 35°N–40°N, 150°E–170°E. Slivers of active PAC-FAR ridge and recently formed Farallon plate survive offshore the northwest United States and Vancouver Island. Today's west coast is located further west than the intra-oceanic FAR trench in B, implying that the latter was overridden and "accreted" in the (relatively recent) past to form the current, coast-hugging Cascadia subduction zone.

TABLE 1. CORDILLERAN KEY COMPONENTS INCLUDING SUPERTERRANES, MAGMATIC BELTS AND INDIVIDUAL TERRANES, AND THEIR SLAB/BASIN AFFILIATIONS FOR EARLY JURASSIC AND LATER TIMES (UNTIL AMALGAMATION WITH NORTH AMERICA)

	Description of constituent components	Relation to geological superterranes	Geophysically affiliated Mesozoic SLAB and ocean basin
Cordilleran superterranes			
Alaskan Cretaceous arc terranes	Koyukuk, Nyak, and Togiak terranes.		ANG slab and Angayucham Ocean.
Insular superterrane (INS)	Wrangellia (WR), Alexander (AX) and Peninsular (PE) arc terranes in Canada and Alaska.		Northern MEZ slab and northern Mezcalera Ocean.
Intermontane superterrane (IMS)	In Canada, Quesnel (QN) and Stikine (ST) arc terranes, and Cache Creek Ocean terrane (CC); in conterminous U.S., terranes of Blue Mountains (BM); farther south, Native Triassic-Jurassic arc (NJ), which includes Triassic-Jurassic episode of the Sierra Nevada batholith; in Mexico, Nazas arc, the southward continuation of NJ arc.		Cache Creek Ocean, a precursor of Mezcalera Ocean. No slab imaged (yet).
Guerrero superterrane (GUS) of Mexico	Considerations range from an intraoceanic arc complex united by Mesozoic volcanic crust (Dickinson and Lawton, 2001; which includes Guerrero, Arteaga, Papanoa, Santa Ana, and upper plate components of Vizcaino and Magdalena terranes of Silberling et al., 1992) to a composite of various terranes related to a long-lived Andean-type arc (e.g. Tahue, Arcelia, Zihuatanejo, and Guanajuato terranes of Centeno-Garcia et al., 2011).		Southern MEZ slab and southern Mezcalera Ocean.
Cordilleran magmatic belts			
Coast Cascades Orogen	1600-km-long belt extending from Yukon to Washington, cored by 105-45 Ma plutonic and metamorphic rock (Monger, 2014). Overprints older parts of the Mezcalera Ocean suture between IMS and INS.		Formed by eastward Farallon subduction after override of INS arcs.
Cretaceous Sierra Nevada batholith of California (SN)	Cretaceous magmatic pulse (ca. 125–85 Ma) overprints the suture of Mezcalera Ocean between older Native arc (IMS) and recently accreted INS.		Formed by eastward Farallon subduction, after override of INS arcs.
Peninsular batholith of Mexico	Cretaceous magmatic pulse (ca. 125–85 Ma) in north overprints the suture of Mezcalera Ocean between older Triassic-Jurassic arc (IMS) and recently accreted GUS. Zircon ages on the western zone (Silver and Chappell, 1988) range from 140 to 105 Ma, whereas those of the easternmost side of the batholith are much younger at 85–75 Ma (Grove et al., 2003).		Formed by eastward Farallon subduction, after override of GUS arcs.
Cordilleran terranes			
Alexander terrane (AX)	Metamorphosed Neoproterozoic arc (Gehrels et al., 1996); Cambro-Ordovician arc (Beranek et al., 2012); Ordovician to Triassic marine quartzo-feldspathic clastic and carbonate shelf, deep water off-shelf and Late Triassic rift assemblages; pinned to Wrangellia by ca. 308 Ma (Gardner et al., 1988).	Part of INS.	Stationed above MEZ slab in Mesozoic, underridden by Mezcalera Ocean.
Angayucham terrane	Imbricated Middle Devonian to Jurassic oceanic crustal succession including pelagic strata, greywacke and limestone.	Part of the Alaskan arc complex.	Early Angayucham Ocean floor.
Bridge River terrane (BR)	Mississippian to Jurassic oceanic crustal succession, disrupted within accretionary complex, includes Late Triassic blueschist.	Part of INS.	Mezcalera Ocean and its precursor.
Cache Creek terrane (CC)	Mississippian to Early (and perhaps Middle) Jurassic oceanic assemblage including mantle tectonite, Mid Permian gabbro (Mihalynuk et al., 2003), supra-subduction zone basalt (Ash, 1994), radiolarian chert, primitive arc basalt, ocean island basalt and carbonate platform succession containing exotic Tethyan faunas of Middle Permian (Monger and Ross, 1971) to Middle Triassic age (Orchard et al., 2001); blueschist of Late Triassic (Paterson and Harakal, 1974) and Middle Jurassic age (174 Ma, Mihalynuk et. al, 2004).	Part of IMS.	Cache Creek Ocean, a precursor of Mezcalera Ocean.
Chugach terrane (CH)	Turbiditic wacke and argillite assemblages of Late Jurassic to Early Cretaceous, mid Cretaceous and Late Cretaceous ages (Amato et al., 2013); interpreted as an accretionary complex (Berg et al., 1972). Inner (older) parts include Triassic to Cretaceous chert and Permian limestone with Tethyan faunas and 205–192 Ma blueschist (Roeske et al., 1989; López-Carmona et al., 2011).	Outboard of Cretaceous INS.	Offscrapings of northern Farallon Ocean/Cascadia Root slabs CR and CR2.
Franciscan composite terrane (FR)	Cretaceous and Tertiary accretionary complex including many fault-bounded subterranes. Maximum depositional age for inboard (oldest) portion is ca. 123 Ma (Dumitru et al., 2010).	Outboard of Cretaceous INS.	Offscrapings of southern Farallon Ocean/southern Farallon slabs.
Guerrero (GU) and Santa Ana (SA) terranes of Mexico	Late Jurassic to Early Cretaceous andesitic volcanic rocks and coeval marine to non-marine sedimentary rocks.	Part of GUS.	Arc complex stationed above southern MEZ slab/ underridden by Mezcalera Ocean.
Mystic (Farewell) terrane of Alaska	Strongly deformed Ordovician to Permian argillite, chert, sandstone and limestone; undated mélange; Ordovician and Triassic pillow basalt; Devonian and Triassic black shale and phosphorite; faunal ties with Siberia (Bradley et al., 2007).	Substrate of Alaskan/ ANG arcs.	ANG slab/Angayucham Ocean.
Pacific Rim terrane (PR)	Late Jurassic to Early Cretaceous, tectonized sedimentary and volcanic rocks, and Late Triassic limestone; Cretaceous high P/T metamorphism (Brandon, 1989); final emplacement and cooling between Early and Mid-Eocene (Groome et al., 2003) during underthrusting of Siletz-Crescent terrane (SC).	Outboard of INS.	Farallon Ocean/CR slab.

(*continued*)

TABLE 1. CORDILLERAN KEY COMPONENTS INCLUDING SUPERTERRANES, MAGMATIC BELTS AND INDIVIDUAL TERRANES, AND THEIR SLAB/BASIN AFFILIATIONS FOR EARLY JURASSIC AND LATER TIMES (UNTIL AMALGAMATION WITH NORTH AMERICA) (*continued*)

	Description of constituent components	Relation to geological superterranes	Geophysically affiliated Mesozoic SLAB and ocean basin
Cordilleran terranes (*continued*)			
Peninsular terrane in Alaska (PE)	Permian limestone, Late Triassic limestone, argillite and basalt, Lower Jurassic volcaniclastic rocks and coeval plutons, Middle Jurassic to Cretaceous marine sedimentary rocks.	Part of INS.	Stationed above northern MEZ slab, underridden by northern Mezcalera Ocean.
Quesnel terrane (QN)	Late Triassic and Early Jurassic arcs constructed on relicts of Silurian to Mid Triassic arc volcanic and marine sedimentary strata with oceanic to pericratonic substrate.	Part of IMS.	Built by subduction of Cache Creek Ocean, a precursor of Mezcalera Ocean.
San Juan composite terrane	Multiple nappes variably composed of Paleozoic to Mesozoic argillite-chert, basalt, ultramafite, limestone with Tethyan faunas in mélange; blueschist of Permian, Late Jurassic and Early Cretaceous age; youngest rocks in nappes are 114 Ma and overlying sediments are ca. 50 Ma (Brown, 2012).	Forms part of INS-IMS suture.	Mezcalera Ocean?
Siletz-Crescent terrane (SC)	Eocene tholeiitic pillow basalt, breccia and subaerial flows; lower parts include sheeted dykes and gabbro of a partial oceanic crustal section; upper parts intercalated with continentally derived sediment (Massey, 1986); aged 46–56 Ma (references in McCrory and Wilson, 2013).	Outboard of Cretaceous INS.	Farallon Ocean crustal welt/ CR slab.
Stikine terrane (ST)	Late Triassic to early Middle Jurassic arc constructed on Early to mid-Triassic chert, widespread Permian limestone and Early Devonian to Permian arc with oceanic to pericratonic substrate (Logan et al., 2000).	Part of IMS.	Built by subduction of Cache Creek Ocean, a precursor of Mezcalera Ocean.
Vizcaino terrane (VC)	Triassic to Cretaceous oceanic crustal and arc strata and extension of Franciscan accretionary complex.	Outboard edge of GUS.	Farallon Ocean and offscrapings.
Western Jurassic/ Foothills composite terrane (WF)	Late Triassic to Late Jurassic arc, oceanic crustal and volcaniclastic strata includes numerous terranes in Klamaths and western Sierra Nevada metamorphic province that are west of the Calaveras terrane/belt as per Dickinson (2008) and Schweickert (2015).	Part of INS.	Products of Mezcalera Ocean subduction.
Wrangellia composite terrane (WR)	Devono-Mississippian arc, Pennsylvanian-Permian volcanic and marine strata including widespread limestone and Late Permian to Mid Triassic chert, up to ~6 km of intraplate ca. 230–225 Ma submarine to subaerial basaltic plateau flows capped by Late Triassic deep water limestone and spiculitic argillaceous strata (Greene et al., 2010). Interbedded and overlying Late Triassic to Middle Jurassic volcanic and clastic rocks and coeval plutons (Nixon and Orr, 2007).	Part of INS.	Stationed above northern MEZ slab (after Triassic), underridden by Mezcalera Ocean.
Yukon-Tanana composite terrane (YTT)	Pericratonic strata and Paleozoic to early Mesozoic arc (Stikine/Quesnel equivalents), lesser oceanic crust, polydeformed and metamorphosed to amphibolite and rare eclogite facies; terrane-specific cooling ca. 200–190 Ma (Mortensen and Jilson, 1985; Newberry et al., 1998; Dusel-Bacon et al., 2002; Knight et al., 2013; Staples et al., 2013).	Part of IMS.	Ophiolitic components may be old Angayucham basin, associated with a precursor of ANG slab.

Note: Terranes or geological belts composed of Jurassic–Cretaceous basinal strata trapped within the INS-IMS suture are described within the text. Descriptions are after Silberling et al. (1992) unless otherwise noted. Acronyms for terranes are defined only if they are used in Fig. 4 or in the main text.

this is stymied by large uncertainties about mantle rheology. The archipelago model implies tight spatio-temporal correlation between slab and paleotrench geometries, and thus a uniformity of slab sinking (rheology) that is geophysically appealing and a fundamental constraint for mantle convection models. In contrast, the Andean-analogue model implies weak correlation of slab to paleotrench geometries and hence complicated sinking (limited predictive power on rheology), but the trench lines would have been relatively simple (a single, margin-hugging Farallon trench). The apparent simplicity of the Andean model presumably accounts for much of its appeal over the past decades. Contributing factors have been the non-consideration of subsurface observations and the limitations of geologic observations in challenging terrain.

Investigation of the archipelago model is facilitated by the presence of a special-case slab geometry under North America: very steep and voluminous belts of slab "walls," which are difficult to explain by any sinking process other than just vertically down under stationary trenches. Slab walls thus appear to directly map out paleotrench positions. Guided by the vertical sinking hypothesis, volcanic arc terranes can be positioned in a mantle reference frame because they must have grown above the subduction zones feeding the slab walls; i.e., surviving tectonic blocks can be paleopositioned without reference to geologic observations. The geologic land record then remains as an independent data set for testing the predictions made by geophysical observations and the vertical sinking hypothesis, i.e., that terrane collisions occurred when the drifting continental margin (as reconstructed, e.g., by Seton et al., 2012) started to laterally overlap the imaged slab walls (e.g., Sigloch, 2011). Such absolute paleopositioning constraints on where, when, and how North America overrode the intra-oceanic arcs are not available for archipelago models based purely on land geology (Moores, 1970, 1998; Schweickert and Cowan, 1975; Ingersoll and Schweickert, 1986; Ingersoll, 2008; Dickinson, 2004, 2008).

Section 2 (geophysical observations) and Section 3 (geological observations) act as two complementary halves that form the core of this study. Sigloch and Mihalynuk (2013) laid out the premises for testing geologic predictions made by geophysics, and started this testing by arguing that the orogenic deformation record of the Cretaceous Cordillera is more consistent with archipelago paleogeography than with the prevailing Andean analogue. Here, we focus on geologic evidence for the starkest prediction of the archipelago model: the existence of a major Jurassic–Cretaceous ocean in addition to the Farallon Ocean, and its diachronous closure by westward subduction under the archipelago, ahead of North America riding into its arc terranes. The implied Late Jurassic–Cretaceous suture, which should span the entire western North American margin, is imminently testable against the land record. The spatial scope of this investigation extends back to Early Jurassic (201–174 Ma, based on the time scale of Cohen et al. [2013], which is used throughout), as

compared to mainly Cretaceous units in Sigloch and Mihalynuk (2013).

The discussion of the premises for geologic hypothesis testing is also extended in several respects. We give a detailed accounting of Farallon subduction because lack of this discussion made it difficult for geophysicists to engage with archipelago models based in geology. We also lay out the close tectonic analogy between diachronous archipelago override by Mesozoic North America, and override of the southwest Pacific archipelago by present-day Australia. This makes the geologic predictions of section 3 more tangible, especially the generalized consequences of diachronous ocean basin suturing at both flanks of northern Australia and expectations of analogous suturing recorded by Cordilleran geology.

Section 4 delineates our findings from archipelago models based purely on geology (Moores, 1970, 1998; Schweickert and Cowan, 1975; Ingersoll and Schweickert, 1986; Ingersoll, 2008; Dickinson, 2004, 2008) and distinguishes it from ribbon continent models (Chamberlain and Lambert, 1985; Lambert and Chamberlain, 1988; Johnston, 2001, 2008; Hildebrand, 2009, 2012, 2015).

Section 5 raises discussion points, such as oblique collisions as the default regime; the relevance of geodynamic convection modeling; prior engagement of geophysicists with (only) the Andean-analogue model; slab sinking rates; and the current limitations of our approach in revealing paleogeography older than Early Jurassic. Mantle convection modeling has not engaged with either the archipelago model (ours or earlier versions) or ribbon continent scenarios and so has not tested them nor weighed their merits relative to the Andean-analogue model. The Andean analogue has been investigated and found to require complex mantle rheologies and sinking behaviors in order to deposit slabs that resemble the observed, lower-mantle assemblage under North America (e.g., Bunge and Grand, 2000; Liu et al., 2008). Our archipelago scenario would produce the observed slabs without needing to invoke such complexities, because the near-vertical sinking it implies has been observed in some numerical convection simulations (e.g., Steinberger et al., 2012). Newer studies of viscous slab folding (e.g., Ribe et al., 2007; Stegman et al., 2010; Gibert et al., 2012; Čížková and Bina, 2013) lend further credence to near-vertical sinking because they reveal a formation mechanism for the wide, voluminous slab walls that are central to our argument for old, intra-oceanic subduction. (Note that we use the following conventions: Slab "height" refers to the slab's vertical dimension, slab "length" is the trench-parallel dimension, and slab "width" is the trench perpendicular dimension.)

Ultimately our study is centered in observations, which we argue are sufficient to falsify the Andean-analogue model for North America, because observations directly contradict a Farallon trench continuously hugging the ancestral continental margin from 180+ Ma to present.

2. SUBDUCTED SLABS CONSTRAIN CORDILLERAN TECTONICS

This section describes geophysical observations and the predictions (or hindcasts) they make about paleogeography, to be tested against the geological observations in section 3. Steep, wall-like slabs stand out among the geometries of subducted lithosphere surveyed in section 2.1 This geometry suggests almost vertical slab sinking relative to the lower mantle as the formation mechanism, combined with deposition beneath stationary trenches (section 2.2), which could only have been intra-oceanic. Massive slab volumes suggest long-lived and hence old (i.e., Jurassic) subduction (section 2.3), which again implies intra-oceanic trenches, because the North American margin lay further east at that time. After matching the magnetic isochron record of the Farallon plate to subducted lithosphere (section 2.4), much slab remains unaccounted for. It must represent an additional, major ocean (section 2.5), which again implies intra-oceanic subduction, of both it and the Farallon Ocean from opposite sides, i.e., an archipelago geography. Certain eastward-dipping slab geometries are consistent with this hypothesis, rather than supporting Andean-style subduction, as previously interpreted (section 2.6). These slabs are ideal for estimating slab sinking rates. Section 2.7 spells out the predicted sequence of archipelago override by North America, a scenario that may seem complex but is in fact closely analogous to the override of today's southwest Pacific archipelagos by Australia (section 2.8), predicting similar observable geological consequences.

2.1. Subducted Lithosphere Under North America and the Problem of Provenance

The mantle under North America has long been known to hold one of the largest accumulations of subducted lithosphere observed anywhere. Revealed by early regional-scale tomographies (Grand, 1994; Grand et al., 1997; van der Hilst et al., 1997), this finding has been confirmed by all global tomography studies since (e.g., Montelli et al., 2006; Li et al., 2008; van der Meer et al., 2010; Ritsema et al., 2011; Obayashi et al., 2013). Imaging resolution of subducted slabs beneath North America has improved enormously over the past decade thanks to the continent-spanning USArray seismological experiment (e.g., Burdick et al., 2008; Sigloch et al., 2008; Schmandt and Humphreys, 2010; reviewed and compared by Pavlis et al., 2012).

Here, we interpret the finite-frequency inversion of broadband, teleseismic P waveforms by Sigloch (2011). This study resolves deeper structure than most, because, alongside the dense array data from the United States, it incorporates data from most North American broadband stations deployed since 1999. Finite-frequency modeling of realistic wave sensitivities on a global grid adds resolution at depth, compared to conventional, ray theoretical imaging (Dahlen et al., 2000; Sigloch, 2008). Figure 2A is a three-dimensional bird's-eye rendering of the North American slabs, showing sublithospheric areas of faster-than-average P-wave velocities relative to the spherically symmetric mantle reference model IASP91 of Kennett and Engdahl (1991).

As a first-order observation, the lower-mantle slab assemblage in Figure 2A is strikingly segmented, and it reaches equally deep in the east and in the west. Steep, wall-like slabs run in two linear belts totaling >10,000 km in length. The Angayucham slab wall (ANG) strikes northwest from present-day Nova Scotia to Yukon, and the Mezcalera slab wall (MEZ) runs from Nova Scotia south beneath the eastern seaboard and the Caribbean. In depth extent, both belts fill the middle third of the mantle from ~800 to 2000+ km deep. An equally deep slab is found further west, labeled "CR" for Cascadia root, which extends from the lower mantle to the active Cascadia subduction zone at the surface. (For better viewing of this western subduction, the eastern slab above 800 km is not rendered in the foreground of Figure 2A, but can be inspected in Supplementary Movie M1.[1] Figure 3 provides an oblique 3-D rendering of only Cascadia/CR subduction.

Figure 4A shows the same slab assemblage as Figure 2, but in map view and rendered only at depths below 1100 km. MEZ and ANG are seen to be paralleled by several shorter and more scattered, but equally deep fragments further west (CR, CR2, SF1). (We write slab names such as MEZ and ANG in uppercase to conceptually distinguish them from their associated paleo-oceans and arc terranes, e.g., Mezcalera and Angayucham.) The name "Mezcalera Ocean" is adopted from Dickinson and Lawton's (2001) review of Mexican arc geology. Angayucham Ocean is named after an ophiolitic terrane in Alaska (Coney et al., 1980, p. 197).

[1]GSA Data Repository item 2017185, Movie M1, is available at http://www.geosociety.org/datarepository/2017 or by request to editing@geosociety.org.

Effective use of slabs for paleogeographic reconstruction requires the validation of a key postulate: Slab geometries preserve paleo-ocean and paleotrench geometries. Although the youngest (shallowest) ends of some slabs, such as CR, can be traced to present-day subduction zones, older and deeper parts of slabs are not dateable per se, unless they can be confidently linked to a well-constrained geologic record. If lower-mantle slabs are heavily deformed by mantle currents, paleotrench locations could be difficult to reconstruct. The rheological properties of slab and ambient mantle are unconstrained enough that deformation styles and sinking rates have remained uncertain. It is debatable how much lateral displacement any given parcel of slab might have undergone while sinking in the mantle, i.e., how much its current latitude and longitude differ from its trench entry point. How can we then approach the inference of paleotrench locations and timing from slab geometries?

Figure 4A superimposes on the slabs the position of North America ca. 110 Ma, and Figure 4B shows North America for 170 Ma, 140 Ma, and present-day. Taken together, they trace out the westward migration of the continent and its west coast relative to the lower mantle. (Movie M1 shows more detail, in 5 m.y. increments [see footnote 1].) The continent's drift relative to Africa and Europe is constrained by magnetic seafloor isochrons from the fully preserved Atlantic spreading record, with uncertainties of generally only ~1° or <2 m.y. (Müller et al., 2008).

A lower-mantle reference frame is the natural choice for this surface reconstruction because the slab walls are located in the lower mantle, and our goal is to establish their paleotrench locations relative to the continent's west coast. The best observational proxy for a lower-mantle reference frame is given by volcanic hotspot tracks (Morgan, 1981; Duncan and Richards, 1991), and Figure 4 uses an Indo-Atlantic hotspot frame back to 100 Ma (O'Neill et al., 2005) and a hybrid paleomagnetism frame for earlier times (Steinberger and Torsvik, 2008), subject to uncertainties of less than 5°. Even with additional uncertainties considered, for example, on the shape of North America's paleomargin, all reconstructions of this type agree that Pangean North America (reconstruction for 170 Ma) was located well east of the most easterly slab walls MEZ and ANG in Figure 4 (cf. Sigloch and Mihalynuk, 2013; GSA Data Repository material [see footnote 1]).

Assuming the lower-mantle slabs did not enter the mantle thousands of kilometers east of their current location, then two alternatives for their formation must be entertained: If the oldest (lower) parts of the MEZ and ANG slabs had subducted by the time Pangea started to break up, then they were deposited west of western North America beneath intra-oceanic arcs (the archipelago) and were fed by westward subduction of the seafloor shaded cyan in Figures 4A and 3B. If they subducted later, while the west coast was already traversing the current slab resting area, then their trenches were proximal to the continental margin and presumably right along it (the Andean-type scenario). The latter leaves the challenge of explaining how a (Farallon) trench that migrated continuously and smoothly with the west coast generated the steep, linear slab belts that bear no resemblance to the shape of the continental margin and are separated by slab-free zones (an issue revisited in section 5.3). Our main purpose, however, is to argue the opposite scenario, i.e., of early, intra-oceanic subduction.

2.2. Null Hypothesis of Vertical Slab Sinking in the Lower Mantle

These paleopositioning arguments can be quantified. Figures 4A and 4B draw trench locations vertically above the slab walls, illustrating our null hypothesis that every parcel of slab wall entered the mantle above its present-day location and simply sank downward; i.e., it is still located at the same longitude and latitude where it entered its trench, analogous to hotspots not moving significantly relative to the lower mantle (Morgan, 1981). To the extent that this vertical sinking hypothesis is correct, and to the extent that the plate reconstruction is correct, Figure 4 gives absolute paleodistances of the continent to the trenches and their attendant arc terranes. The cumulative observational uncertainties of tomographic model, reconstruction, and continental margin shape over time are a few hundred

Figure 2 (*on following page*). (A) Seismically fast domains in the lower mantle beneath North America, according to the tomographic P-velocity model of Sigloch (2011). Isovelocity contours, with color changing every 200 km in depth, enclose mantle regions where wave velocities are dVp/Vp > 0.35% faster than average. These regions are interpreted as subducted, cool lithosphere that was deposited beneath volcanic arcs and accumulated to form slabs. Three-dimensional (3-D) image is an oblique elevation view from the east-northeast. Spherical geometries have been flattened so as to minimize horizontal or vertical distortion at the center of the rendering volume. Slabs names are capitalized acronyms that allude to each slab's interpreted plate origins: MEZ slab consisting of Mezcalera Ocean lithosphere; ANG—Angayucham; CR and CR2—Cascadia Root, i.e., northern Farallon Ocean; SF1—Southern Farallon; K—Kula. The 10,000-km-long and near-vertical MEZ/ANG slab walls in the lower mantle (formerly presumed Farallon slabs) are seen in the foreground (east and north). In the background (west), the lower-mantle CR is upward-continuous to today's Farallon/Juan de Fuca Trench in the Cascadia subduction zone (shallowest, purple material). The MEZ/ANG slabs have been masked above 800 km to leave an unobstructed view of this entire Farallon subduction system; note the near verticality of the CR slab in the lower mantle. The interpreted Mesozoic Mezcalera-Angayucham Oceans were located at the surface to the east and north of the MEZ/ANG slab walls, i.e., closest to the viewer. (B) Cartoons show interpreted generation of the slabs; they are drawn to scale. Panels B1 (Early Cretaceous) and B2 (today) interpret slab and surface evolution along southerly cross section X-X′-X″ of panel A. Panels C1 and C2 interpret slab evolution under northerly cross-section Y-Y′-Y″. (B1) MEZ slab wall was deposited by Jurassic–Cretaceous westward subduction of the Mezcalera Ocean into a stationary, intra-oceanic trench and beneath the Insular superterrane (INS), until the Mezcalera Ocean was consumed and the Insular superterrane had accreted. NJ arc is the older Native Jurassic arc intruded in stable North America. (B2) Subsequently, the southern Farallon Ocean subducted eastward beneath a migrating, continental trench, depositing the eastward-dipping slab L1 (not rendered above 800 km in A but visible in Movie M1 [see text footnote 1] and contoured green in Fig. 4A). MEZ slab continued to sink in place. (C1) Double-sided, intra-oceanic subduction of Angayucham and northern Farallon oceans in Jurassic–Cretaceous times generated the ANG and CR slab walls. Consumption of the Angayucham Ocean ended with accretion of the Alaskan arcs to the continental margin pre-modified by earlier accretion of the Intermontane superterrane (IMS). Later, the Farallon trench converted from intra-oceanic to continental upon override, and proceeded to deposit a laterally sprawling, upper-mantle slab (blue-purple shades in panels C2 and A). Observed thickening of slabs is attributed to folding in the transition zone. All slabs sink vertically relative to the lower mantle; stationary trenches produce vertical slab walls; migrating trenches produce dipping slabs.

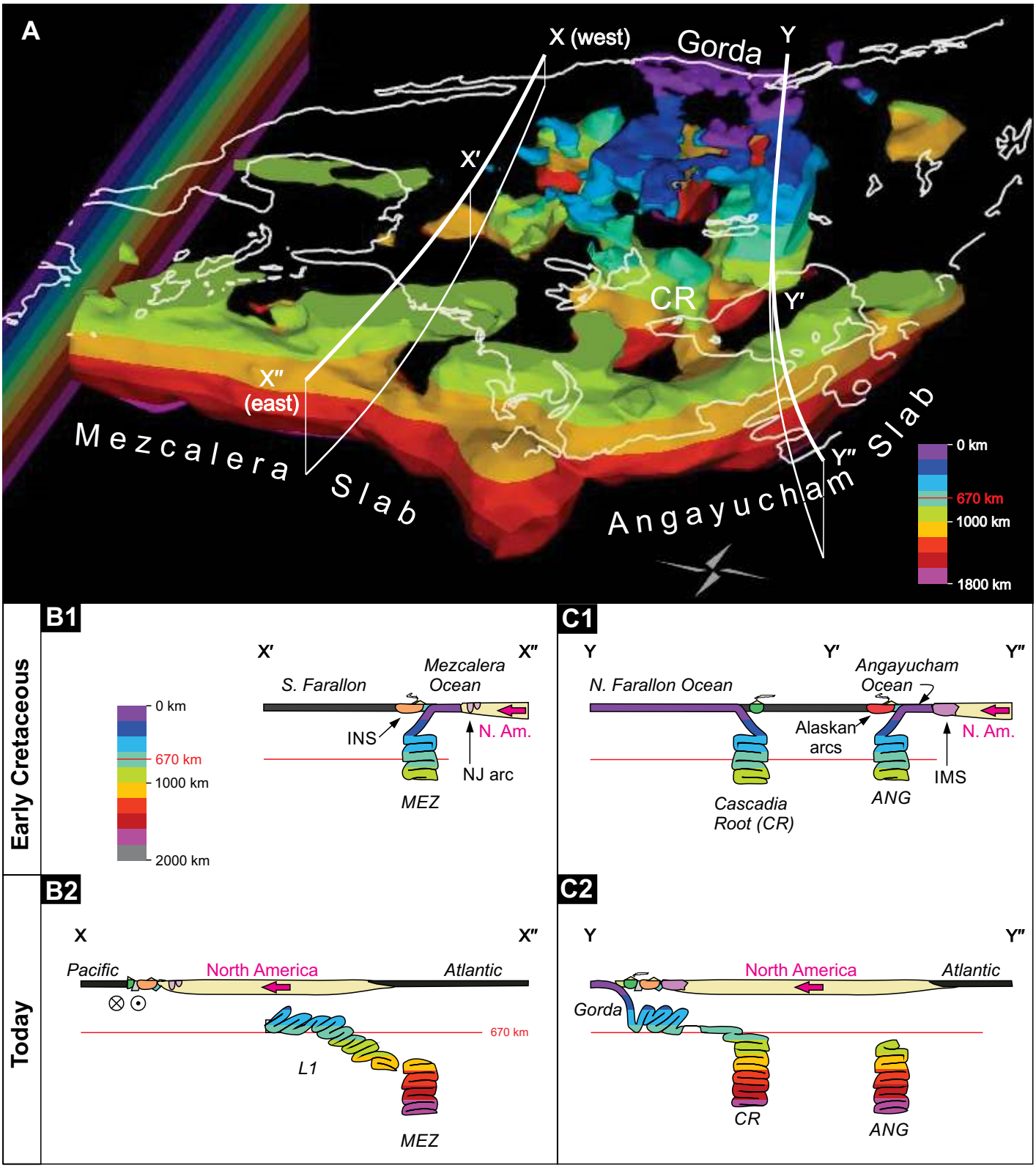

Figure 2.

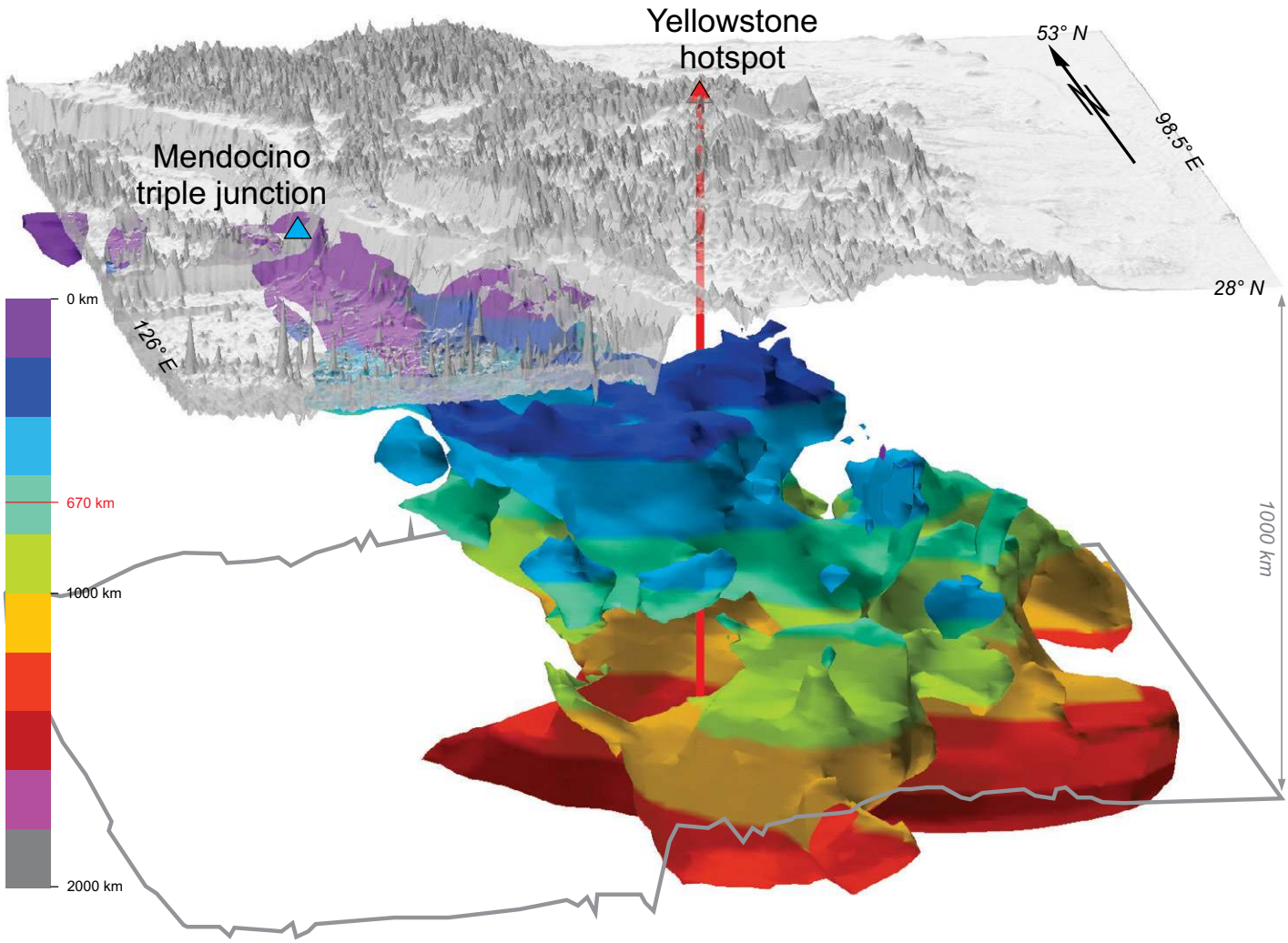

Figure 3. Farallon subduction beneath the Cascadia subduction zone, from trench to ~1500 km depth. Three-dimensional, oblique elevation view from the southwest; topography and bathymetry of the western U.S. are shown as translucent surface (elevations strongly exaggerated; same surface is also shown schematically translated to 1000 km depth for spatial reference). Seismically fast domains according to the tomographic P-velocity model of Sigloch (2011) are iso-contoured in 3-D where wave velocities are dVp/Vp > 0.35% faster than average (as in Figs. 2 and 4, and using same rainbow color scale to indicate depth). Fast velocities that are clearly separate from this continuous system are masked out, including cratonic root and transition zone slab to the east, and lower-mantle slabs CR2 and K to the north and west (the latter are visible in Figs. 2 and 4 and Movie M1 [see footnote 1]). The slab dips eastward, but extends not farther east than the Rocky Mountain front (see also Figs. 4A/B). The slab's lower-mantle parts, termed "CR" or "Cascadia Root" in the text, are much more massive than in the uppermost mantle; slab thickening happens mostly in the transition zone (light blue level, 400–600 km). Comparison to the different perspectives of Figures 2A and 4A reveals a rotation in deposition direction. The base of CR at the red/yellow levels strikes NW-SE (almost perpendicular to this viewing angle) and is built steep and wall-like. From the blue-green level (~800 km) up, the slab is less massive, heavily fragmented, and shows a clear slope toward the trench, i.e., westward-shallowing; the strike of this material is more N-S, c.f. Figure 2A. (We interpret this upper-mantle slab as deposited after CR trench had accreted and while it was dragged westward as an Andean-style trench, i.e., post-ca. 60 Ma. This matches a clockwise rotation of conjugate magnetic isochrons on the Pacific plate from NW-SE to more N-S, recording the fracturing of the Vancouver fragment from the northern Farallon ca. 52 Ma, as discussed in Sigloch, 2011.)

kilometers, or 3–24 m.y., when converted to temporal uncertainties via the drift rate of North America (for this uncertainty analysis, see supplement *in* Sigloch and Mihalynuk, 2013).

At the times and locations that North America's west coast in Figure 4A starts to overlap the MEZ and ANG slabs, it is predicted to collide with their arc terranes, and the oceans that intervened between the west coast and the trenches would have closed (the Mezcalera and Angayucham Oceans). This prediction, which follows from the null hypothesis of vertical sinking, and which uses only geophysical observations (tomography, plate reconstructions from magnetized seafloor, the hotspot reference frame) to build the collision model, is testable against the geologic record of arc terrane collisions along the margin, which constitutes a completely independent set of observations. Sigloch and Mihalynuk (2013) tested it against the Cretaceous record of marginal deformation in time

and space, and here we show that the predicted closure of the Jurassic–Cretaceous Mezcalera and Angayucham Oceans can also be demonstrated in the geologic record. Hence, we argue that the vertical slab sinking hypothesis is holding up to scrutiny.

The potential for demonstrating a new lower-mantle reference frame, equivalent to the hotspot frame but reaching further back in time, provides the strongest motivation for vetting the vertical sinking hypothesis. Its simplicity requires no input of uncertain mantle rheologies in order to build a subduction model, and it permits rigorous integration of geological observations into what has been a largely geophysical debate.

Even if more complicated slab sinking were expected a priori, falsification of this simplest possible sinking mode should be attempted first. This cannot happen so long as intra-oceanic trenches are not considered to be an option. Earlier work has only shown the incompatibility of vertical sinking with an Andean-style Farallon trench (cf. section 5.3).

Vertical sinking of massive slabs is plausible a priori because gravity is the only primary force acting on them. Nonvertical displacement of slabs would require their entrainment in the lateral flow of ambient mantle ("mantle wind"), which is driven by lateral pressure gradients. In order to be effective, the driving agents would need to be even larger slabs (or plumes), which do not exist nearby. The North American slab walls are among the most massive in the entire mantle and should therefore sink more vertically than anything else. Also, the lower-mantle reference frame empirically "works" for plumes (Morgan, 1981; O'Neill et al. 2005), confirming sluggish lateral convection at those depths. It may therefore work equally well, or better, for slabs that are much more massive than plumes.

The cartoons of Figure 2 illustrate "vertical" slab sinking in a lower-mantle sense, i.e., of thickened slabs. In panel C1, two slab walls, ANG and CR, initially grow under two stationary, intra-oceanic trenches. By the time of panel C2, the Angayucham Ocean has closed, and its arcs have accreted to migrating North America, while the ANG slab wall continues to sink vertically in the mantle. The CR (Farallon) arcs have also accreted to the continent, which is now forcing the Farallon trench westward. Combined with vertical sinking, this forced trench rollback deposits a laterally extended slab from the transition zone downward. Thus, vertical sinking can generate both vertical and shallowly dipping slab geometries, depending on trench motion. Figure 3, showing a different oblique view of CR/Cascadia subduction, and its comparison to Figures 2A and 4A, permits examination of this idea on actual slab observations. Southern Farallon slab L1 is another dipping slab deposited by a migrating, continental trench, as discussed in the caption of Figure 2.

2.3. How Much Lithosphere Is in the Slabs?

The near-vertical MEZ and ANG slab walls in the foreground of Figure 2A fill more than 1000 km of the mantle column, from ~800 km to >1800 km in depth, and run over 10,000 km long in an angled, highly structured geometry. In this depth range, the CR slab is also near vertical; it only slopes toward its Cascadia trench in the upper ~800 km (most clearly seen in Fig. 3). In their narrowest dimension, the MEZ, ANG, and CR slab walls are 400–700 km wide, best seen in Figure 4A. If each represented a single sheet of lithosphere dipping steeply into the lower mantle, then their width should equal typical lithospheric thickness, on the order of 100 km. Widening of steep lower-mantle slabs under North America is a robust, consistent observation that was evident in the earliest tomographic images (Grand, 1994) and has been reproduced consistently by all later studies. This slab widening might not have been interpreted due to lingering doubts about artificial image smearing, but with modern waveform imaging methods and much denser instrumentation, these doubts have been settled (see Discussion, section 5.2).

Assuming mature lithospheric thickness of 100 km, a 1000-km-"high" and 400–700-km-wide slab wall would contain a paleo-ocean in which at least 4000–7000 km of lithosphere would have been generated, and even more if the subducted lithosphere was young and proportionally thinner. It takes time to subduct ocean basins many thousands of kilometers wide, implying a commensurate age for the slab walls, i.e., older than previous estimates, which did not factor in the excess width of the walls. Old age is important to our hypothesis because the slabs, if old enough, could not have subducted beneath the western margin of North America—the continent lay too far east during Jurassic times, when it was still part of the supercontinent Pangea or just breaking away. Hence, the significance of widened slab walls (regardless of the exact widening mechanism) lies in the sheer volume of lithosphere contained and the long memory of mantle history recorded. Their steepness suggests both vertical sinking and stationary trench positions over those long periods of time.

Slab wall widening probably occurs through lithospheric bending and folding when subducting lithosphere approaches the viscosity interface near 670 km depth. This would lay down piles of periodic folds, as cartooned in Figures 2B and 2C, where individual folds are not (yet) resolvable by tomography. This folding mechanism for viscous thin sheets against a backstop has been revealed by recent geodynamic modeling studies (Bellahsen et al., 2005; Ribe et al., 2007; Funiciello et al., 2003; Stegman et al., 2010; Čížková and Bina, 2013; Garel et al., 2014; see Discussion, section 5.2).

A folding process that lays down a 400–700-km-wide slab wall can be expected to generate a few hundred kilometers of deviation from strictly vertical slab descent, unless trench motion exactly tracks the oscillatory slab folding motion. It is unclear whether to picture the trench as firmly centered above the slab wall, or always off to one side, or oscillating back and forth as folds are laid down. Hence, the concept of "vertical sinking" of thickened lower-mantle slabs is meaningful only within observational uncertainties of a few hundred kilometers (roughly the half-width of the slab wall), but this is still narrow compared to lower-mantle features or plate dimensions at the surface.

2.4. Which Slabs Are Farallon Lithosphere?

Of the lower-mantle slabs in Figure 2A, only CR connects upward to the currently active subduction zone of the Farallon plate (Juan de Fuca and Gorda) and can hence be reliably considered Farallon lithosphere (see also Fig. 3). Provenance of the remaining slabs is a priori questionable, but given that the Farallon Ocean undoubtedly existed and spread since 180+ Ma (Engebretson et al., 1985; Atwater, 1989), it is not warranted to hypothesize additional oceans until all inferred Farallon seafloor has been matched to appropriate slabs. Farallon trench location is not directly constrained by isochrons (cf. Fig. 1A vs. Fig. 1B), but given a number of equally deep (equally old?) candidate slabs, e.g., CR, CR2, SF1, MEZ, and ANG, those closest to the Farallon-Pacific spreading ridge should represent Farallon lithosphere. The Farallon-Pacific ridge ran just east of reconstructed Pacific isochrons, as in Figure 4A, where the ridge is backstripped to 110 Ma. The slabs closest to it are CR, CR2, and SF1, and hence these should be Farallon slabs—a reasoning confirmed by ongoing Farallon subduction into CR.

SF1 truncates upward at depths of ~1050 km, and CR2 truncates upward at depths of between 1050 and 650 km, as seen in Supplementary Movie M1 (see footnote 1; although these numbers may be too shallow because resolution tests indicate upward smearing due to the slabs' residence beneath the uninstrumented Pacific; Sigloch, 2011). Hence, subduction into SF1 and CR2 terminated long ago, quite con-

sistent with the Farallon's fragmented history as inferred from isochrons. Sager et al. (1988) reconstructed a clockwise rotation of the northern Farallon plate ca. 147 Ma, suggesting a change in trench strike from roughly E-W to its more recent NW-SE direction. Indeed, CR and CR2 strike NW-SE, but at depths below ~1400 km (red shades in Fig. 4A), an E-W–striking connection between CR and CR2 is imaged, which we interpret as Farallon slab deposited before this rotation (the implied sinking rate of 1400 km/147 Ma is 9.5 mm/yr, consistent with the estimate of 10 ± 2 mm/yr by Sigloch and Mihalynuk, 2013). Following rotation, the coexistence of CR and CR2 en echelon was presumably not stable, and CR2 subduction ceased in the Cretaceous. When SF1 died out, a suitable shallower slab, L1, is imaged further east, which would have accommodated subsequent Farallon subduction. L1 is a slab that fills the transition zone at ~400–800 km depth, which is too shallow to be rendered in Figure 2A or Figure 4A, but it is outlined in dashed green in Figure 4A, and it can be inspected in Supplementary Movie M1 (see footnote 1). Initiation of L1's trench is marked as the easternmost green trench barb in Figure 4A; the slab itself is discussed as the "Laramide slab" by Sigloch (2011), although we now think that it spans a wider time range than the Laramide flat subduction episode.

Judging by its depths of 900–1200 km, slab K may be the direct "successor" of CR2. Its E-W strike and location north and west of CR (which represents the northern Farallon plate) make it tempting to identify K with the Kula plate (Fig. 3A). Isochrons indicate that the Kula plate broke away from the northern Farallon plate and subducted northward between ca. 85 Ma and ca. 55 Ma (Woods and Davies, 1982; Engebretson et al., 1985; Atwater, 1989). While slab K's limited depth span of 300 km would be consistent with the Kula plate's 30 m.y. life span and a deposition rate of 10 mm/yr, its absolute depth exceeds the 550–850 km expected for a 10 mm/yr sinking rate. On the other hand, this slab is not underlain by a massive wall, and an argument could be made that it fell through the upper mantle at a much faster velocity. If slab K is not Kula lithosphere, it could instead represent northward subduction prior to Kula breakoff. During the Cretaceous superchron (ca. 120–83 Ma), spreading was not recorded magnetically, and the transition from (northward) Izanagi to (northward) Kula subduction is poorly known (Woods and Davies, 1982).

Thus, all Farallon seafloor known to have existed can be accounted for by the western half of the observed slab assemblage (slabs CR, CR2, K, SF1, L1). At least 180 m.y. of northern Farallon subduction can be directly accommodated by deposition into the CR slab, which reaches sufficiently deep (>1800 km), is voluminous enough (widened to 400–700 km), and connects upward to ongoing Farallon subduction. Sufficiently deep and voluminous slabs (SF1, L1) can also account for southern Farallon subduction (which may or may not have initiated as early as 180+ Ma). Even known isochron complications such as rotations and plate break-offs are matched by slab geometries.

Slabs CR2 and K point to a problem with the Andean analogue in that they must represent Farallon slabs (being most proximal to the reconstructed Farallon spreading ridge; Fig. 4A). Yet, they could never have subducted beneath the continental margin because even today they are located west of the west coast. So at least these old parts of the Farallon plate must have subducted offshore, raising the question: What else did?

Figure 4 (*on following page*). Reconstruction of North American drift and its impingement on the Archipelago of Jurassic–Cretaceous island arcs, with the resulting assemblage of accreted arc terranes and continent-spanning suture of the Mezcalera-Angayucham Oceans. (A) Superposition of subducted slab walls (as in Fig. 2A) with quantitative plate reconstruction of Müller et al. (2008) in the lower-mantle reference frame of Steinberger and Torsvik (2008). Paleo-position of North America is in black; seafloor isochrons are in dark blue. Reconstructed time is 110 Ma; only slabs presumably deposited by that time are rendered (and are currently located below 1100 km depth, based on a sinking rate of 10 mm/a; Sigloch and Mihalynuk, 2013). Colored text labels and lines are used to group genetically related tectonic elements: in orange, the Mezcalera slab wall (MEZ), interpreted Mezcalera trench locations, and the Mezcalera Ocean (westward-subducting); in red, the Angayucham slab wall (ANG), Angayucham trench, and ocean (westward-subducting). These inferred oceans fill the space between westward-migrating North America and the MEZ and ANG slabs, as outlined by the cyan-colored patches. All other slabs and trenches, labeled green, are associated with the eastward-subducting Farallon plate. CR, CR2, L1, SF1, K—see section 2.4. Paleo-arcs are being extinguished and accreted where North America has started to impinge on the eastward-projecting MEZ slab (dashed orange barbs), followed by subduction flip to eastward below the newly established Andean-style margin (slab L1, solid green barbs). (B) Current versus former positions of accreted terranes. North America's position is reconstructed for 170 Ma, 140 Ma, and present day; one intermediate position of western margin at 90 Ma is shown by dark green coastline contour. Arc terranes are shown in their current locations (left half of plot) and in their inferred paleo-positions, i.e., behind the intra-oceanic trenches of panel A, and above the slab walls, which are outlined as translucent patches. The same color scheme as in panel A is used to group related tectonic units across time periods: in orange, Mezcalera slab, ocean, paleo-arcs, and accreted terranes (Insular and Guerrero Superterranes); in red, Angayucham slab, ocean, arcs and terranes (Alaska and Siberia); in green, Farallon slabs, arcs, and terranes; in purple, Intermontane Superterrane (IMS), which had accreted by 170 Ma. The superterranes in their present positions are subdivided as described in Table 1: in orange, MEZ-affiliated arc terranes PE (Peninsular), WR (Wrangellia), AX (Alexander), WF (Western Jurassic, Western Hayfork, Foothills, and related terranes), SA (Santa Ana), and GU (Guerrero). The purple terranes QN (Quesnel), ST (Stikine), CC (Cache Creek), and YTT (Yukon Tanana) are all considered part of Jurassic IMS Superterrane. Equivalents in the conterminous U.S. are shown together as BM (Blue Mountains terranes), which are linked to the Native Jurassic arc (NJ) and its continuation into Mexico ("Nazas arc," diagrammatically shown by purple asterisks). The collapsed basins that mark the Mezcalera-Angayucham suture are shown in solid cyan, also annotated by numbers and listed in the legend. These basins represent the surface remains of the large paleo-oceans shown as translucent cyan patches, and straddle the boundary between orange (MEZ) and purple (IMS/NJ) terranes as predicted. Between basin relicts 4 and 8, the Insular-Intermontane boundary is extensively overprinted by Coast Cascades orogen. Where adjacent arc terranes were expansively below sea level, suture basin strata may have extended well beyond the suture zone, such as northeast of suture relict 5, where coeval Bowser Basin (BB) is observed as onlapping Intermontane Superterrane (IMS). Sierra Nevada batholith, located immediately east of basin 10, overprints the basin and the Native Jurassic arc. Green terranes are associated with Farallon subduction: CG—Chugach; PR—Pacific Rim; SC—Siletz-Crescent; FR—Franciscan; VC—Vizcaino. Abbreviations and terrane attributions are explained further in Table 1.

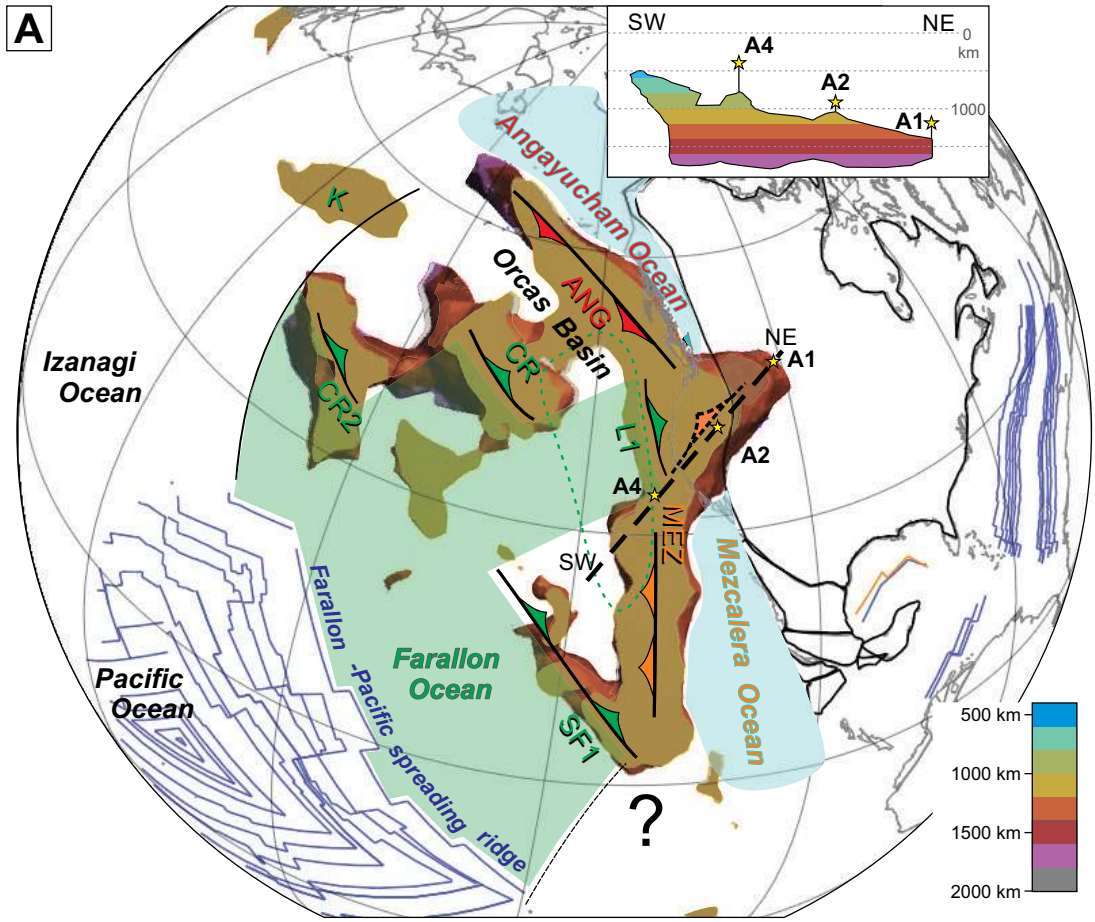

Figure 4

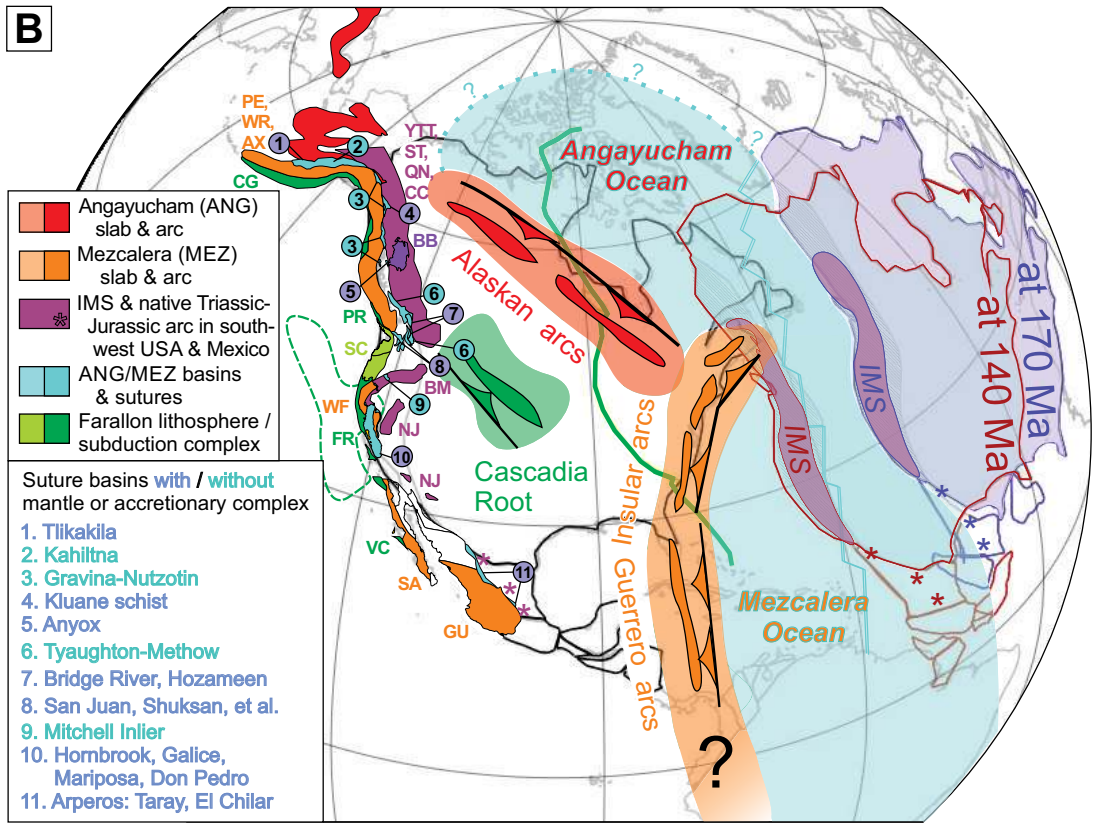

2.5. MEZ and ANG Slab Walls Cannot Be Farallon Lithosphere

Strikingly, the matching of Farallon seafloor to subducted slabs leaves the huge MEZ and ANG slabs unaccounted for. Associating MEZ and ANG with Farallon lithosphere is implausible for other reasons as well:

(1) Wrong depth—The Farallon plate could not have subducted into CR, CR2, SF, and into the more distal MEZ/ANG slabs at the same time. If MEZ and ANG were Farallon slabs, they would need to represent older Farallon subduction, despite residing at the same depths as CR, CR2, and SF. This implies vastly slower sinking or complete stagnation of MEZ and ANG, despite being the more massive slabs.

(2) Slab longitudes—A coast-hugging Farallon trench would have swept across all longitudes between the 170 Ma margin and today's coastline (as reconstructed in Fig. 4B). Yet, beneath much of this area, no slabs are observed, especially not beneath the cyan-shaded areas of today's Atlantic Ocean.

(3) Steep, narrow geometries—A marginal trench would have constantly migrated westward with the continent, but the near-vertical MEZ/ANG slab walls suggest stationary trenches, over sufficiently long times to have deposited the massive volumes observed.

(4) Slab shape—The outlines of the MEZ and ANG slabs do not conform to the shape of the North American margin, against expectations for slabs deposited at the margin.

(5) Uniform extent in depth—Both the ANG and MEZ slab walls extend equally deep at their eastern and western limits (Figs. 2A and 4A; cross section in Fig. 4A inset for MEZ; Fig. 5 and Movie M1 [see footnote 1]), suggesting simultaneous deposition rather than westward-younging deposition by a migrating, marginal trench.

(6) Slab curvature—The eastward-protruding shape of the MEZ-ANG chevron is inconsistent with long-lived eastward subduction because this would have created a space problem for the incoming Farallon plate; i.e., had the MEZ-ANG structure been a singular Farallon arc, its "correct" curvature would be westward convex.

In summary, if the North American slab walls were generated by continuous eastward subduction beneath the continental margin since 180+ Ma, then there is no recognizable geometrical signature of such a relationship. This problem disappears if the MEZ and ANG slabs were of intra-oceanic and non-Farallon origin. Intra-oceanic trenches could have remained stationary in the seas west of Pangea and deposited the observed, steep slab walls. Making these most easterly slabs intra-oceanic implies that all lower-mantle slabs of Figures 2A and 4A initially grew under separate, but coeval, intra-oceanic trenches (the archipelago), including the green Farallon trenches.

2.6. Archipelago Override—Geophysical Predictions

Supplementary Movie M1 visualizes the four-dimensional model predictions for archipelago override (see footnote 1). As North America migrates westward from 200 Ma to 0 Ma in 5 m.y. increments, the slab is rendered (deposited) at increasingly shallow depths, at a rate of 10.5 mm/yr (see section 2.7 for rate derivation). Interpreted trenches are placed vertically above actively growing slabs and evolve with the slab geometries. Figure 5 summarizes this trench evolution from 200 Ma to present. The first-order contrast is between older trenches hovering stationary above slab walls versus younger trenches dispersing in a westward-younging pattern. In all cases, the transition coincides with the arrival (override) of North America at the slab walls, i.e., trench override. Westward subduction into stationary MEZ is replaced by eastward subduction into the westward-migrating Farallon (L1) slab. Stationary CR transitions into the west-migrating Gorda slab; both are deposited via eastward subduction of Farallon lithosphere.

Override of the archipelago must have taken roughly 100 m.y. This geophysical prediction follows from the east-west extent of the MEZ, ANG, and CR slab walls in Figure 4 (~2800 km, measured at latitude 65°N), divided by the rate of North American westward drift, which is well constrained by Atlantic spreading (~25 mm/yr over the past 155 m.y., measured at latitude 40°N; e.g., Engebretson et al., 1985; Müller et al., 2008). This rough averaging of $(2800 \times 10^6$ mm)/(25 mm/yr) yields 112 m.y. In a more granular accounting that propagated observational uncertainties, Sigloch and Mihalynuk (2013) predicted onset of archipelago override at 146 ± 24 Ma when the North American margin reached point A1 in Figure 4A (the easternmost extent of MEZ slab/arc). Thus, first collisions would have been in the Late Jurassic. Tomography and plate reconstruction predict end of archipelago override at 55 ± 7 Ma, when the margin reached the CR trench.

On its continued westward drift past the first MEZ arcs at point A1, the west coast diachronously closed the wedge-shaped Mezcalera Ocean from north to south, and the Angayucham Ocean from south to north, accreting increasingly broader swaths of Mezcalera and Angayucham arc terranes to the south and north, respectively (Figs. 4A and 4B). The Mezcalera-Angayucham Oceans must have closed by westward subduction, because no slabs are imaged to the east of MEZ and ANG, and because MEZ/ANG cannot represent Farallon lithosphere, as argued earlier herein.

As North American rode over Mezcalera-Angayucham trenches and into the archipelago, it encountered Farallon lithosphere or smaller microplates. Subduction regimes for this lithosphere were variable and complex but can be roughly inferred from slab geometries. In Figure 2A, southerly cross-section X-X′-X″ slices through the MEZ slab at a latitude where it was overridden by the southern U.S./Mexican west coast. Panels B1 and B2 of Figure 2 interpret observed slab geometries along this section: Westward closure of the Mezcalera Ocean (panel B1) was followed by a forced subduction flip to eastward Farallon subduction (B2). While the stationary, intra-oceanic Mezcalera trench had built a vertical slab wall, the migrating, margin-hugging Farallon trench built a dipping slab L1 (which is too shallow to be rendered in Figure 2A but can be inspected in Movie M1 [see footnote 1] and Fig. 5).

Northerly section Y-Y′-Y″ in Figure 2A cuts through the two equally deep slab walls ANG and CR indicating a subduction history quite different from that of section X-X′-X″. Both the ANG and the Farallon trench were intra-oceanic and stationary (panel C1). After closure of Angayucham Ocean and extinction of Angayucham arc, there was still no subduction beneath the west coast (because no shallow slab equivalent to L1 is imaged between ANG and CR; this microplate presumably escaped to the north, with margin-parallel motion). The CR (Farallon) slab wall continued to grow until the west coast impinged on its trench and started dragging it westward (panel C2). This initiated the Andean-analogue subduction regime along the Cascadia margin and has since built a dipping slab that connects to the current trench, which is clearly observed in panel A, and is cartooned in panel C2. Hence, the conversion to Andean-style subduction happened much later along Y-Y′-Y″ than along X-X′-X.″ At even more northerly latitudes, the conversion is not expected to have happened at all.

Such predictions make our hypothesis testable and falsifiable. Spatio-temporal collision predictions can be checked against the geologic record (e.g., Dickinson and Lawton, 2001; Dickinson, 2004, 2006, 2008; Sigloch and Mihalynuk, 2013). If no matching collisions or sutures are observed, then slab sinking must have been more complex than just vertically down, and error bounds can be put on these deviations.

The geologic deformation record indicates a completely consistent time span for override: onset of southern Canadian Rocky Mountain

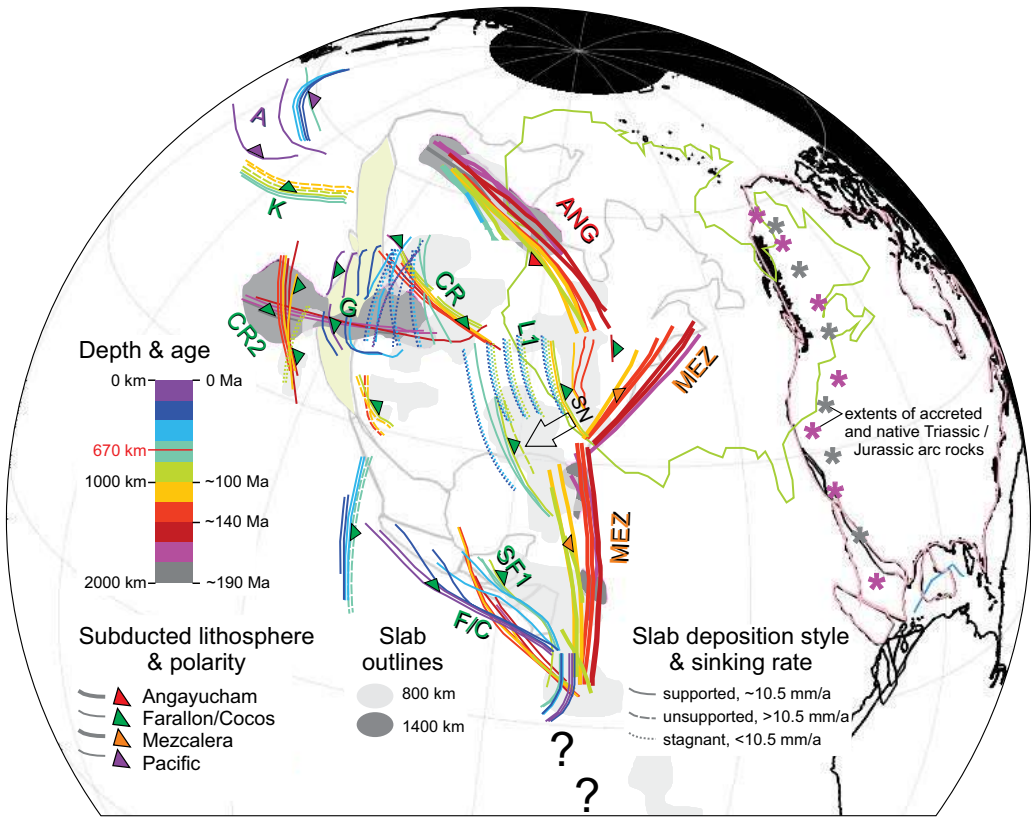

Figure 5. Volcanic arc and trench migrations west of Jura-Cretaceous North America over time and space: summary of the four-dimensional paleo-reconstruction of Supplementary Movie M1. Colored lines are absolute trench positions over time, with respect to the lower mantle, as inferred from slab geometries. Colors are chosen to match the depth-to-color mapping used to visualize the 3-D tomography model in Figures 2 and 4, and Movie M1 (see footnote 1). At depth increments of 100 km, trench geometries were inferred from the geometries of "actively growing" slabs, as explained in the caption of Movie M1 (see footnote 1). A slab-wall sinking rate of 10.5 mm/yr, which is estimated from slab geometries rather than just assumed, produces a mapping of slab depth to trench age; see the color bar. This mapping is derived from the geometries of the MEZ, ANG, and CR slab walls (c.f. Section 2.7); such "supported" trenches are drawn as solid lines. Barbs on trench lines point in direction of subduction; barb colors denote the ocean basin origin of subducting lithosphere: Farallon (dark green), Mezcalera (orange), Angayucham (red), or Pacific (maroon). Slabs that sank slower or faster than 10 ± 2 mm/yr are marked by dotted or dashed trench lines, respectively, and their deviating sinking styles are expected and discussed in the caption of movie M1 (see footnote 1). Arguments for MezAng suturing do not depend on these younger Farallon slabs. Slab outlines at 1400 km and 800 km depth are given for reference, as are continent locations in a lower-mantle frame at 170 Ma, 80 Ma, and present day, with accreted belt shaded beige. (Additional times are omitted in order to avoid clutter. The movie reconstructs 3-D slab deposition, continental drift, and seafloor isochrons in time increments of 5 m.y., from 200 Ma to present.)

deformation at ca. 163–146 Ma (Pană and van der Pluijm, 2015), and the Nevadan orogeny in California 163–152 Ma, terminating around 155 ± 3 Ma in the Sierra Nevada foothills (Schweickert et al., 1984) or 145–155 Ma (Harper et al., 1994), although some workers posit ongoing deformation for ~30 m.y., to ca. 123 Ma (Tobisch et al., 1989; Saleeby et al., 1989), significantly overlapping the onset of Sevier orogenic events (e.g., DeCelles, 2004). This matches our predictions of deformation onset (collisions at MEZ promontory → Nevadan orogeny), followed by more interior deformation as MEZ-ANG arcs were overridden (→ Sevier). The last arc terrane accretion along the Cascadia margin at 55–50 Ma (Sigloch and Mihalynuk, 2013) corresponds to a fundamental change in the Coast-Cascade orogenic belt (e.g., Crawford et al., 2009).

The temporally least constrained match is for deformation onset: 146 ± 24 Ma from geophysics versus 163–145 Ma from geology. The likely reason is that the continental margin protruded at least 200–300 km farther west than today (relative to stable North America), considering the previous addition of the Intermontane microcontinent to the margin in Canada (Evenchick et al. 2007, and references therein), subsequent shortening in the Rocky Mountain and Skeena fold-and-thrust belts, and similar minimum cumulative shortening in thrust belts of the United States (e.g., DeCelles, 2004). In that case, the margin would have impinged on MEZ arc ~10–15 m.y. earlier, consistent with the age of the Nevadan orogeny (Schweickert et al., 1984; Harper et al., 1994).

Also, depending on the width of these pre-accreted terranes (shaded belts in Fig. 4B and 5; and Movie M1 [see footnote 1]) at the latitude of California, override of MEZ (cross section X-X′-X″ and panels B1/B2 in Fig. 2) should have commenced between 135 Ma and 110 Ma, consistent with the onset of both the main pulse of Sierra Nevadan magmatism (Ducea, 2001; Cecil et al., 2012) and the Franciscan accretionary complex (Dumitru et al., 2010).

2.7. East-Dipping Slab Geometries Support Archipelago Hypothesis and Provide Rate Estimates for Slab Deposition

The eastward-protruding chevron where the MEZ and ANG slabs meet is probably the most discussed geometric feature of the North American slabs and has been interpreted to support Andean-analogue subduction, including our own work prior to Sigloch and Mihalynuk (2013). Tomography models have typically been presented in two-dimensional (2-D) cross sections that cut obliquely to the strike of either slab wall, most often east-west sections (an example is Fig. 1 *in* Sigloch et al., 2008, cut at 42°N). This gives MEZ the appearance of a thick, eastward-dipping sheet, i.e., a dipping upper surface paralleled by a dipping lower surface. A section parallel to the MEZ wall reveals a different geometry, as shown by the inset of Figure 4A, which strikes SW-NE. The upper surface of the MEZ slab plunges from SW to NE, from depths of 500 km (light-blue level)

down to 1500 km (red). The bottom surface, however, runs almost flat, at ~1800 km depth (magenta level). The Andean analogue suggests no reasonable explanation, but this geometry is expected if the lower surface records the onset of MEZ subduction, synchronous along the entire sectioned segment, because a continuous plate boundary came into being (see Movie M1 [see footnote 1]). Subduction into this trench segment would have been roughly NW-ward (trench-perpendicular). Any cross-section in NW direction would perpendicularly intersect the MEZ wall, which would look like the cartoon in Figure 2B1. However, a section through A1 would show earlier subduction termination than a section through A2 or A4. This illustrates that the slab's NE-dipping upper surface in the inset of Figure 4A records the diachronous extinction times of subduction along the Mezcalera trench, as North America overrode more and more of it (and subduction was forced outboard, e.g., to trench L1 in Fig. 4A). At A1, the slab wall was only built to a depth of 1500 km (red color level) and thus a "wall height" of 300 km (= 1500–1800 km). At point A2, the west coast arrived later, so the slab wall was built to the yellow level of ~1000 km depth (or "wall height" of 800 km = 1000–1800 km). How long did it take to deposit those 300 km or 800 km of slab wall?

The plate reconstruction gives the arrival times of the west coast at points A1, A2, etc. In Figure 4A, for example, the western margin at 110 Ma has overridden the Mezcalera trench (dashed orange barb) up to point A2 or A4 (there is a geological uncertainty of several hundred kilometers about the exact shape of the margin, cf. section 2.6). The slab wall sinking rate can be estimated at any point A_i by dividing the (current) depth of the upper surface of the slab wall by the time since the margin arrived there, e.g., 1050 km/110 Ma at point A2. An arbitrary number of sinking rate estimates can be made along the MEZ and ANG slab walls, including much farther west. Sigloch and Mihalynuk (2013) chose five points that could be independently verified and dated by the geologic record, for example, first arc collision and deformation at the continental margin for A1. This ensemble of points yielded relatively uniform sinking rates of 10 ± 2 mm/yr, i.e., relative regional variations in slab wall sinking of only 20%. Thus, slab sinking rates are not assumed by our methodology but were estimated from observations. Across the lower-mantle slab assemblage, whether MEZ, ANG, or CR, only this one relatively uniform sinking rate is consistent with the geophysical observations and the vertical sinking hypothesis.

Although 10 mm/yr is the (averaged) sinking rate since end of arc activity, the slab walls presumably sank at the same rate while the arc was active, so that 10 mm/yr is also the rate at which the slab wall grew in "height": ~10 km were added every 1 m.y., or 100 m.y. of deposition to build a wall to a vertical extent of 1000 km. (This rate does not hold for upper-mantle slabs that are not supported from below by the lower mantle.)

Figure 4A is calibrated to 10 mm/yr sinking rate: matching the reconstruction at 110 Ma, only slabs at and below 1100 km depth are rendered. In the same manner, Movie M1 shows reconstructions and tomography slices in increments of 5 m.y. and 50 km (see footnote 1).

2.8. Archipelago Override—Today's Southwest Pacific as a Modern Analogue

Today's southwest Pacific Ocean is a remarkably close analogue to the Mesozoic archipelago suggested by tomography and plate reconstructions. Some detailed comparison is warranted, given that an archipelago setting is more complex and has been given less consideration than the Andean analogue, especially by the geophysical community.

The overarching similarity between the two archipelagos is that both accommodate(d) the simultaneous and long-lived subduction of two major ocean basins from opposite directions. Their convergent plate boundaries form outer bounds of the archipelagos. Beneath the southwest Pacific, the Indo-Australian plate subducts northeastward, and the Pacific plate subducts westward. Beneath the Mesozoic American archipelago, the proto-Pacific Farallon plate subducted eastward, and the Mezcalera-Angayucham Oceans (the North American plate) subducted westward. In both cases, one of the plates carries(carried) a major continent that obliquely overrides(overrode) the archipelago and slowly extinguishes(ed) its trenches: present-day Australia plays the same role as late Mesozoic North America.

In a remarkable coincidence(?), the connectivity of the major, convergent plate boundaries is almost identical for both archipelagos. This becomes evident if a map of today's southwest Pacific is mirrored and then rotated 90° counterclockwise (Fig. 6). Comparison of Figure 6 with Figure 4A (at ca. 110 Ma) shows that trench topologies are basically the same, which is made explicit by the use of identical colors for corresponding trenches and by labeling today's southwest Pacific map with the names of its corresponding Mesozoic American elements of Figure 4. The Angayucham Ocean corresponds to the Indian Ocean; the ANG arc terranes correspond to Sumatra-Java; the Nevadan and Sevier orogenies correspond to the Papuan fold-and-thrust belt; the Cretaceous Interior Seaway corresponds to the Gulf of Carpentaria–Arafura Sea, etc. Hence, the southwest Pacific provides rather detailed predictions and actualistic examples for the geologic structures expected in the Cordillera if the Archipelago hypothesis is correct, such as arc accretions, subduction flips, and formation of interior seaways (e.g., Silver and Smith, 1983). The analogy is detailed further in Table 2, which compares the sequences of North American versus Australian archipelago override side-by-side.

Section 3 focuses on geological arguments for the existence and diachronous closure of the inferred Angayucham-Mezcalera Ocean. Its counterparts are the Indian Ocean and Coral Sea to either side of Australia. Oceanic lithosphere ahead (north) of Australia, which formerly connected the two ocean basins, has subducted beneath the archipelago's arc terranes, which have now accreted to formerly "native arc" (northern New Guinea) as Australia has started to override the archipelago. This situation reflects the North American archipelago at ca. 110 Ma (Fig. 4A), when the formerly continuous Mezcalera-Angayucham Ocean had been separated into two basins as North America overrode the NE-protruding part of Mezcalera trench and its arc terranes (the Insular superterrane, consisting of the Wrangellia, Alexander, and Peninsular terranes). The phase of Mezcalera-Angayucham suturing represents the earlier (Jurassic to Early Cretaceous) parts of override, equivalent to Australia's past. In Australia's tectonic future presumably lies a messy sequence of terrane accretions, causing frequent reconfigurations of secondary trenches in the archipelago's interior (black barbs in Fig. 6), which will produce significant slab complexity. Figure 5 clearly demonstrates the transitions upon override, from simple to complex trench geometries. Slab geometries in the upper mantle and transition zone under North America, which recorded archipelago override in full swing, are less voluminous and more fragmented than the massive, clear-cut, and vertical slab walls that were built before the continent collided with the first Mezcalera-Angayucham terranes. Thus, the archipelago hypothesis offers a new framework for assessing upper-mantle slab geometries, which have been imaged consistently and in great detail since the advent of the USArray experiment (e.g., review by Pavlis et al., 2012; Burdick et al., 2014), and which can for example be inspected in Supplementary Movie M1 (see footnote 1). Interpretation of upper-mantle structure is beyond the scope of this study, as is a detailed discussion of corresponding geologic events since the Late Cretaceous (ca. 110 Ma), or of slab geometries imaged under the southwest Pacific.

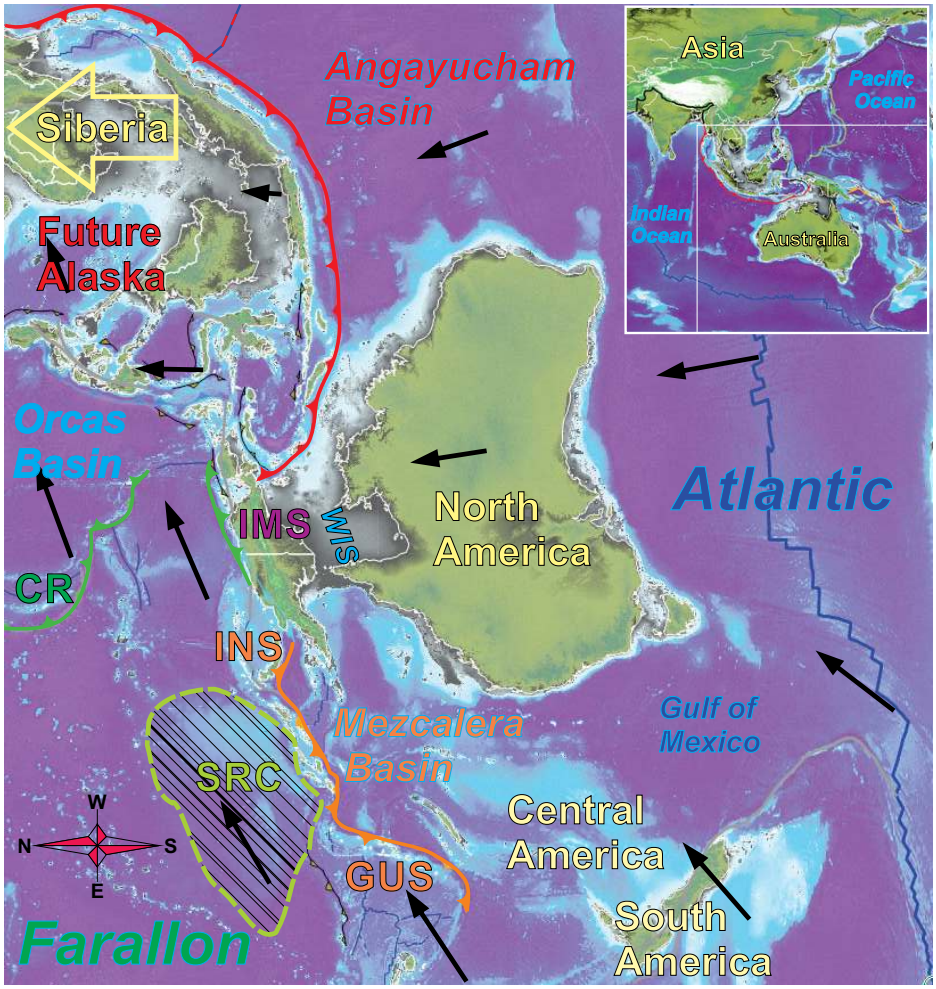

Figure 6. Today's southwest Pacific is a close analogue to the archipelago inferred for the seas west of North America in Early Cretaceous times. A 90° counterclockwise rotation of a mirrored map transforms the larger Australian region (map inset in top right) to a trench-continent configuration that is topologically almost identical to that inferred from the slab geometries of Figure 4A for Mesozoic North America. (Standard geographic directions N-E-S-W transform to W-S-E-N; see compass rose in bottom left.) Present-day tectonic elements are labeled with the names of their corresponding Cretaceous analogues of Figure 4, so that Australia becomes "North America," the Indian Ocean becomes the "Angayucham Basin," etc. Trenches are marked by the same colors as their counterparts in Figure 4. Secondary trenches without counterparts are colored black. Corresponding geological elements and their roles in archipelago override are explained in Table 2. IMS—Intermontane superterrane; INS—Insular superterrane; GUS—Guerrero superterrane; SRC—Shatsky Rise conjugate; WIS—Western Interior Seaway.

3. GEOLOGICAL EVIDENCE FOR THE MESOZOIC ARCHIPELAGO MODEL

From geophysical observations alone (section 2), we can ultimately only make plausible arguments about paleogeography: Uncertain mantle rheologies mean that the scenario of much more complicated, heterogeneous slab sinking (under an Andean-style trench) cannot be definitively rejected. This section argues that the Andean analogue can, however, be rejected based on direct geological evidence for the Mezcalera-Angayucham Oceans and for its spatio-temporal closure as predicted by the paleotrench configuration of Figure 4A.

Geologic relicts of the Mezcalera-Angayucham Oceans are preserved in a tract of at least 11 collapsed basins extending from Alaska to Mexico. These had been described previously, but they had not been recognized as a continuous, continent-spanning suture of a wide and mature paleo-ocean. As predicted, basin relicts of appropriate age straddle the boundary of two microcontinents, which are introduced in section 3.1: the Intermontane superterrane, pre-accreted to the continent by ca. 170 Ma, and the Insular-Guerrero superterrane, accreted as the Mezcalera-Angayucham Oceans sutured. Section 3.2 distributes the inventory of North American terranes along the geophysically inferred trenches (slab walls) such that the predicted override sequence reproduces the tectonostratigraphic relationships of the accreted Cordilleran terrane assemblage.

Interpretations of the Cordilleran geologic record have mostly focused on arguing consistency with the Andean-analogue model. A relatively late (post–Late Jurassic) suture of the Insular-Guerrero superterrane to the Intermontane superterrane is inconsistent with this model because there was arc activity on the Insular superterrane, which could not have been due to a continent-hugging Farallon arc if the Insular superterrane was not sutured to the Intermontane superterrane (the latter had accreted prior to 170 Ma and hence represents continental margin for our purposes). Section 3.3 argues that all supposed geologic evidence against late Insular-Intermontane superterrane suturing is controvertible because none of said evidence demonstrates stitching or overlap sensu stricto. To the contrary, sections 3.4, 3.5, and 3.6 demonstrate direct observational support for late suturing, and for the preceding Mezcalera-Angayucham arc activity built atop the Insular superterrane (by westward subduction), west of the suture. Hence, neither land geology nor geophysical evidence is consistent with Farallon-beneath-continent subduction since 180+ Ma, or with the early (pre–mid-Jurassic) accretion of the Insular superterrane required by Andean-analogue models of the Cordillera.

3.1. Cordilleran Superterranes

Table 1 lists the characteristics and mutual relationships of all superterranes and terranes discussed, and for which paleopositions and current positions are shown in Figure 4B. In the Andean-versus-Archipelago controversy, decisive geologic evidence must be held by the Insular superterrane in the Canadian and Alaskan Cordillera. Consisting of the Peninsular and Alexander-Wrangellia terranes, the Insular superterrane is a Paleozoic–Mesozoic terrane composite constructed from several generations of arcs. Located inboard (east) of the Insular superterrane, there are the "native Triassic–Jurassic arc" (Dickinson, 2008) and the Intermontane superterrane, another Paleozoic–Mesozoic microcontinent consisting of Quesnellia, Stikinia, Yukon-Tanana,

TABLE 2. ANALOGIES IN ARCHIPELAGO TECTONICS AND COMPARISON OF EARLY CRETACEOUS NORTH AMERICA TO TODAY'S SOUTHWEST PACIFIC

Figure 4	Figure 6
Corresponding tectonic elements	
Seas west of Cretaceous North America	Southwest Pacific today
North America (NAM) at ca. 120 Ma.	Australia (AUS) today.
Green: Farallon trenches. Orange: Mezcalera trenches. Red: Angayucham trenches.	Green: Pacific trenches (Izu-Bonin, Mariana). Orange: Coral/Solomon Seas trenches. Red: Indian Ocean trenches (Sunda-Java-Banda).
Westward spreading of central Atlantic Ocean since ca. 170 Ma.	Northward spreading of Southern Ocean since ca. 95 Ma (Brown et al., 2003).
Mezcalera-Angayucham Ocean, closed by westward subduction under the archipelago. Subdivided into Angayucham and Mezcalera Oceans, following impingement of North America on the archipelago.	Neo-Tethys Ocean, closed by north/northwestward subduction under the archipelago. Subdivided into Indian Ocean and Coral/Solomon Seas, following impingement of Australia on the archipelago.
Farallon Ocean in the proto–Pacific basin, subducting eastward.	Pacific Ocean, subducting westward.
Mezcalera and Angayucham trenches formed a continuous and stationary eastern boundary of the archipelago (as evidenced by continuous, steep slab walls).	Sunda-Java–Banda Trench forms a smooth, continuous and stationary western boundary of the archipelago (as evidenced by continuous trench lines and steep slabs underneath).
Farallon Ocean trenches formed the ragged western boundary of the archipelago. Eastward subduction into slab fragments CR, CR2, SF1, L1.	Pacific Ocean trenches form the ragged eastern boundary of the archipelago. Westward subduction into the fragmented Izu-Bonin, Mariana, Yap, and Pulau trenches.
Shatsky Rise conjugate (SRC), the subducted other half of today's Shatsky Rise, a huge oceanic plateau on the Farallon plate.	Ontong-Java Plateau, world's largest oceanic plateau on the Pacific plate.
Western Interior Seaway (WIS)	Arafura Sea/Gulf of Carpentaria
Prior to archipelago override	
The archipelago was bounded by two major oceans subducting in opposite directions: the Farallon Ocean versus the Mezcalera-Angayucham Ocean (and its successor basins).	The SW Pacific archipelago is bounded by two major oceans subducting in opposite directions: The Pacific Ocean versus the Neo-Tethys Ocean (and its successor basins, including the Indian Ocean).
North America rifted from supercontinent Pangea (African margin) to drift westward, opening the central Atlantic Ocean in its wake.	Australia rifted from supercontinent Gondwana (Antarctic margin) to drift northward, opening the Southern Ocean in its wake.
Ahead of NAM, the Mezcalera-Angayucham Ocean closed, by westward subduction under the archipelago.	Ahead of Australia, the Neo-Tethys Ocean closed, by northward subduction under the archipelago.
On its westward drift, NAM first accreted the microcontinent IMS (Intermontane superterrane) ca. 185 Ma.	On its northward drift, AUS first accreted the outer Melanesian arc (sensu Cloos et al., 2005) of Papua New Guinea (PNG) as ocean crust at the leading edge of AUS was totally consumed by northward subduction.
Archipelago override	
North America's impingement on the archipelago divided the Mezcalera-Angayucham Ocean into two basins on either side of the continent: Angayucham Ocean and Mezcalera Ocean. These two basins closed over the next 100 m.y. as NAM rode into the archipelago.	Australia's impingement on the archipelago divided the Neo-Tethys into two basins on either side of the continent: the Indian Ocean and the Coral/Solomon/Tasman Seas. These two basins continue to close as Australia continues to ride into the archipelago.
Collision of INS produced the Mezcalera-Angayucham suture and a continent-verging fold-and-thrust belt (Nevadan and Sevier orogenies).	Melanesian arc collision generated a suture and the continent-verging Papuan fold-and-thrust belt.
Riding into the archipelago, NAM accreted the active arcs behind the red ANG trenches (future Alaska) and behind the orange MEZ trenches (INS-GUS microcontinent). Collisions were diachronous because the MEZ-ANG trench lines (slabs) were eastward convex.	Riding into the archipelago, AUS will continue to accrete active arc terranes behind the red trenches (Sunda-Java-Banda) and orange trenches (New Britain, New Ireland, Solomon Islands). Collisions will be diachronous because the trench lines are curved, mostly southward convex.
Since NAM did not subduct, its collisions with MEZ-ANG arcs forced subduction flip from westward to eastward. This started outboard of INS and IMS, at latitudes of the United States, initiating the Franciscan subduction complex ca. 125 Ma.	Since AUS will not subduct, its collisions will force subduction flip, from northward to southward. This has already started in northwest (outboard) PNG with subduction of the Pacific plate.
Override of archipelago interior and subduction of its lithosphere (e.g., the small Orcas basin) was messy, as reflected by complex slab geometries in the upper mantle.	Override of archipelago interior and subduction of its oceanic lithosphere will be messy; many small trenches and basins exist already.
From the Farallon realm, no continent approached. However, two major oceanic Farallon plateaus, the Shatsky Rise conjugate (SRC) and Hess Rise conjugate, impinged on the archipelago and ultimately on the NAM margin (after ca. 90 Ma). Presumable cause of the Laramide orogeny was resistance to subduction of buoyant plateau.	From the Pacific realm, no continent is approaching, but the world's largest oceanic plateau (30-km-thick Ontong-Java) is headed for the archipelago.
Cretaceous Western Interior Seaway was formed by crustal thickening of IMS and continental terrace, causing loading of the continental margin via fold and thrust deformation (Beaumont et al., 1993; Evenchick et al., 2007) during accretion of INS.	Epicontinental "interior seaway" Arafura Sea/Gulf of Carpentaria between AUS and Papua New Guinea is formed by crustal thickening of continental terrace via fold and thrust deformation and accretion, causing loading of the continental margin (Hamilton, 1979; Edgar, 2003).
Thick clastic blankets were shed from the structurally thickened belt, eastward across a broad alluvial plain and coal-forming swamplands and into the Western Interior Seaway (e.g., Pană and van der Pluijm, 2015).	Thick clastic blankets (molasse) are shed southward from structural highlands across the broad alluvial plains and swamps of the Fly-Strickland lowlands and into the Arafura Sea (flysch).
Completion of Archipelago override	
NAM took ~100 m.y. to override the archipelago, accreting all terranes to its western margin. Finished with the override of the most distal Farallon trench, CR, at ca. 55–50 Ma. Final accretion did not result in a flip in polarity, but conversion from intra-oceanic to margin-hugging trench.	AUS might ultimately override the entire archipelago, accreting all terranes to its northern margin. Before fully colliding with eastern Asia, Australia might override the most distal Pacific trenches, Yap, Mariana, and Izu-Bonin.

Note: The table refers to Figures 4A, 4B, and 6, listing corresponding tectonic elements and their respective roles in the two archipelago override sequences.

and the Cache Creek terranes. Like today's Aleutian, Kuril, and Sumatra-Banda arcs, the inner, Quesnellian part of the Intermontane superterrane extended from ocean in the north onto the continent in the south, i.e., the arc on Quesnellia transitioned into the native arc anchored in today's southwest, cratonic United States (e.g., Asmerom et al., 1990; Lawton and Garza, 2014). Hence, the Intermontane superterrane was bound to the native arc, and offshore portions began to accrete to cratonic North America by ca. 185 Ma (Nixon et al., 1993; Murphy et al., 1995; Colpron et al., 1998). Final collapse of the Intermontane superterrane against the margin (at least loosely) occurred by ca. 173 Ma in the north (Mihalynuk et al., 2004) and ca. 170 Ma at the latitude of California (Dickinson, 2008). After that time, well-defined arc magmatism did not affect the ancestral North American margin, only the more outboard Insular superterrane.

Hence, the crucial question becomes: Where were the Insular superterrane and its trench located after 170 Ma, relative to the North American/Intermontane superterrane margin? If they were offshore and separate from the pre-accreted Intermontane superterrane, then an ocean intervened between the Insular superterrane and Intermontane superterrane (our Mezcalera-Angayucham Oceans), and its suture must be sought between those two superterranes. By contrast, if the Insular superterrane was bound to the Intermontane superterrane and hence the craton since ca. 170 Ma (van der Heyden, 1992; or even since 200+ Ma), then no Mezcalera-Angayucham Oceans existed, and subduction beneath the composite Insular-Intermontane superterrane margin must have been eastward. The latter alternative is a key assertion of the Andean model. Alternative scenarios, such as ours, are not "Andean" because they imply a gap in arc activity along the continental west coast while Jurassic–Cretaceous westward subduction beneath the offshore Insular superterrane was closing the Mezcalera-Angayucham basin. Intermediate scenarios have invoked simultaneous subduction beneath a marginal trench and beneath the Insular superterrane, either eastward (e.g., Monger et al., 1982) or westward (e.g., Dickinson, 2013), and thus at least a small intervening ocean.

3.2. Location Constraints on Intermontane and Insular Superterranes—Regional Context

It follows that the archipelago model must assign the Intermontane superterrane to the North American margin but the Insular superterrane and its Jurassic–Cretaceous arc to the MEZ slab, so that the Mezcalera-Angayucham Oceans closed between the Intermontane superterrane and Insular superterrane while building the MEZ slab wall by westward subduction (Figs. 4A and 4B). Placement of Insular superterrane along the intra-oceanic MEZ slab permits a sensible placement of the remaining Cordilleran superterranes:

(1) Arc terranes that now make up Alaska must always have been located north of the Insular superterrane. This is satisfied if Alaskan terranes are attributed to formation above the ANG slab—a huge slab that is a plausible generation region for Alaska's voluminous, Jurassic–Cretaceous arc rocks (not including Arctic Alaska and the northward-translated Alaskan parts of the Insular superterrane).

(2) The Guerrero superterrane of Mexico, considered to be a southern extension of the Insular superterrane, must always have been located south of the Insular superterrane. This is satisfied if the Guerrero superterrane was located atop the southern MEZ slab, immediately south of the Insular superterrane.

(3) The most recent accretions of (Farallon) terranes must have been associated with the westerly CR slab and trench. The Chugach subduction complex and Pacific Rim arc terrane can be explained as having grown above the eastward-subducting CR.

Items 1 to 3 express the plate-tectonic understanding that relative inboard/outboard positions of major terrane belts should not have changed over time, despite deformation and variable margin-parallel translation. They also express the expectation that some substantial arc terrane should be matched to each of the huge slab walls.

The terrane configuration surrounding the Intermontane and Insular superterranes passes some important geological plausibility checks. Much of Alaska consists of Jurassic–Cretaceous island-arc terranes and basins (red in Fig. 4B), which overprint and overlap older crustal fragments. The presence and growth of these arcs are causally explained by the presence of the ANG slab. As North America slowly and obliquely overrode the ANG trenches from SE to NW, ending only ca. 55 Ma according to slab geometries and plate reconstructions (Sigloch and Mihalynuk, 2013), it would have deformed and translated the accreting Alaskan arc terranes along its margin. This prediction is consistent with paleomagnetic evidence for compaction of the Alaskan arcs through variable rotations in oroclinal folds, and with northward transport by hundreds to a few thousand kilometers between 85 Ma and 55 Ma (Hillhouse and Coe, 1994; Johnston, 2001). Hence, the Angayucham part of the Mezcalera-Angayucham suture spatially tracks the oroclinal folding of the Alaskan arcs.

West of the Insular superterrane, override of the CR slab is similarly predicted for 60–50 Ma (Sigloch and Mihalynuk, 2013). In good agreement, the last major arc accretion occurred ca. 50 Ma with the Pacific Rim terrane (Cowan, 2003; Groome et al., 2003; Jakob and Johnston, 2015). Much of this Farallon/CR arc material might currently be underplated (Clowes et al., 1987), still to be tectonically exhumed as the modern Cascades accretionary prism continues to be underthrust and accumulates. Later and further outboard, oceanic plateau rocks of the Siletz-Crescent terrane accreted ca. 48–40 Ma (McCrory and Wilson, 2013). They must reflect early-stage subduction along the (Andean-style) Cascades arc that replaced the intra-oceanic CR arc. Hence, the Siletz-Crescent terrane could be thought of as the top/oldest part of the Cascades accretionary prism. Magmatic rocks of the northern Cascades are as old as 35 Ma (Phillips et al., 1989), although ancestral Cascade arc precursors in California and Nevada date to ca. 45 Ma (du Bray et al., 2014).

From arc geology in western Mexico, Dickinson and Lawton (2001) inferred Cretaceous westward subduction of more than just a narrow backarc basin under the Guerrero superterrane. Assignment of the Guerrero superterrane to the same topological position as the Insular superterrane, only farther south along the MEZ slab, is consistent with substantial, late westward subduction because the geometrically inferred Mezcalera Ocean widens to the south (Fig. 4B) and thus must have closed later there than between the Intermontane superterrane and Insular superterrane to the north.

3.3. No Geological Evidence for Intermontane-Insular Superterrane Suturing Prior to the Late Jurassic

The decisive test between archipelago versus Andean-style subduction history is the timing of Intermontane-Insular superterrane suturing, near the narrow nexus of the Mezcalera-Angayucham Oceans. It should be post–ca. 155 Ma (the reconstruction of Figure 4B predicts it was under way by 140 Ma), or post–146 Ma ± 24 Ma, when considering geophysical timing uncertainties and uncertainties about the westward extent of pre-accreted the Intermontane superterrane (Sigloch and Mihalynuk, 2013).

In the Canadian Cordillera and northwest Washington State, the Intermontane-Insular superterrane contact is located in the strongly metamorphosed and extensively intruded Coast-Cascades orogen. The true extent of this Coast-Cascades orogen suture is continental in scale

because the two superterranes once flanked much of the U.S. and Canadian margins (Fig. 4B). During and after accretion, parts of the Intermontane and Insular superterranes were translated, mainly northward according to paleomagnetic evidence (Enkin, 2006; Kent and Irving, 2010; Hillhouse and Coe, 1994), with the Insular superterrane now flanking British Columbia and Alaska, and only discontinuous relicts of the Intermontane superterrane still present in the United States, e.g., the Blue Mountains and Klamaths (Dickinson, 1976, 1979; Coney et al., 1980; Silberling et al., 1992; and many others).

Our proposed, relatively young Intermontane-Insular superterrane suture in the Coast-Cascades orogen is widely considered to be negated by geological evidence. Monger (2014) summarized the arguments against Late Jurassic–Early Cretaceous suturing as:

(1) There is scant evidence of a suture of the correct age in the Coast-Cascades orogen, where evidence is limited to the Bridge River terrane.

(2) There is evidence of plutons stitching the Intermontane-Insular superterrane boundary by the Early Jurassic.

(3) There is evidence of overlap between the Intermontane superterrane and Insular superterrane by the Early Jurassic.

(4) The Intermontane superterrane and Insular superterrane can be correlated by ca. 180 Ma on the basis of temporal and faunal affiliations.

In subsections 3.3.1–3.3.4, we argue that all four points are controvertible, because none of the evidence constitutes a stitch or overlap sensu stricto.

3.3.1. Evidence for the Mezcalera-Angayucham Suture

Far from being limited to the small Bridge River terrane or even to Canada, the predicted Mezcalera-Angayucham suture runs the length of the North American Cordillera. Although the large-scale connections may not have been made, the predicted trail of Late Jurassic to Early Cretaceous collapsed basins has been observed by previous workers. It extends from Alaska and Canada (Hampton et al., 2010) through the southwest United States (McClelland et al., 1992; Anderson and Mahoney, 2006) to Mexico (Dickinson and Lawton, 2001; Anderson et al., 2005). The basins include the Kahiltna and Nutzotin Basins in Alaska; Dezadeash Formation in Yukon; Gravina, Tyaughton, and Methow Basins in British Columbia and Washington State; the Mariposa and Galice Formations in California; and relicts of the Arperos Basin in Mexico, along with the Taray "Formation" and El Chilar subduction complexes. The bulk of the basin fills consists of turbidite deposits (those basin relicts are colored cyan in Fig. 4B), but some include arc, ocean crust, and mantle substrate (purple number labels in Fig. 4B). They have the correct distribution, age, and composition for surface remnants of the closed Mezcalera-Angayucham Oceans—the suture we seek, almost in plain sight.

Starting in the north, in south-central Alaska, much of the border between the Insular and Intermontane superterranes is marked by the Late Jurassic to Early Cretaceous Kahiltna assemblage in a region that has long been recognized as a tectonic suture (Jones et al., 1982; Csejtey et al., 1982) and has thus been named the "Alaska Range suture zone" (Ridgway et al., 2002). Detrital zircon analysis shows that the Kahiltna Basin received detritus from the Insular superterrane, and increasingly in the early Late Cretaceous, from the Intermontane superterrane (Hampton et al., 2010). Kahiltna has been regarded as a syncollisional basin (Ridgway et al., 2002; Hampton et al., 2007) formed by suturing that proceeded from east to west (Kalbas et al., 2007), or from south to north in Jurassic coordinates. This is consistent with diachronous metamorphism of Kahiltna basin strata ranging from Late Cretaceous to early Paleocene, and evidence of older and ~14 km deeper metamorphism in the east (Davidson and McPhillips, 2007).

The Kahiltna Basin displays along-strike equivalence with the Nutzotin and Gravina Basins, which extend from eastern Alaska through western Yukon (known there as the Dezadeash Formation) and along the Alaska panhandle, well into the Coast belt (e.g., McClelland et al., 1992; Manuszak et al., 2007; Ridgway et al., 2002). Gravina and its metamorphosed equivalents separate magmatic belts that, prior to 110 Ma, were restricted to either the Intermontane superterrane or the Insular superterrane but were overprinted by 100–50 Ma plutons that span the boundary (fig. 5 *in* Gehrels et al., 2009). Intermontane superterrane and Gravina Belt strata are interleaved by thrusts (Rubin et al., 1990; McClelland et al., 1992) and synkinematic, mid-Cretaceous plutons (Crawford et al., 1987; Himmelberg et al., 2004) that may have acted to facilitate and enhance thrusting (Hollister and Crawford, 1986). Possible equivalents of these strata known as the Kluane schist in southwest Yukon contain detrital zircons as young as ca. 95 Ma, with metamorphic overgrowths of ca. 82 Ma (Israel et al., 2010), and are structurally interleaved with slices of Triassic ocean lithosphere (trondhjemite ages: 206.3 ± 2.0 Ma to 206.8 ± 3.2 Ma; Mónica Escayola, 2015, personal commun.). In the northern Coast Mountains of northwest British Columbia, metasedimentary rocks that are undated but possibly correlative with the Gravina belt contain ultramafic lenses interpreted as slivers of mantle (Mihalynuk et al., 1994).

Near the southern end of the Alaska panhandle, surrounded by plutons in the heart of the Coast belt, is the Anyox pendant. It is extensively faulted and in part composed of a volcanogenic succession of early Middle Jurassic and perhaps Early Jurassic age, including tholeiitic pillow basalt and serpentinized ultramafite (Evenchick and McNicoll, 2002). The clastic strata overlying the Anyox pendant are correlated with those of the Late Jurassic and Early Cretaceous Bowser Lake Group (Evenchick and McNicoll, 2002), which contain open-water faunas (Poulton et al., 1994) and were affected by the same east-directed, mid- through Late Cretaceous deformation that formed the Skeena fold-and-thrust belt (Evenchick et al., 2007), a consequence of Intermontane-Insular superterrane suturing.

In southwest British Columbia and northern Washington State, basinal strata akin to the Gravina-Nutzotin extend through the eastern Coast Cascades orogen to the coeval Tyaughton-Methow Basin (McClelland et al., 1992; Hampton et al., 2010). Early Cretaceous strata near the top of the basin succession (the Relay Mountain Group) are recognized to be the oldest probable link between the southeastern and southwestern Coast belts and thus between the Intermontane and Insular superterranes (dated ca. 110 Ma by Garver, 1992; but revised to ca. 130 Ma by Umhoefer et al., 2002).

At the base of the Methow Basin, the Cayoosh assemblage consists of Early Jurassic to Early Cretaceous, mainly deep-water strata that conformably overlie oceanic crustal units of the Bridge River Ocean complex (Journeay and Northcote, 1992). Cayoosh strata have been interpreted as the last vestiges of the Mississippian to Jurassic (Cordey and Schiarizza, 1993) Bridge River Ocean within the southern Coast belt (Mahoney and Journeay, 1993; Journeay and Mahoney, 1994). We regard this long-lived Bridge River Ocean as part of the Mezcalera Ocean. Other workers seeking to accommodate such evidence of old oceanic crust between the Insular superterrane and Intermontane superterrane have proposed sinistral strike-slip entrapment of the ocean relict (Monger et al., 1994; Gehrels et al., 2009). While sinistral faults undoubtedly exist, invoking regional strike-slip duplication of the Bridge River–Cayoosh basin is an incidental complication because this Mezcalera Ocean relict is situated exactly where it should be—exposed within the Insular-Intermontane superterrane suture.

Farther south, Late Jurassic to Early Cretaceous amalgamation of terranes may be recorded by quartz-rich overlap strata. Late Juras-

sic granitic boulders contained in these strata provide a maximum overlap age that "links" Wrangellia to Bridge River–Methow terranes (Friedman and Armstrong, 1995; Riddell, 1991). However, strata as young as Cenomanian (ca. 95 Ma) contain radiolarian and foraminifer fossils indicating open-ocean conditions (Haggart et al., 2011) prior to the onset of Late Cretaceous thrusting (Journeay and Friedman, 1993). Pervasive faulting within this part of the Coast-Cascades orogen means that overlap cannot be unequivocally proven, a problem that is exacerbated in older, more deformed, and more extensively intruded rocks.

Detrital zircons from the mid-Cretaceous Methow Basin strata record no definitive evidence for provenance linkage to the Precambrian North American interior (Haggart et al., 2011, Surpless et al., 2014), which is unexpected if the Methow Basin formed as a margin-proximal, Andean-style forearc. By contrast, the lack of continental zircons is more probable if a trench east of the Methow Basin, marked by the Cayoosh subduction complex, separated and isolated the basin from North America. In our interpretation, Methow was the forearc basin, and Cayoosh was the accretionary prism above the westward-subducting MEZ slab.

Near the latitude of the Canada-USA border (49°N), Jurassic to Early Cretaceous strata of the Methow trough unconformably overlie ocean-ridge–type pillow basalt and gabbro, which are in fault contact with belts of serpentinized mantle (Ray, 1986). This marks the suture between the deformed leading edge of the Intermontane superterrane (Mount Lytton complex included in Quesnellia) and outboard gneissic rocks of the Coast-Cascades orogen.

South of 49°N, the southern ends of the 1500-km-long Coast-Cascades orogen and of adjacent Wrangellia (Insular superterrane) are curiously enveloped by Late Jurassic to Cretaceous rocks. In the west, this includes ophiolite and blueschist in the thrust nappes of the San Juan Islands, e.g., rocks overprinted by 124 ± 0.7 Ma blueschist metamorphism (mid–Early Cretaceous; Brown et al., 2005). The nappes are interpreted to have been emplaced over Wrangellia terrane from the south or possibly southeast (Brown, 2012) and may record Insular superterrane–Intermontane superterrane collision. Terminal San Juan deformation is bracketed by the age of the youngest strata involved in thrusting (112–115 Ma, late Early Cretaceous) and the oldest postthrusting strata (ca. 84 Ma, Late Cretaceous). The uppermost thrust nappe contains detrital zircons as young as 87 Ma (Brown, 2012). Late suturing at low latitudes is predicted by our kinematic model, which shows a wedge-like widening of the Mezcalera Ocean to the south. A reconstruction of the North American margin at 80 Ma is plotted as a green line in Figure 4B, which crosses the southern limit of the Insular superterrane arc and subduction zone, thus predicting final ocean closure, possibly including blueschist emplacement, on the southernmost Insular superterrane around this time.

3.3.2. No Evidence of Plutons Stitching the Insular-Intermontane Superterrane Boundary by the Early Jurassic

Until plutons across most of the Insular-Intermontane superterrane boundary have been subjected to robust isotopic studies, arguments for or against pluton stitching will lack credence. Utilization of cooling ages and multigrain zircon U-Pb dating, or even dating of single zircon crystals containing xenocrystic cores or mantled by overgrowths, obscures the geological story. To illustrate, multigrain U-Pb zircon age data were used to argue for an Andean margin in an influential paper by van der Heyden (1992), but none of the older ages of stitching plutons reported by van der Heyden (1989, 1992) could be confirmed by subsequent workers. All ages had to be revised downward when found to have been compound ages compromised by zircon inheritance (Butler et al., 2006; Gehrels et al. 2009). Pluton ages now stand at 100–120 Ma, down from previously 230 Ma, 120–140 Ma, and 100–120 Ma, and consistent with Early Cretaceous suturing, as predicted by tomography and plate reconstructions (see "Magmatic Response to Archipelago Override" section later herein).

3.3.3. No Conclusive Evidence for Overlap of the Insular Superterrane and Intermontane Superterrane by the Early Jurassic

Examples of Insular-Intermontane superterrane overlap basins older than the Middle Jurassic do not exist, nor can the Late Jurassic and Cretaceous basins discussed earlier be demonstrated to form incontrovertible "overlap." Rather, they are collapsed remnant basins, in the sense of Ingersoll et al. (2003). All have undergone postdepositional structural overprinting, as a consequence of collision that outlasted sedimentation. Overlap could only be demonstrated if strata depositionally rested on both the Insular superterrane and Intermontane superterrane and could be traced from one to the other.

Perhaps the most-cited example of Early Jurassic overlap is the Moffatt volcanics. Isotopic age dates reported from allegedly correlative portions on the Insular superterrane (177 ± 4 Ma, "ca. 175 Ma"; Gehrels, 2001, p. 1589) and Intermontane superterrane (173 ± 8 Ma and 170 ± 5 Ma) are coeval only near the limits of their large error envelopes (Gehrels, 2001). In addition, these ages fall within the acknowledged range of arc magmatism in both the Insular superterrane and Intermontane superterrane (ca. 210–170 Ma; see earlier herein), so until facies of Moffatt volcanics can be traced from the Insular superterrane to the Intermontane superterrane, they do not strictly constitute an overlap. However, confident tracking of the volcanic units from the Intermontane superterrane to the Insular superterrane may not be possible because contacts of Moffatt volcanics in the Insular superterrane are described as faults, or unconformities modified by faults (Gehrels, 2001), which contradicts and/or calls into question their "overlap" status (although at a few localities, fault disruption of the unconformity appears to be minimal; Brew and Karl, 1988).

One of the best opportunities to demonstrate overlap of the Insular-Intermontane superterrane boundary is the westward extension of the Intermontane superterrane–derived, distinctive, chert pebble conglomerates of the Late Jurassic to Early Cretaceous Bowser Basin ("BB" in Fig. 4B). Into the Coast belt, these strata have been traced as far west as the Anyox pendant (Evenchick and McNicoll, 2002). However, in the adjacent Insular superterrane, west of the Coast belt, the nearest coeval conglomeratic strata (Gravina belt) are dominated by igneous clasts derived from the underlying Insular superterrane (Brew and Karl, 1988). Such observations are consistent with the observations of Monger et al. (1983), who stated that all clastic rocks of the Gravina-Nutzotin belt appear to have westerly sources. Conclusions drawn by these early authors still apply: The simplest solution, and best fit to available data, is that the Insular superterrane accreted to the Intermontane superterrane late, trapping the Jurassic–Cretaceous Gravina-Nutzotin basin in between.

3.3.4. No Correlation via Temporal Affiliation of Arc Ages or Faunal Assemblages

The Intermontane superterrane and Insular superterrane should be expected to display an overlap in magmatic ages. Intermontane superterrane Stikinian arc subduction was active until termination ca. 173 Ma in the north (Mihalynuk et al., 2004), and perhaps slightly later in the south (Cordey et al., 1987). Westward subduction into the MEZ slab (beneath the Insular superterrane) should have overlapped the last ~20–30 m.y. of Intermontane superterrane subduction, according to slab depths and volumes (Sigloch and Mihalynuk, 2013). Thus, we do not agree with workers who assert that the similarity of the Insular superterrane and Intermontane superterrane arc ages, or even synchronous initiation of arc segments, implies formation along the same margin. Although

instances exist where this is demonstrably the case, one need not look beyond the modern-day western Pacific to see counterexamples. In the case of Early Jurassic North America, cessation of eastward subduction beneath western Pangea (Intermontane superterrane and native arcs), and initiation of westward-pulling subduction (into the Insular superterrane and Alaskan arcs by the MEZ and ANG slabs) were probably even geodynamically linked, because both would have facilitated the breakup of Pangea and central Atlantic spreading.

Jurassic faunal affiliations shared by the Intermontane superterrane and Insular superterrane have been used to argue that the Insular superterrane and Intermontane superterrane (Stikine) arcs were built in close proximity by ca. 200–180 Ma (Smith, 2006). Faunal affiliations are primarily controlled by water temperatures and ocean currents. We will not speculate on currents in the Mezcalera Ocean, but we point out that the Intermontane superterrane and Insular superterrane would have been located at similar latitudes on either side of Mezcalera Ocean, so that surface-water temperatures should have been similar. Despite its substantial width, Mezcalera Ocean did not span two thirds of Earth's equator, as the proto-Pacific (Panthalassa) did, so that Triassic to Cretaceous endemism across it should have been proportionally less pronounced, with eastern and western faunal affiliations largely shared. Hence, ocean fossil faunas are unlikely to discriminate between the Andean analogue and our archipelago model.

3.4. Exotic Basin Substrates Indicate Large, Long-Lived Mezcalera-Angayucham Oceans

There is additional, direct evidence for the Mezcalera and Angayucham Oceans and a late suture. The oceans' large dimensions and longevity are indicated not just by the voluminous MEZ and ANG slabs and by direct size estimates from plate reconstructions (Fig. 4B), but also by exotic substrates that underlie some of the Mezcalera-Angayucham suture basins. Exotic substrates are well demonstrated outside of the Coast belt, where metamorphic overprinting and destruction of fossils are not extensive. On either end of the Coast-Cascades orogen, exotic substrates sit stratigraphically and/or structurally beneath remnant ocean basin strata: Bridge River terrane beneath Methow Basin strata (in southern British Columbia), and Mystic subterrane beneath Kahiltna strata (in the Alaska Range suture zone).

The Bridge River accretionary complex contains an old oceanic record spanning ~170 m.y. (Cordey and Schiarizza, 1993) of pelagic chert, oceanic crust, and mantle with local lenses of blueschist. An overlying conglomerate that contains Na-amphibole grains and clasts from Bridge River blueschist provides the first depositional ties across the Intermontane-Insular superterrane boundary in the mid- to Early Cretaceous (Garver, 1992; Umhoefer et al., 2002).

In Alaska, Kahiltna strata are at least partly deposited unconformably atop the Silurian to Triassic Mystic subterrane, which includes fossiliferous limestone, conglomerate, phosphatic shale, well-preserved pillow basalt, mélange, and turbiditic sandstone (Bradley et al., 2007; Kalbas et al., 2007). Paleozoic fossils of the Mystic subterrane are more closely allied with Siberian than North American faunas (Blodgett et al., 2002), and detrital zircons are not easily interpretable, displaying mixed North American and Siberian provenance (Bradley et al., 2007).

Such evidence helps to discriminate between archipelago paleogeography and slightly modified Andean-analogue models (for the United States—McClelland et al., 1992; Saleeby, 1983; Harper et al., 1994; for Canada—van der Heyden, 1992), which explain the string of Jurassic basins as transtensional retro-arc basins to eastward Farallon subduction beneath the Insular superterrane arc, formed subsequent to a hard collision of the Insular superterrane with the Intermontane superterrane by Early Jurassic times. We are unaware of any other case where a continental-scale orogenic scar reopened along its exact suture location. Still, this scenario might account for the persistence of these basins at the boundary of the Intermontane superterrane and Insular superterrane, and possibly even for their deep-sea nature, but the exotic suture substrates and open-ocean faunas of the Bowser Basin (Poulton et al., 1994) deposited on the Intermontane superterrane, and of the Methow Basin (Kleinspehn, 1985) deposited between the Intermontane superterrane and Insular superterrane are difficult to reconcile with the retro-arc model.

If relicts of Late Jurassic to Early Cretaceous basinal strata were deposited in transtensional or backarc basins, their substrates should dominantly be extended portions of the adjacent Intermontane superterrane and Insular superterrane, not seafloor that formed up to 170 m.y. earlier containing exotic fauna. In principle, exotic terrane fragments might have been trapped during an earlier episode of suturing and re-exposed by formation of backarc or transtensional basins. However, in that case, evidence of earlier suturing should be demonstrated by age-appropriate regional deformation, extending the length of the continent, like the Jurassic–Cretaceous basins. Such evidence seems to be lacking until Mezcalera-Angayucham suturing in Late Jurassic to Cretaceous times.

3.5. Insular Superterrane as the Substrate for the Mezcalera Arc

Magmatic and tectonic lulls recognized in land geology are compatible with separation of the Insular superterrane from the Intermontane superterrane before the Late Jurassic (and hence location of the Insular superterrane above the first outboard slab to the west). Proponents of the Andean-margin hypothesis might argue that since ca. 207 Ma in the Late Triassic (Amato et al., 2007b), the Insular superterrane magmatic arc in Alaska, the Talkeetna arc, had been coupled with a subduction complex outboard of the Insular superterrane, the Chugach terrane, which includes blueschists dated between ca. 204 and 185 Ma (Roeske et al., 1989), thus proving eastward subduction beneath both terranes throughout this period. This is one of the most persistent myths supporting an Andean margin in Alaska. In fact, high-pressure–low-temperature metamorphic mineral assemblages occur in two modes: within the McHugh complex, the innermost (oldest) part of the Chugach terrane; and as slivers within the Border Ranges, a crustal-scale fault system that separates the Chugach complex from the Insular superterrane. Blueschists are important markers of fossil subduction zones, but in the Chugach terrane, they predate the assembly of their supposedly associated accretionary complex by tens of millions of years and are, therefore, clearly reworked from a much earlier high-pressure–high-temperature event. Even the inner McHugh complex, presumably the oldest part of the Chugach accretionary complex (with individual structural panels of sandstone having maximum depositional ages as old as 169 ± 2 Ma; Amato et al., 2013), is constrained by detrital zircons to have been assembled after 146 ± 5 Ma (Amato and Pavlis, 2010; Clift et al., 2012), and hence >50–60 m.y. after the oldest blueschist metamorphism. Similarly incompatible ages are seen 200 km south of Anchorage, where maximum depositional ages of 160 Ma at Iceberg Lake (Day et al., 2011) contrast with a 185 Ma blueschist age (Sisson and Onstott, 1986).

Initiation of subduction recorded in the Chugach complex followed termination of Talkeetna arc volcanism around 167 Ma (Amato et al., 2007b; although plutonism may have extended to ca. 153 Ma according to Rioux et al., 2007). Our model suggests that the Talkeetna arc was not paired with the Chugach complex, but rather grew above the west-subducting MEZ slab that drew the Intermontane superterrane toward the Insular superterrane (similarly proposed by Dickinson, 2004). Diachronous Insular-Intermontane superterrane collision, starting in the Late Jurassic, terminated Talkeetna arc

growth and forced a subduction jump outboard of the arc, and a polarity flip to (north-) eastward subduction of the Farallon plate. This explains the subsequent onset of Chugach complex accretion, recording Andean-style subduction of the Farallon realm, but only since the latest Jurassic, not since the Late Triassic.

3.6. Magmatic Response to Archipelago Override

Magmatism is a faithful recorder of plate interactions. Arc magmatism records subduction. Termination of arc magmatism and attendant deformation record collision with a buoyant crustal welt. Unfortunately, normal arc magmatism can be challenging to distinguish from subduction-termination magmatism caused by asthenospheric inflow after slab break (e.g., van de Zedde and Wortel, 2001) or from orogenic magmatism caused by crustal thickening and collapse (Dewey, 1988; Li et al., 2016) and/or superimposed convective delamination (Houseman and Molnar, 1997; Molnar and Houseman, 2013). We focus on spatio-temporal predictions for arc activity as determined from slab geometries, which guide the scrutiny of the existing magmatic record and its episodicity.

The lack of a slab to the east of the MEZ-ANG slab walls, beneath the Atlantic Ocean, predicts an arc hiatus on the North American west coast while it was overriding those longitudes. However, as described, we also accept 174–170 Ma as the timing for the collapse of the Intermontane superterrane and its native arc equivalents against the paleo-Canadian and U.S. margins, by eastward subduction. In principle, the Mezcalera Ocean might have closed by simultaneous eastward and westward subduction, as envisioned by Dickinson (2013, his fig. 7). This would have created arc magmatism along both the Intermontane superterrane and Insular superterrane margins right up to the time of ocean closure, and it would render the demonstration of a suture and of two separate arcs more challenging. However, this scenario is not supported by slab geometries, because no additional "native-arc slab" has been imaged in the mantle beneath the region formerly occupied by the west coast of Triassic–Jurassic North America (today's central Atlantic) at the same midmantle depths that farther west are filled by the MEZ slab. Hence, westward subduction should have persisted after termination of eastward subduction under the "native arc." (A deeper, older "native-arc slab" may be present as expected; see discussion in section 5.5.)

Can we demonstrate this hiatus of the native arc, which is negated by Andean-analogue models? Duration of the hiatus should be ~15–20 m.y., starting with terminal collapse of the Intermontane superterrane (174–170 Ma) and ending with reestablishment of arc magmatism after continental override of the Insular superterrane ca. 155 Ma (we attribute the initial pulse of Nevadan deformation [Harper et al., 1994] to first impingement of the Insular superterrane into North America and its pre-accreted Intermontane superterrane). Compared to this tectonic lull between arc collision events, the magmatic lull on the Intermontane superterrane appears to have been somewhat shorter, which can be ascribed to three factors: old, misleading geochronology (as described earlier herein); predictable slab break-off magmatism on the Intermontane superterrane; and Intermontane superterrane magmatism related to deformation rather than subduction. During the magmatic lull in the Intermontane superterrane, arc magmatism in the Insular superterrane was ongoing, as expected from westward Mezcalera subduction.

Demonstrating the existence of a magmatic lull in the Intermontane superterrane is easiest within a 300 km stretch where the magmatic slate was wiped clean by the Bowser Basin (labeled "BB" in Fig. 4B; e.g., Wheeler and McFeely, 1991; Evenchick et al., 2010). The Intermontane superterrane basement of the Bowser Basin includes intrusions as young as 185 Ma, overlain by Aalenian strata (172–176 Ma) intercalated with 175–172 Ma shallow submarine volcanic rocks and their feeders and volcaniclastic strata (which were considered the youngest Intermontane superterrane magmatism at this latitude of 56.5°N by Cutts et al., 2015). These rocks form the substrate for the diachronous sediments of the Bowser Lake Group (Evenchick et al., 2010): deltaic strata, prograding southwestward (from Bajocian to Oxfordian, ca. 172–156 Ma) over basinal turbidites, dominated by chert pebble conglomerates derived from the uplifted Cache Creek terrane (Intermontane superterrane). Post–172 Ma magmatic arc rocks are absent in the Bowser Basin (Intermontane superterrane), while they are abundant in the coeval Insular superterrane.

Plutonic rocks intrusive into other parts of the Intermontane superterrane are rare during the intercollisional magmatic lull in the latest Jurassic. Following collapse of the Intermontane superterrane arc around 173 Ma, a suite of ca. 172–170 Ma intrusions cuts the axis of the Intermontane superterrane (Cache Creek terrane). North of the Bowser Basin, their cooling ages smear to ca. 165 Ma (Fourth of July batholith, 59.5°N; Ash, 1994). South of the basin at Spike Peak (~55°N), their youngest phase is 166.5 ± 1.8 Ma (MacIntyre et al., 2001). Since this magmatism directly followed the end of Cache Creek subduction (Mihalynuk et al., 2004), it is tentatively related to slab break-off.

Despite a paucity of magmatic rocks between the Middle and latest Jurassic, continuous volcanic ash air fall is recorded in Bowser Basin strata by U-Pb detrital zircon ages and by biochronology of coeval ammonites (Evenchick et al., 2010). However, recognizable ash beds are extremely rare in the basin, suggesting a distant source, such as the approaching Insular superterrane volcanic arc. It was not until the end of the Early Cretaceous that intrusions began to abundantly cut the Bowser Group strata (e.g., Wheeler and McFeely, 1991; Mihalynuk and Friedman, 2006; Evenchick et al., 2007). This plutonism is consistent with eastward Farallon subduction that initiated after Insular-Intermontane superterrane collision and the forced flip of subduction polarity (Fig. 4A: dashed orange trench turns into solid green trench near the MEZ-ANG arc chevron). In summary, bona fide arc magmatism in the Intermontane superterrane on the continental margin ended before 172 Ma and resumed only around 130 Ma. However, during this interval, distal ash sourced in the active, offshore Insular superterrane arc contributed zircons to the sediment budget of the Bowser Basin.

Local records of intercollisional magmatism in the Intermontane superterrane exist. Perhaps the most comprehensively studied example is the composite Endako batholith, located ~70–200 km south of the Bowser Basin. Its magmatism apparently ranges from ca. 219 Ma (Late Triassic) to ca. 145 Ma (youngest Cretaceous; Villeneuve et al., 2001). The isotopic and geochemical character of the youngest Endako phases is consistent with wholesale remelting of juvenile arc crust, not mantle contributions from arc magmatism (Whalen et al., 2001). Intermediate-aged Endako phases are plagued with dating uncertainties due to selection of multigrain zircon fractions and the possibility that some of these grains contained inherited cores.

In the northwest United States, the Idaho batholith preserves a geological history much like that of the Endako batholith. Oldest phases show mantle contributions, but younger phases show increasing evidence of melting of subjacent crust (Gaschnig et al., 2011), indicating they were not subduction related.

In the southwest United States, an enormous body of isotopic age data constrains the location and timing of three Mesozoic arc belts, as summarized by Snow and Scherer (2006), Dickinson (2008), Schweickert (2015), and Saleeby and Dunne (2015). In California, the oldest and youngest arc-like belts overlap spa-

tially in an inboard (eastern) location: A mid-Triassic to Early Jurassic belt (ca. 240–170 Ma) is intruded and overprinted by an arc that ignited ca. 153 Ma with emplacement of post-Nevadan intrusions (such as the Guadalupe pluton; Ernst et al., 2009), which peaked around 90 Ma with a spectacular flux of magmatism in the Sierra Nevada batholith. Both arcs must reflect eastward subduction beneath the southwest United States: The older "native arc" developed across the craton, and the younger Sierra Nevada–Peninsular Ranges arc (a Farallon arc associated with slab L1 in Fig. 5) sutured the new crustal addition of the southern Insular superterrane to the craton (e.g., Kistler and Peterman, 1978).

A third arc of intermediate magmatic ages (ca. 193–155 Ma; Dickinson, 2008) is preserved in accreted, more westerly terranes and is separated from the two eastern arcs by relicts of blueschist and broken formation that accumulated outboard of the Intermontane superterrane/native arc in the so-called compound suture belt (Dickinson, 2008). Arc rocks west of the suture belt comprise much of the Foothills and San Pedro terranes (as defined by Schweickert, 2015) and also include the Smartville block, Foothills arc, and Slate Creek–Lake Combie arc belts (of Dickinson, 2008). In the Klamaths, the arc includes the Western Jurassic, Western Hayfork, and Rattlesnake Creek belts of Dickinson (2008). In detail, the compound suture belt is resolved into constituents, like the Calaveras mélange belt of the western Sierra Nevada range (Dickinson, 2008), and to its immediate west, the Don Pedro terrane (Schweickert, 2015).

In our interpretation, the western arc formed above the westward-subducting Mezcalera Ocean (in agreement with Dickinson, 2008; Schweickert, 2015). The Calaveras mélange belt and Don Pedro terrane that separate the arc from the more easterly, but partly coeval native arc are thus hypothesized to hold two subduction complexes of overlapping ages: recording the Mezcalera basin's initially double-sided closure from the Late Triassic to shutdown of the native arc (ca. 170 Ma, Calaveras mélange belt), finalized by one-sided, westward closure in the Late Jurassic (up to ca. 155 Ma, Don Pedro terrane). This interpretation seems to satisfy both geological and slab geometrical constraints and makes the Calaveras mélange–Don Pedro terrane units part of our continent-spanning Mezcalera-Angayucham suture.

Collision of the Mezcalera arc (Insular superterrane) in the Late Jurassic forced subduction outboard of the western arc, as evidenced by the accretionary phase of Franciscan complex growth beginning in the Early Cretaceous (ca. 123 Ma—Dumitru et al., 2010; or <144 Ma—Snow et al., 2010), and resumption of eastward subduction, as evidenced by the Early to Late Cretaceous magmatic inflation of the Sierra Nevada batholith (Cecil et al., 2012; Ducea, 2001). Figure 5 illustrates the setting of the youngest Sierra Nevada arc ("SN") associated with Andean-style Farallon subduction into slab L1. The geometry shows how earlier at these latitudes, the MEZ trench and subduction complex would have collapsed against a continental margin hosting the even older native arc.

Like the Bowser Basin of Canada, the Western Interior Basin of the United States holds a record of volcanic eruptions near the leading edge of North America, both as ash beds and detrital zircons (e.g., Christiansen et al., 1994; Laskowski et al., 2013). These reflect cessation of vigorous native arc magmatism near the end Triassic (by 200 Ma) and approach of the Mezcalera arc (ca. 170–146 Ma, by westward subduction). Magmatism ebbed following Mezcalera collision and then resumed with vigor as new, eastward Farallon subduction was established outboard of the sutured Mezcalera arc (slab L1 in Figs. 2 and 4). As outlined in Sigloch and Mihalynuk (2013), but not discussed herein, collision of the Hess-Shatsky conjugate plateau (Livaccari et al., 1981), starting ca. 93 Ma, extinguished the Sierra Nevada batholith, and collision of the Cascadia Root arc (starting ca. 55 Ma) extinguished the Coast-Cascades orogen; in both cases, terminal peaks in magmatic flux may have been enhanced by slab breaking. In Figure 5, the approximate location and east-west extent of the Hess-Shatsky plateau during collision are indicated by the wide unfilled arrow.

4. EARLIER CHALLENGES TO THE ANDEAN-STYLE SUBDUCTION MODEL

This section puts our findings in the context of the four different categories of models found in the geologic literature for Mesozoic Cordilleran evolution: the Andean analogue of eastward subduction (Fig. 7A); a variant featuring staggered eastward subduction (Fig. 7B); archipelago models of westward subduction beneath the archipelago (Fig. 7C); and models of offshore "ribbon continents" that contained allochthonous pericratonic terranes (and even craton) of acknowledged North American origin (Fig. 7D). Challengers of 180+ m.y. of eastward, Andean-style subduction have included Moores (1970, 1998); Schweickert and Cowan (1975); Chamberlain and Lambert (1985); Lambert and Chamberlain (1988); Ingersoll and Schweickert (1986); Ingersoll (2008); Dickinson (2004, 2008); Johnston (2001, 2008); and Hildebrand (2009, 2012, 2015). Challenges were presented by Dickinson and Lawton (2001) for Mexico and Box and Patton (1989) for Alaska. In some scenarios, westward subduction may have related to the earlier collapse of the Intermontane superterrane against North America, but others related to closure of variations of the Mezcalera-Angayucham Ocean basins, and some models have incorporated both.

4.1. Archipelago Models

Both eastward and westward consumption of oceanic crust has been invoked in models explaining delivery of island archipelago terranes to the western margin of North America. Monger et al. (1982) posited that the two metamorphic belts extending along the Canadian Cordillera arose from mid-Jurassic and Cretaceous collisions of two microcontinental archipelagos: the Intermontane superterrane and Insular superterrane, both transported to North America via eastward consumption of oceanic crust (Monger et al., 1972; Monger and Price, 1979; Fig. 7B).

Moores (1970, 1998) hypothesized an intra-oceanic archipelago at the origin of Cordilleran mountain building, which included eastward (Farallon) subduction as required by the Pacific magnetic record, but also westward subduction beneath an archipelago, ahead of North America's westward migration (Fig. 7C). Farther south, at the latitude of the Sierra Nevada batholith in the western United States, workers have recognized that arc and oceanic crustal remnants and their ages of deformation ("Nevadan orogeny") are most consistent with Late Jurassic collision of an intra-oceanic Jurassic archipelago that formed above a west-dipping subduction zone (Schweickert and Cowan, 1975; Ingersoll and Schweickert, 1986; Ingersoll, 2012; Fig. 7C). Transport to the continental margin was by double-sided consumption of ocean crust beneath the archipelago and beneath the margin of North America.

For the seas offshore Jurassic–Cretaceous Mexico, Dickinson and Lawton (2001) proposed a westward subduction scenario similar to ours (Fig. 7C), abandoning an earlier model of the type in Figure 7A, whereby deposition of the Mezcalera formation had been attributed to westward closure of a narrow backarc basin (Dickinson, 1981; Goldhammer and Johnson, 1999), which was presumed to have opened due to eastward Farallon subduction beneath an Andean-type margin. Dickinson and Lawton (2001) concluded instead that this "Mezcalera"

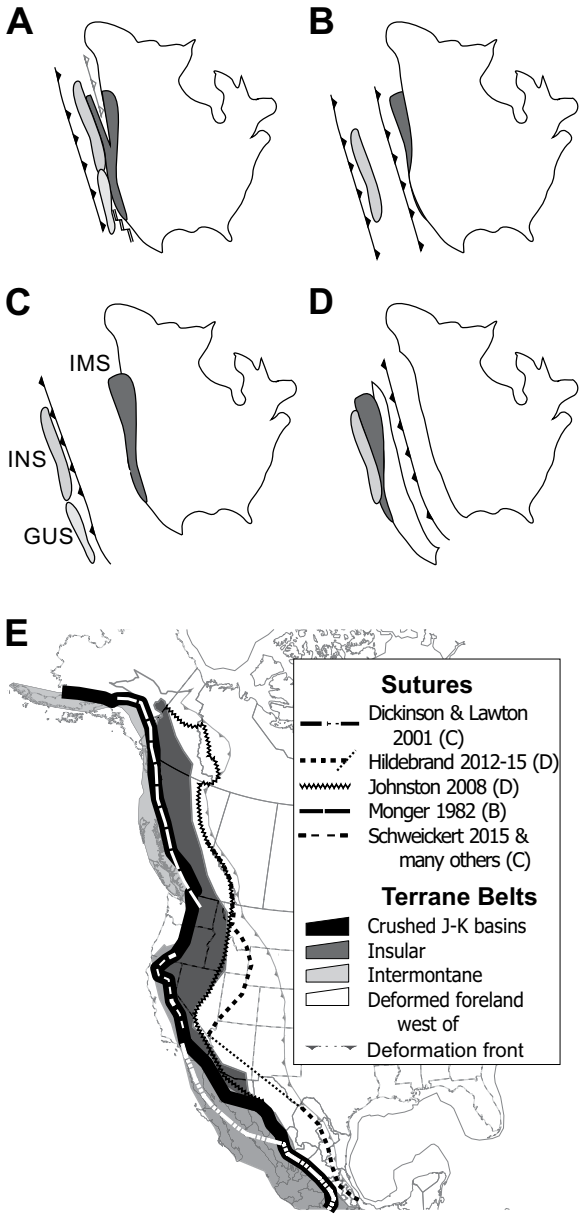

Figure 7. Competing models for the Jurassic–Cretaceous development of the Cordillera (A–D), and the oceanic sutures they predict (E). Models disagree about collision times of North America with Insular (INS) and Guerrero (GUS) superterranes (medium and light gray), and about the subduction regimes that closed the surrounding oceans. Intermontane microcontinent (IMS) is shown in dark gray. (A) Andean analogue model: long-lived eastward subduction beneath a prefused and pre-accreted Insular-Intermontane superterrane package (e.g., Burchfiel et al., 1992). Variants: mid-Jurassic collapse of an ocean basin within Intermontane superterrane (gray barbs; e.g., van der Heyden, 1992), or backarc/transtensional basin formation along the Intermontane-Insular superterrane boundary (stylized ridge; e.g., McClelland et al., 1992). (B) Modified Andean-margin model: collapse of Insular superterrane onto Intermontane superterrane via staggered eastward subduction (Monger et al., 1972; Monger and Price, 1979). (C) Archipelago models: Westward subduction of North America (with pre-accreted Intermontane superterrane) beneath Insular-Guerrero superterrane (Moores, 1970, 1998; Dickinson, 2004, 2008; Dickinson and Lawton, 2001; Schweickert and Cowan, 1975; Ingersoll and Schweickert, 1986; Ingersoll, 2008; Sigloch and Mihalynuk, 2013; this study). Variants: Some models consider synchronous or slightly older eastward subduction in addition to westward subduction. Not all models consider the Guerrero superterrane. (D) "Ribbon continent" models, including Intermontane superterrane and pericratonic terranes with an offshore microcontinent that accreted by westward subduction (Chamberlain and Lambert, 1985; Lambert and Chamberlain, 1988; Johnston, 2001, 2008). Variant: The ribbon continent also included Proterozoic cratonic domains (Hildebrand, 2009, 2012, 2015). Ribbon continents are the only model category that does not have the Intermontane superterrane pre-accreted by ca. 170 Ma. (E) Ocean suture locations predicted by authors advocating models in B to D. Solid black—Mezcalera-Angayucham suture predicted here (archipelago, part C), which largely coincides with Monger (1982) in Canada (dashed white, part B) and with Schweickert (2015) and others in California (dashed white, part C), and partly coincides with Dickinson and Lawton (2001) in Mexico (dash-dotted white; part C). Ribbon continent models by Johnston (black sawtooth; part D) or Hildebrand (dotted black; part D) predict more easterly, inboard sutures within the Intermontane superterrane and/or the (peri-)cratonic foreland. Hildebrand suture is pictured as offset by Texas lineament (thin dotted). J-K—Late Jurassic–Cretaceous.

basin must have been a sizeable, deep ocean—in good agreement with evidence for the size, timing, and subduction direction of the geophysically inferred Mezcalera Ocean. Like us, and supporters of the archipelago model for the western United States, they inferred simultaneous, double-sided subduction in Jurassic times, westward under the Guerrero superterrane (the southern extension of the Insular superterrane), and eastward under the native arc (called "Nazas arc" in Mexico), followed by exclusively westward subduction (Fig. 7C). When the Mezcalera basin had been fully consumed, a flip to eastward Farallon subduction beneath the outboard edge of the Guerrero superterrane ensued (the modern-day configuration, aside from more recent Gulf of California spreading). Given the consistency of this Mexican scenario with our interpreted paleography further north, we adopted their name "Mezcalera Ocean" for the entire basin.

4.2. Ribbon Continent Models

Considering only slab geometries without additional geological constraints, the joint placement of the Insular superterrane and Intermontane superterrane behind the Mezcalera arc (i.e., fused since the Early Jurassic or longer) would be reasonable per se. Including pieces of pericratonic terranes farther east would essentially equate to the ribbon continent scenario of Johnston (2001, 2008) and Hildebrand (2009, 2012), and if limited to north of latitude ~48°N, to "Cordilleria" of Chamberlain and Lambert (1985). However, these scenarios require the Mezcalera-Angayucham suture to run east (inboard) of the Intermontane superterrane (Fig. 7D). This is negated by geological evidence of the older, Triassic–Jurassic native arc rooted in the craton in the southwestern United States, which probably connected to Quesnellia on the Intermontane superterrane. Given this tie to the craton, the native arc must have formed above eastward-subducting ocean lithosphere. Like most workers in the Cordillera, we consider the evidence for this arc very solid. Plutons along the trail of the native arc cut deformed continent-fringing strata and Proterozoic craton alike. In addition, Late Triassic detritus from the native arc extends atop the craton as far as the Colorado Plateau, e.g., the Chinle Formation (Stewart et al., 1986; Asmerom et al., 1990; Riggs et al., 2013), and Jurassic eolianites extend discontinuously from the craton to the native arc in southern California–Arizona and northern Sonora (Bilodeau and Keith, 1986; Dickinson and Gehrels, 2009, 2010; Dickinson et al., 2010; Lawton and Garza, 2014).

Additional issues with ribbon continent scenarios are that they do not explain the presence of the Late Jurassic–Cretaceous suture basins that stretch from Alaska to Mexico (Fig. 4B), and, in the case of Hildebrand (2012), suturing times postulated for the Late Cretaceous ("Laramide orogeny," Lewis thrust) are too late to be explained by subduction into the MEZ-ANG slabs. Plate reconstructions confidently superimpose North America with the imaged slabs by Late Jurassic–Early Cretaceous times (Figs. 4A and 4B), implying earlier collision with MEZ and ANG arc terranes. Evidence of the earliest phase of this collision is the well-documented Late Jurassic shortening cratonward of the Mezcalera-Angayucham suture ("Nevadan orogeny"; Harper et al., 1994; Schweickert and Cowan, 1975; Ingersoll and Schweickert, 1986). Deformation persisted through Cretaceous times ("Sevier orogeny"; Armstrong, 1968; Monger and Price, 1979; DeCelles, 2004; DeCelles and Coogan, 2006; Evenchick et al., 2007; Pană and van der Pluijm, 2015; and many others).

Models that focus exclusively on westward subduction beneath a ribbon continent, such as the "Cordilleria" of Chamberlain and Lambert (1985), "Saybia" of Johnston (2008), and "Rubia" of Hildebrand (2009), are also incomplete in that they do not explain how the ribbon continents have related to, and transitioned into, eastward Farallon subduction since 180+ Ma, which is required by the magnetic seafloor record on the Pacific plate (e.g., Engebretson et al., 1985; Atwater, 1989; Sager et al., 1988).

Our archipelago model differs from ribbon continent models in several important aspects, most fundamentally, in its constituent parts, since it includes no western Laurentian peri-cratonic terranes in the archipelago. Still, the term "Cordilleria," introduced by Chamberlain and Lambert (1985), is a particularly fitting and self-explanatory name for the intra-oceanic paleogeography that became the western North American Cordillera. Hence, "Cordilleria" might be readopted as a proper name for "the archipelago," a name inclusive enough to survive further refinements of the archipelago concept.

With regard to Alaskan terranes, our archipelago model generally agrees with the "terrane wreck" of Johnston (2001, 2008). We associate the ANG terranes with the railcars of his "wreck," and the ANG slab wall with the absolute spatial location of his ribbon continent. The slab runs from beneath Nova Scotia to Yukon and thus grew arcs at more southerly latitudes than occupied by (central) Alaska today—in good agreement with paleomagnetic constraints on Alaska, which generally show northward displacement relative to cratonic North America. More specifically, strong northward displacement is indicated for Early to Late Cretaceous Alaskan rocks, which were deposited along the southeastern ANG and accreted early, whereas weaker and variable, north or south displacements are indicated for latest Cretaceous to Paleocene rocks (Hillhouse and Coe, 1994), which were deposited farther northwest and accreted late. Such timing reflects diachronous, southeast-to-northwest closure of the Angayucham Ocean, in two stages. First, between Late Jurassic to earliest Cretaceous times, the North American margin ploughed northward and obliquely into the trench marked by the ANG slab, trapping Angayucham arc terranes and their substrates between North America and Siberia. Later, between latest Cretaceous and mid-Eocene times, North America moved relatively southwestward (Enkin, 2006), resulting in dextral strike-slip faulting that accentuated Alaskan oroclines, rotating them 44° ± 11° counterclockwise (Coe et al., 1989). Together, these events produced the "terrane wreck"–style of oroclinal compaction described by Johnston (2001).

5. DISCUSSION

5.1. Oblique Collision as the Default Regime—Not Captured by Andean nor Ribbon Continent Models

The 3-D slab geometries that do not strike parallel to the reconstructed North American margin indicate that oblique collision was the default state along the Mesozoic west coast. These geometries imply formation of slab windows, alternating stress regimes, persistent indenters, and margin-parallel escape, consistent with findings from synoptic paleomagnetic studies (Enkin, 2006; Kent and Irving, 2010). At any time between ca. 155 Ma and ca. 50 Ma, parts of the continent were colliding with limbs of the MEZ-ANG arc chevron, while others were not yet colliding, were overriding seafloor inside the archipelago, or were already abutting the Farallon plate.

Although Andean and ribbon continent models are commonly seen as opposite end members of Cordilleran tectonic interpretations, they share the 2-D, special-case character of margin-perpendicular subduction. Both model types ignore or deemphasize gradual, margin-parallel changes that arise from unstable plate-boundary configurations and terrane translations, which are inevitable consequences of plate interactions on a spherical planet. Hence, simple, purely margin-perpendicular models of subduction should not be expected to capture the essence of Cordilleran evolution, at least not on a whole-orogen scale, over 10–100 m.y. To re-create a paleotectonic history that has any semblance of accuracy, there is no way around assimilating observations and modeling in 3-D (plus time).

5.2. Slab Widening—Observational Robustness and Formation Mechanism

The observed widening of American lower-mantle slab walls to 4–7 times the thickness of subducted oceanic lithosphere plays a crucial part in our argument for old and intra-oceanic subduction. Several lines of reasoning indicate that this observation is robust.

(1) If the slabs were much narrower than 400–700 km, then the dominant artifact afflicting ray-based tomography methods would be wave-front healing. It tends to smear out imaged features but acts even more strongly to render them invisible (Nolet and Dahlen, 2000). Yet, the slab walls have always been among the most robust features imaged in the mantle, and they are truly massive.

(2) Waveform-based or finite-frequency tomography methods such as we employed here (Sigloch, 2011) largely compensate for wave-front healing by modeling finite-wavelength effects. Yet, the width of the lower-mantle slabs has not decreased significantly compared to ray-based studies (including comparison tests of our own). Again, this means the slabs must be sufficiently wide that waveform healing is not a severe problem.

(3) Even with ray-based methods, it has always been easier to resolve the lower-mantle slab walls than, for example, the Juan de Fuca plate, just a few hundred kilometers below its trench. This should not be the case if the slab had the same thickness of ~100 km in both locations, because wave-front healing and smearing act more detrimentally on structures far from sources and receivers (i.e., in the lower mantle, not near a well-instrumented surface region).

Slabs in the upper and lower mantle have often been imaged by different studies using different methods, which might have put this comparability in question. With the advent of USArray however, individual tomographic studies have imaged through both upper and lower mantle (e.g., review by Pavlis et al., 2012; Burdick et al., 2014). They resolve a sharply defined, thin slab near the trench as expected, and pronounced thickening from the transition zone down (e.g., fig. 1 *in* Sigloch et al., 2008, transect at 42°N). This striking contrast in slab character—thin and ragged near the trench versus massive and continuous in the lower mantle—is also evident in Figure 2A and especially in Figure 3. A more subtle effect of artificial slab widening was described by Bezada et al. (2013), due to unaccounted wave path bending into the slab when using a spherically symmetric reference model. In principle, this effect should affect our images, but in a much-attenuated manner because our tomography is

dominated by longer wave periods of 30–10 s and uses less approximate sensitivity kernels than those of Bezada et al. (2013). Also the North American slab walls are 2–3 times wider than their Mediterranean upper-mantle slab and so are relatively less affected.

In summary, lower-mantle slabs are clearly several times wider than slabs in the upper 300 km, and our basic argument of massive volumes does not depend on whether they are 4 or 7 times wider. Instead, the existence, width, and age of the Mezcalera-Angayucham Oceans are argued from the distances of reconstructed North America to the slab walls, from the timing of the suture, and from the ocean floor sediments found in the suture basins; sinking rates are inferred from upward truncations of the slab walls. While "unfolding" and "obducting" the slabs walls back to the surface might test the reconstruction of the Mezcalera-Angayucham Oceans (e.g., Wu et al., 2016), we currently consider the uncertainties rather large, not just in the exact slab width, but also the tightness of its folds, and the likely existence of a spreading ridge in the Mezcalera-Angayucham Oceans that generated additional lithosphere.

Our deductions remain valid regardless of how exactly the slabs widened, but recent geodynamic modeling studies confirm that folding was the probable widening mechanism. Folding of viscous thin sheets (lithosphere) at the viscosity interface between the upper and lower mantle, as shown diagrammatically in our cartoons in Figure 2, has been observed in fluid dynamic tank experiments (Guillou-Frottier et al., 1995; Bellahsen et al., 2005; Schellart, 2008) and numerical convection modeling (Ribe et al., 2007; Stegman et al., 2010; Ribe, 2010; Gibert et al., 2012; Čížková and Bina, 2013; Garel et al., 2014). The simulations show that folding occurs in certain subspaces of a priori plausible parameter spaces for slab and ambient mantle rheologies, which means that observations of ubiquitous slab walls (hence ubiquitous slab folding) and of quantifiable sinking velocities put strong constraints on mantle rheology. Gibert et al. (2012) suggested that the oscillatory motion of slab folding in the mantle transition zone might transmit upward into trench oscillations, possibly expressed in periodically alternating compressive and extensive stress regimes along the South American Andes arc.

5.3. Andean-Margin Analogue in Geophysics

All slab interpretations prior to Sigloch and Mihalynuk (2013) followed the primacy of the Andean-analogue model, positing only Farallon subduction beneath the continent (e.g., Grand, 1994; Grand et al., 1997; van der Hilst et al., 1997; van der Lee and Nolet, 1997; Bunge and Grand, 2000; Ren et al., 2007; Sigloch et al., 2008; Liu et al., 2008). In part, this is explained by the relatively late discovery that the surviving Farallon plate fragment, the Juan de Fuca plate, does not connect downward into the MEZ and ANG slabs, as had been assumed, but instead into the much more westerly Cascadia Root slab (CR; Sigloch et al., 2008), which had been only vaguely visible in earlier tomographic images (e.g., Bijwaard et al., 1998; Montelli et al., 2006). Until then, the MEZ and ANG slabs had to be presumed to be Farallon slabs to match the undisputed seafloor magnetization for 180+ m.y. of Farallon spreading and thus subduction (Engebretson et al., 1985; Atwater, 1989; Seton et al., 2012).

Geodynamic simulations of subduction history under North America found the observed slab geometries challenging to reproduce unless unusual rheological regimes were invoked. Generation of the pronounced, eastward-pointing chevron of the MEZ-ANG slabs from a relatively straight margin-hugging trench proved especially problematic. Bunge and Grand (2000) could produce the chevron shape only by inserting the "Farallon" trench along the Rocky Mountain thrust front during Cretaceous times, an extremely easterly position that they acknowledged as geologically impossible. Instead, they hypothesized that from its actual coastal trench, Farallon lithosphere had reached its easterly resting place (MEZ/ANG slab) by extremely shallow ("Laramide") subduction, even though their simulations did not produce this lateral translation. Simulations by Liu et al. (2008) did achieve shallow Farallon slab transport over large lateral distances (~1000 km) by implementing a >3000-km-long low-viscosity channel ("stress guide") beneath stable North America. This modeling complexity was driven by the presumed requirement of a margin-hugging Farallon trench rather than a priori expectations about anomalous mantle rheologies, and the extensive low-viscosity layer it implied under an old continent is not evident in surface-wave tomography (e.g., review by Schaeffer and Lebedev, 2015).

Liu (2014) contrasted slab deposition in the Andean versus archipelago scenarios and argued for the former. It is, however, unclear how his 2-D simulations (depth plus a lateral dimension) could have implemented the essence of the archipelago's oblique and shifting trenches of Figure 5 (no details of trench evolution were given). An indication that the essence of our model was not captured is that twice as much lithosphere was subducted than for the Andean model, a major kinematic inconsistency, because total amounts should be the same in both cases (our model subtracts from the Farallon Ocean what it adds to the Mezcalera-Angayucham Oceans; cf. Fig. 1A vs. Fig. 1B).

To our knowledge, no convection simulation has produced the full, 3-D assemblage of North American slabs discovered since the advent of USArray, and especially not the slabs that are most problematic to the Andean-analogue model: the equally deep extent of the ANG slab wall at its eastern and western ends, or of the MEZ wall at its northern and southern ends, nor the presence of the deep, westerly CR slab. We expect that generating this full assemblage will be nearly impossible with a margin-hugging trench configuration and the known constraints on Farallon spreading, but it would be relatively straightforward with the trench evolution we propose because many convection simulations model do show near-vertical sinking. For example, Steinberger et al. (2012) found that in standard rheologies, lateral slab displacement from the surface to the core-mantle boundary did not exceed a few hundred kilometers, i.e., within the observational uncertainties of vertical sinking as hypothesized here. Bunge and Grand's (1994) model did not produce sufficient lateral slab displacement to deposit the MEZ/ANG slabs under a marginal Farallon trench. The modeling of Lithgow-Bertelloni and Richards (1998) enforced vertical sinking beneath trenches globally, including a marginal Farallon trench, and did not produce the observed MEZ-ANG slab chevron (their fig. 6 and plate 3).

In a simulation-free approach, van der Meer et al. (2010) assumed vertical sinking globally, including beneath a margin-hugging Farallon trench. Depositing the steep slab walls then required invoking a longitudinal, time-dependent rotation of the global lithospheric shell relative to the lower mantle. This net lithospheric rotation would have acted to effectively cancel out Atlantic opening during Cretaceous times, in order to hold the coastal Farallon trench stationary above the MEZ-ANG slabs, though again without fitting the chevron shape of MEZ-ANG slabs (their fig. 2c). This longitudinal shift was argued from the fit of three "anchor slabs," but for the relevant times, only the Farallon plate provides a real constraint: The east-west–striking Tethys slab yields only weak constraints on longitude, and the Mongol-Okhotsk slab is too old.

The net lithospheric rotation hypothesis can be tested and rejected by our investigation of MEZ-ANG arc collisions. We show that the Mezcalera trench was intra-oceanic, which negates the need to westward-translate the continental margin during Cretaceous times. Our accretion events indicate no net lithospheric

rotation with respect to the lower mantle, other than that contained in the hotspot/hybrid reference frame we use (O'Neill et al., 2005; Steinberger and Torsvik, 2008).

Taken together, the prior work can be read as having falsified the hypothesis of vertical sinking and uniform rheologies given a margin-hugging trench, but having left open the possibility of vertical sinking for the archipelago alternative.

To our knowledge, the only other slab interpretations to discuss similarly old arc accretions as ours were van der Meer et al. (2012), who associated Wrangellia (Insular superterrane) with a slab beneath the central Pacific, and Shephard et al. (2013), who acknowledged that the predicted position of Wrangellia corresponds with MEZ, but who supported a conventional interpretation of MEZ as a post–100 Ma Farallon slab. Both models imply that that Insular superterrane accreted after eastward transport on the Farallon plate (a modified Andean scenario; Fig. 7B), although consistency with isochron data was not argued. For some relatively recent accretions of oceanic plateaus, possible signatures left on slabs have been discussed. Accretions of the Hess and Shatsky Rise conjugates between 90 Ma and 70 Ma were invoked as explanations for the chevron shape of the "Farallon" (MEZ-ANG) slabs (Liu et al., 2010), and for the tomographically visible thickening of the Wyoming craton, via underplating of the Shatsky conjugate (Humphreys et al., 2015). Accretion of the Siletzia oceanic plateau ca. 50 Ma has been associated with a stalled Farallon slab under the Challis magmatic arc of the northwest United States (Schmandt and Humphreys, 2011). None of these relatively recent accretions was an arc terrane, and there is no doubt that they arrived on the Farallon plate.

5.4. Slab Sinking Rates

In sections 2.6 and 2.7, we inferred an averaged sinking rate for the MEZ-ANG slab walls of 10 ± 2 mm/yr since subduction, and we discussed how this was not an assumption but rather the only rate that is consistent with the observed slope of the westward-shallowing upper truncation surfaces of the MEZ and ANG slabs. Sigloch and Mihalynuk (2013) included the CR slab wall in this sinking rate estimate.

A lower-mantle sinking rate of 10 ± 2 mm/yr might appear slow compared to other rates suggested in the literature (see review by Butterworth et al., 2014). All such estimates have suffered from uncertainties in trench positions, possibly quite large and unrecognized, as argued here, and from ambiguous matches of trenches to slabs. Faster sinking rates tend to arise in convection simulations, but the small number of slab interpretations that have incorporated extensive geological evidence have yielded slow sinking rates consistent with ours, implying ~10 mm/yr for lower-mantle slabs under Asia (Van der Voo et al., 1999a, 1999b) and 12 ± 3 mm/yr for lower-mantle slabs globally (van der Meer et al., 2010). The latter study scrutinized the geologic record for volcanic arc activity (similar to our approach), and although they assumed vertical sinking rather than treating it as a null hypothesis to be tested, we generally agree with their results on sinking rates because our tests do support vertical sinking.

Our sinking estimate was inferred only for the special-case geometry of massive, steep slab walls in the lower mantle. We claim no validity for other slab types. In fact, Movie M1 (see footnote 1) implies clearly slower sinking for Farallon slabs L1 and G sprawling in the transition zone—the type of "stagnant slab" first discovered under the archipelagos of today's west and southwest Pacific (Fukao et al., 2009)—and faster sinking for some younger Farallon fragments of limited vertical extent, including the presumed Kula slab K of section 2.4. There are plausible reasons for their different sinking styles, as discussed in the caption of Movie M1 (see footnote 1). The present study does not depend on deciphering these young Farallon slabs in detail, as long as the cumulative volume of Farallon fragments is sufficient to account for the entire Farallon isochron record, which is the case (section 2.4). The complexity of Farallon fragments and trench evolution (Fig. 5) is considerable but not more so than in today's southwest Pacific (Fig. 6). The MEZ/ANG slabs have much simpler geometries, permitting robust predictions about Mezcalera-Angayucham Oceans suturing by westward subduction, and about the early transition phase into eastward, Andean-style Farallon subduction. Sinking rates can be robustly estimated as a side product of reconciling slab wall geometries with plate reconstructions, and they have been validated against the geologic record.

5.5. Temporal Limitations of our Archipelago Model—Where Is the Slab that Generated the Triassic–Jurassic "Native Arc"?

For Early Jurassic times, our model agrees with the Andean analogue as far as (eastward) subduction under the native arc (and linked Intermontane superterrane) is concerned, subduction that had shut down by ca. 170 Ma. From reconstructions of the Pangean North American margin and from observed systematics of slab sinking, the slab that drove this subduction is expected in the lower third of the mantle under today's central Atlantic (at depths corresponding to the lowest 200 km of the MEZ slab wall and deeper). Beyond the reach of the regional tomography of Sigloch (2011), such ultradeep imaging poses the challenge of adequately modeling seismic wave propagation in proximity to Earth's core, although tomographic imaging methods are advancing rapidly. We predict that this slab will soon be imaged directly, which will further quantify the spatial and temporal separation of eastward subduction under the Intermontane superterrane versus westward subduction under the Insular superterrane. In fact, suitable slab candidates under the central Atlantic Ocean lowermost mantle have started to appear, e.g., in the global model of van der Meer et al. (2010, their supplement) or the compilation of core-diffracted waveform measurements for tomography of Hosseini and Sigloch (2015). Despite the current lack of confident, direct observations of this paleo-seafloor, our argument about the longitudinal separation of the Intermontane superterrane from the Insular superterrane remains solid because reconstructions of the absolute location of Pangea, and thus of the Triassic–Jurassic native arc on its western margin, are already constrained by a range of marine magnetic, land magnetic, and hotspot observations, including the backstripping of Atlantic Ocean opening.

Similarly, the Insular superterrane microcontinent has a volcanic arc history that reaches much further back than the accretion event reconstructed here, but again slabs below 2000 km depth, which will probably account for this history, are only vaguely visible beneath North America and the Pacific in global tomographic images (van der Meer et al., 2010, 2012; Li et al., 2008; Obayashi et al., 2013; Ritsema et al., 2011).

6. CONCLUSIONS

Paleoreconstruction of oceanic regions, such as the seas west of Mesozoic North America, are plagued by the double uncertainty of where the trenches ran and how subducted lithosphere deformed into high-velocity slabs in the mantle. Special slab geometries under North America, showing wall-like linear belts, suggest the null hypothesis that they directly trace out stationary paleotrench locations, and that this lithosphere simply sank vertically beneath the trenches. Combined with a complete Atlantic spreading record that allows confident paleopositioning of the continent, these slab geometries permit detailed predictions of the existence, geometry, and closure of a major ocean ahead of westward-drifting North America, the Mezcalera-Angayucham Oceans.

The most conspicuous prediction for the geologic record is the presence of this ocean's suture, which must run along the entire western margin of North America, and which we have demonstrated here. Geological evidence confirms the Mezcalera-Angayucham suture as truly continental in scale, marked by a trail of at least 11 collapsed, Late Jurassic to Late Cretaceous basins, roughly half of which are known to contain mantle rocks (Fig. 4B). They run between the Insular (Peninsular, Alexander, Wrangellia) and Intermontane (Stikinia, Cache Creek, Quesnellia) microcontinents and were closed later than the Middle Jurassic or older suturing ages invoked by popular versions of the Andean-analogue model for the North American Cordillera. Confirmation of the suture's predicted location and timing in turn supports the hypothesis of vertical slab sinking (although we are not yet able to put tighter bounds on it than Sigloch and Mihalynuk [2013] had obtained from the continental deformation record).

Uncertainty in trench locations has generally been underestimated and gone largely unnoticed by the deep subsurface community. They have stuck to the perceived certitude of a single, margin-hugging Farallon trench since 180+ Ma, and eastward subduction under the tightly bound package of Insular superterrane, Intermontane superterrane, and cratonic North America, even though some geologists had considered alternatives such as archipelago paleogeographies and ribbon continents. Against this disconnect, our finding of a large, "missed" paleo-ocean and its margin-spanning suture is not as unlikely it might sound. Also, while geophysical imaging most readily resolves large-scale features such as giant slab walls, this is not the natural length scale for geological field work. In the absence of a guiding hypothesis, there was little reason to investigate a dozen Jurassic–Cretaceous basins from Mexico to Alaska, most of which had been displaced along the margin by hundreds to thousands of kilometers, as a potentially contiguous feature, although some studies have come close (e.g., McClelland et al., 1992).

Our slab-guided reconstruction of Cordilleran evolution is most similar to geologically derived archipelago models (e.g., Moores, 1970, 1998; Monger et al., 1982). It differs from ribbon continent models (Chamberlain and Lambert, 1985; Johnston, 2008; Hildebrand, 2009) in that we place no pericratonic terranes of acknowledged North American derivation in the archipelago. We stress that the southeast Intermontane superterrane was rooted in the cratonic southwest United States along with coeval Triassic–Early Jurassic "native arcs," and that those native and allied accreted arcs had collapsed by 170 Ma to form the then-new leading edge of North America. This modified margin proceeded to override the Mezcalera/Angayucham arcs—Insular-Guerrero microcontinent and Alaskan arcs—during a drawn-out collision from ca. 155 Ma to ca. 50 Ma. All marine geophysical constraints on Farallon plate evolution are satisfied by this model.

The kind of "tomotectonic" integration demonstrated here, with high-resolution tomography, plate reconstructions, and land-geological evidence, offers a blueprint for clarifying similar paleogeographic ambiguities in other accretionary orogens.

ACKNOWLEDGMENTS

We have benefited from discussions with James Monger, Eldridge Moores, W. Jason Morgan, Rob Coe, Edward Mankinen, Stephen Johnston, Terry Poulton, Charles Ferguson, and John Wakabayashi. We have also benefited from detailed reviews by Gene Humphreys, Associate Editor Clinton Conrad, and two anonymous colleagues. This project has received funding from the European Research Council (ERC) under the European Union's Horizon 2020 research and innovation programme (grant agreement 639003 "DEEP TIME"). K.S. acknowledges additional funding from a Philip Leverhulme Prize awarded by The Leverhulme Trust.

REFERENCES CITED

Amato, J.M., and Pavlis, T.L., 2010, Detrital zircon ages from the Chugach terrane, southern Alaska, reveal multiple episodes of accretion and erosion in a subduction complex: Geology, v. 38, p. 459–462, doi:10.1130/G30719.1.

Amato, J.M., Bogar, M.J., Gehrels, G.E., Farmer, G.L., and McIntosh, W.C., 2007a, The Tlikakila complex in southern Alaska: A suprasubduction-zone ophiolite between the Wrangellia composite terrane and North America, *in* Ridgway, K.D., Trop, J.M., Glen, J.M.G., and O'Neill, J.M., eds., Tectonic Growth of a Collisional Continental Margin: Crustal Evolution of Southern Alaska: Geological Society of America Special Paper 431, p. 227–252, doi:10.1130/2007.2431(10).

Amato, J.M., Rioux, M.E., Kelemen, P.B., Gehrels, G.E., Clift, P.D., Pavlis, T.L., and Draut, A.E., 2007b, U-Pb geochronology of volcanic rocks from the Jurassic Talkeetna Formation and detrital zircons from prearc and postarc sequences: Implications for the age of magmatism and inheritance in the Talkeetna arc, *in* Ridgway, K.D., Trop, J.M., Glen, J.M.G., and O'Neill, J.M., eds., Tectonic Growth of a Collisional Continental Margin: Crustal Evolution of Southern Alaska: Geological Society of America Special Paper 431, p. 253–271, doi:10.1130/2007.2431(11).

Amato, J.M., Pavlis, T.L., Clift, P.D., Kochelek, E.J., Hecker, J.P., Worthman, C.M., and Day, E.M., 2013, Architecture of the Chugach accretionary complex as revealed by detrital zircon ages and lithologic variations: Evidence for Mesozoic subduction erosion in south-central Alaska: Geological Society of America Bulletin, v. 125, p. 1891–1911, doi:10.1130/B30818.1.

Anderson, T.H., and Mahoney, J.B., 2006, Late Jurassic basins; the tracks of a continental-scale transform from the Gulf of Mexico to Alaska, *in* Haggart, J.W., Enkin, R.J., and Monger, J.W.H., eds., Paleogeography of the North American Cordillera; Evidence For and Against Large-Scale Displacements: Geological Association of Canada Special Paper 46, p. 369–375.

Anderson, T.H., Jones, N.W., and McKee, J.W., 2005, The Taray Formation; Jurassic(?) mélange in northern Mexico; tectonic implications, *in* Anderson, T.H., Nourse, J.A., McKee, J.W., and Steiner, M.B., eds., The Mojave-Sonora Megashear Hypothesis: Development, Assessment, and Alternatives: Geological Society of America Special Paper 393, p. 427–455, doi:10.1130/0-8137-2393-0.427.

Armstrong, R.L., 1968, Sevier orogenic belt in Nevada and Utah: Geological Society of America Bulletin, v. 79, p. 429–458, doi:10.1130/0016-7606(1968)79[429:SOBINA]2.0.CO;2.

Ash, C.H., 1994, Origin and Tectonic Setting of Ophiolitic Ultramafic and Related Rocks in the Atlin Area, British Columbia (NTS 104N): British Columbia Ministry of Energy, Mines and Petroleum Resources Bulletin 94, 48 p.

Asmerom, Y., Zartman, R.E., Damon, P.E., and Shafiqullah, M., 1990, Zircon U-Th-Pb and whole-rock Rb-Sr age patterns of Lower Mesozoic igneous rocks in the Santa Rita Mountains, southeast Arizona: Implications for Mesozoic magmatism and tectonics in the southern Cordillera: Geological Society of America Bulletin, v. 102, p. 961–968, doi:10.1130/0016-7606(1990)102<0961:ZUTPAW>2.3.CO;2.

Atwater, T., 1970, Implications of plate tectonics for the Cenozoic tectonic evolution of western North America: Geological Society of America Bulletin, v. 81, p. 3513–3536, doi:10.1130/0016-7606(1970)81[3513:IOPTFT]2.0.CO;2.

Atwater, T., 1989, Plate tectonic history of the Northeast Pacific and western North America, *in* Winterer, E.L., Hussong, D.M., and Decker, R.W., eds., The Eastern Pacific Ocean and Hawaii: Boulder, Colorado, Geological Society of America, The Geology of North America, v. N, p. 21–72.

Barth, A.P., Walker, J.D., Wooden, J.L., Riggs, N.R., and Schweickert, R.A., 2011, Birth of the Sierra Nevada magmatic arc: Early Mesozoic plutonism and volcanism in the east-central Sierra Nevada of California: Geosphere, v. 7, p. 877–897, doi:10.1130/GES00661.1.

Beaumont, C., Quinlan, G.M., and Stockmal, G.S., 1993, The evolution of the Western Interior Basin; causes, consequences and unsolved problems, *in* Caldwell, W.G.E., and Kauffman, E.G., eds., Evolution of the Western Interior Basin: Geological Association of Canada Special Paper 39, p. 97–118, https://dalspace.library.dal.ca/handle/10222/26207 (accessed October 2016).

Bellahsen, N., Faccenna, C., and Funiciello, F., 2005, Dynamics of subduction and plate motion in laboratory experiments: Insights into the "plate tectonics" behavior of the Earth: Journal of Geophysical Research, Solid Earth, v. 110, B01401, doi:10.1029/2004JB002999.

Beranek, L.P., Van Staal, C.R., Gordee, S.M., McClelland, W.C., Israel, S., and Mihalynuk, M., 2012, Tectonic significance of Upper Cambrian–Middle Ordovician mafic volcanic rocks on the Alexander terrane, Saint Elias Mountains, northwestern Canada: The Journal of Geology, v. 120, p. 293–314, doi:10.1086/664788.

Berg, H.C., Jones, D.L., and Richter, D.H., 1972, Gravina-Nutzotin belt—Tectonic significance of an Upper Mesozoic sedimentary and volcanic sequence in southern and southeastern Alaska, *in* Geological Survey Research 1972, Chapter D: U.S. Geological Survey Professional Paper 800-D, p. D1–D24, http://www.dggs.alaska.gov/pubs/id/4057 (accessed March 2016).

Bezada, M.J., Humphreys, E.D., Toomey, D.R., Harnafi, M., Dávila, J.M., and Gallart, J., 2013, Evidence for slab rollback in westernmost Mediterranean from improved upper mantle imaging: Earth and Planetary Science Letters, v. 368, p. 51–60, doi:10.1016/j.epsl.2013.02.024.

Bijwaard, H., Spakman, W., and Engdahl, E.R., 1998, Closing the gap between regional and global travel time tomography: Journal of Geophysical Research, ser. B, Solid Earth, v. 103, p. 30,055–30,078, doi:10.1029/98JB02467.

Bilodeau, W.L., and Keith, S.B., 1986, Lower Jurassic Navajo-Aztec–equivalent sandstones in southern Arizona and their paleogeographic significance: American Association of Petroleum Geologists Bulletin, v. 70, p. 690–701.

Blodgett, R.B., Rohr, D.M., and Boucot, A.J., 2002, Paleozoic links among some Alaskan accreted terranes and Siberia based on megafossils, *in* Miller, E.L., Grantz,

A., and Klemperer, S., eds., Tectonic Evolution of the Bering Shelf–Chukchi Sea–Arctic Margin and Adjacent Areas: Geological Society of America Special Paper 360, p. 273–290, doi:10.1130/0-8137-2360-4.273.

Box, S.E., and Patton, W.W., 1989, Igneous history of the Koyukuk terrane, western Alaska; constraints on the origin, evolution, and ultimate collision of an accreted island arc terrane: Journal of Geophysical Research, v. 94, p. 15,843–15,867, doi:10.1029/JB094iB11p15843.

Bradley, D.C., McClelland, W.C., Wooden, J.L., Till, A.B., Roeske, S.M., Miller, M.L., Karl, S.M., and Abbott, J.G., 2007, Detrital zircon geochronology of some Neoproterozoic to Triassic rocks in interior Alaska, *in* Dumoulin, J.A., and Till, A.B., eds., Late Proterozoic to Devonian Continental Sequence, Alaska: Geological Society of America Special Paper 431, p. 155–189, doi:10.1130/2007.2431(07).

Brandon, M.T., 1989, Deformational styles in a sequence of olistostromal mélanges, Pacific Rim complex, western Vancouver Island, Canada (with Suppl. Data 89–16): Geological Society of America Bulletin, v. 101, p. 1520–1542, doi:10.1130/0016-7606(1989)101<1520:DSIASO>2.3.CO;2.

Brew, D.A., and Karl, S.M., 1988, A reexamination of the contacts and other features of the Gravina belt, southeastern Alaska, *in* Galloway, J.P., and Hamilton, T.D., eds., Geologic Studies in Alaska by the U.S. Geological Survey during 1987: U.S. Geological Survey Circular 1016, p. 143–146.

Brown, B.J., Müller, R.D., Gaina, C., Struckmeyer, H.I.M., Stagg, H.M.J., and Symonds, P.A., 2003, Formation and evolution of Australian passive margins: Implications for locating the boundary between continental and oceanic crust, *in* Hillis, R.R., and Müller, R.D., eds., Evolution and Dynamics of the Australian Plate: Geological Society of America Special Paper 372, p. 223–243, doi:10.1130/0-8137-2372-8.223.

Brown, E.H., 2012, Obducted nappe sequence in the San Juan Islands–northwest Cascades thrust system, Washington and British Columbia: Canadian Journal of Earth Sciences, v. 49, p. 796–817, doi:10.1139/e2012-026.

Brown, E.H., Lapen, T.J., Leckie, R.M., Silva, I.P., Verga, D., and Singer, B.S., 2005, Revised ages of blueschist metamorphism and the youngest pre-thrusting rocks in the San Juan Islands, Washington: Canadian Journal of Earth Sciences, v. 42, p. 1389–1400, doi:10.1139/e05-033.

Bunge, H.-P., and Grand, S.P., 2000, Mesozoic plate-motion history below the northeast Pacific Ocean from seismic images of the subducted Farallon slab: Nature, v. 405, p. 337–340, doi:10.1038/35012586.

Burchfiel, B.C., and Davis, G.A., 1972, Structural framework and evolution of the southern part of the Cordilleran orogen, western United States: American Journal of Science, v. 272, p. 97–118, doi:10.2475/ajs.272.2.97.

Burchfiel, B.C., and Davis, G.A., 1975, Nature and controls of Cordilleran orogenesis, western United States—Extensions of an earlier synthesis: American Journal of Science, v. A275, p. 363–396.

Burchfiel, B.C., Cowan, D.S., and Davis, G.A., 1992, Tectonic overview of the Cordilleran orogen in the western United States, *in* Burchfiel, B.C., Lipman, P.W., and Zoback, M.L., eds., The Cordilleran Orogen: Conterminous U.S.: Boulder, Colorado, Geological Society of America, The Geology of North America, v. G-3, p. 407–479.

Burdick, S., Li, C., Martynov, V., Cox, T., Eakins, J., Mulder, T., Astiz, L., Vernon, F.L., Pavlis, G.L., and van der Hilst, R.D., 2008, Upper mantle heterogeneity beneath North America from travel time tomography with global and USArray transportable array data: Seismological Research Letters, v. 79, p. 384–392, doi:10.1785/gssrl.79.3.384.

Burdick, S., Van der Hilst, R.D., Vernon, F.L., Martynov, V., Cox, T., Eakins, J., Karasu, G.H., Tylell, J., Astiz, L., and Pavlis, G.L., 2014, Model update January 2013: Upper mantle heterogeneity beneath North America from travel-time tomography with global and USArray transportable array data: Seismological Research Letters, v. 85, p. 77–81, doi:10.1785/0220130098.

Butler, R.F., Gehrels, G.E., Hart, W., Davidson, C., and Crawford, M.L., 2006, Paleomagnetism of Late Jurassic to mid-Cretaceous plutons near Prince Rupert, British Columbia, *in* Haggart, J., Enkin, R.J., and Monger, J.W.H., eds., Paleogeography of the North American Cordillera: Evidence For and Against Large-Scale Displacements: Geological Association of Canada Special Paper 46, p. 171–200.

Butterworth, N.P., Talsma, A.S., Müller, R.D., Seton, M., Bunge, H.P., Schuberth, B.S.A., Shephard, G.E., and Heine, C., 2014, Geological, tomographic, kinematic and geodynamic constraints on the dynamics of sinking slabs: Journal of Geodynamics, v. 73, p. 1–13, doi:10.1016/j.jog.2013.10.006.

Cecil, M.R., Rotberg, G.L., Ducea, M.N., Saleeby, J.B., and Gehrels, G.E., 2012, Magmatic growth and batholithic root development in the northern Sierra Nevada, California: Geosphere, v. 8, p. 592–606, doi:10.1130/GES00729.1.

Centeno-Garcia, E., Busby, C., Busby, M., and Gehrels, G., 2011, Evolution of the Guerrero composite terrane along the Mexican margin, from extensional fringing arc to contractional continental arc: Geological Society of America Bulletin, v. 123, p. 1776–1797, doi:10.1130/B30057.1.

Chamberlain, V.E., and Lambert, R.S.J., 1985, Cordilleria, a newly defined Canadian microcontinent: Nature, v. 314, p. 707–713, doi:10.1038/314707a0.

Christiansen, E.H., Kowallis, B.J., and Barton, M.D., 1994, Temporal and spatial distribution of volcanic ash in Mesozoic sedimentary rocks of the Western Interior: An alternative record of Mesozoic magmatism, *in* Caputo, M.V., Peterson, J.A., and Franczyk, K.J., eds., Mesozoic Systems of the Rocky Mountain Region, United States: Denver, Colorado, Rocky Mountain Section, Society for Sedimentary Geology (SEPM), p. 73–94.

Čížková, H., and Bina, C.R., 2013, Effects of mantle and subduction-interface rheologies on slab stagnation and trench rollback: Earth and Planetary Science Letters, v. 379, p. 95–103, doi:10.1016/j.epsl.2013.08.011.

Clift, P.D., Wares, N.M., Amato, J.M., Pavlis, T.L., Hole, M.J., Worthman, C., and Day, E., 2012, Evolving heavy mineral assemblages reveal changing exhumation and trench tectonics in the Mesozoic Chugach accretionary complex, south-central Alaska: Geological Society of America Bulletin, v. 124, p. 989–1006, doi:10.1130/B30594.1.

Cloos, M., Sapiie, B., van Ufford, A.Q., Weiland, R.J., Warren, P.Q., and McMahon, T.P., 2005, Collisional delamination in New Guinea: The geotectonics of subducting slab breakoff: Geological Society of America Special Paper 400, 51 p.

Clowes, R.M., Brandon, M.T., Green, A.G., Yorath, C.J., Brown, A.S., Kanasewich, E.R., and Spencer, C., 1987, LITHOPROBE—southern Vancouver Island: Cenozoic subduction complex imaged by deep seismic reflections: Canadian Journal of Earth Sciences, v. 24, p. 31–51, doi:10.1139/e87-004.

Coe, R.S., Globerman, B.R., and Thrupp, G.A., 1989, Rotation of central and southern Alaska in the Early Tertiary: Oroclinal bending by megakinking?, *in* Kissel, C., and Laj, C., eds., Paleomagnetic Rotations and Continental Deformation: Springer, p. 327–342, http://link.springer.com/chapter/10.1007/978-94-009-0869-7_20 (accessed April 2015), doi:10.1007/978-94-009-0869-7_20.

Cohen, K.M., Finney, S.C., Gibbard, P.L., and Fan, J.X., 2013, The ICS International Chronostratigraphic Chart: Episodes, v. 36, p. 199–204.

Colpron, M., Warren, M.J., and Price, R.A., 1998, Selkirk fan structure, southeastern Canadian Cordillera; tectonic wedging against an inherited basement ramp: Geological Society of America Bulletin, v. 110, p. 1060–1074, doi:10.1130/0016-7606(1998)110<1060:SFSSCC>2.3.CO;2.

Coney, P.J., Jones, D.L., and Monger, J.W.H., 1980, Cordilleran suspect terranes: Nature, v. 288, p. 329–333, doi:10.1038/288329a0.

Cordey, F., and Schiarizza, P., 1993, Long-lived Panthalassic remnant; the Bridge River accretionary complex, Canadian Cordillera: Geology, v. 21, p. 263–266, doi:10.1130/0091-7613(1993)021<0263:LLPRTB>2.3.CO;2.

Cordey, F., Mortimer, N., DeWever, P., and Monger, J.W.H., 1987, Significance of Jurassic radiolarians from the Cache Creek terrane, British Columbia: Geology, v. 15, p. 1151–1154, doi:10.1130/0091-7613(1987)15<1151:SOJRFT>2.0.CO;2.

Cowan, D.S., 2003, Revisiting the Baranof–Leech River hypothesis for Early Tertiary coastwise transport of the Chugach–Prince William terrane: Earth and Planetary Science Letters, v. 213, p. 463–475, doi:10.1016/S0012-821X(03)00300-5.

Crawford, M.L., Hollister, L.S., and Woodsworth, G.J., 1987, Crustal deformation and regional metamorphism across a terrane boundary, Coast plutonic complex, British Columbia: Tectonics, v. 6, p. 343–361, doi:10.1029/TC006i003p00343.

Crawford, M.L., Klepeis, K.A., Gehrels, G.E., and Lindline, J., 2009, Mid-Cretaceous–Recent crustal evolution in the central Coast orogen, British Columbia and southeastern Alaska, *in* Miller, R.B., and Snoke, A.W., eds., Crustal Cross Sections from the Western North American Cordillera and Elsewhere: Implications for Tectonic and Petrologic Processes: Geological Society of America Special Paper 456, p. 97–124, doi:10.1130/2009.2456(04).

Csejtey, B., Cox, D.P., Evarts, R.C., Stricker, G.D., and Foster, H.L., 1982, The Cenozoic Denali fault system and the Cretaceous accretionary development of southern Alaska: Journal of Geophysical Research, ser. B, v. 87, Special Issue on Accretion Tectonics, p. 3741–3754, doi:10.1029/JB087iB05p03741.

Cutts, J.A., McNicoll, V.J., Zagorevski, A., Anderson, R.G., and Martin, K., 2015, U-Pb geochronology of the Hazelton Group in the McTagg anticlinorium, Iskut River area, northwestern British Columbia, *in* Geological Fieldwork 2014: British Columbia Geological Survey Paper 2015-1, p. 87–101, http://www.em.gov.bc.ca/Mining/Geoscience/PublicationsCatalogue/Fieldwork/Documents/2014/05_Cutts_etal.pdf.

Dahlen, F.A., Hung, S.-H., and Nolet, G., 2000, Fréchet kernels for finite-frequency traveltimes—I: Theory: Geophysical Journal International, v. 141, p. 157–174, doi:10.1046/j.1365-246X.2000.00070.x.

Davidson, C., and McPhillips, D., 2007, Along strike variations in metamorphism and deformation of the strata of the Kahiltna basin, south-central Alaska, *in* Ridgway, K.D., Trop, J.M., Glen, J.M.G., and O'Neill, J.M., eds., Tectonic Growth of a Collisional Continental Margin: Crustal Evolution of Southern Alaska: Geological Society of America Special Paper 431, p. 439–453, doi:10.1130/2007.2431(17).

Day, E.M., Pavlis, T.L., and Amato, J.M., 2011, Diverging histories of the Liberty Creek and Iceberg Lake blueschist bodies, south central Alaska: San Francisco, California, American Geophysical Union, Fall Meeting abstracts, v. 1, p. 2426.

DeCelles, P.G., 2004, Late Jurassic to Eocene evolution of the Cordilleran thrust belt and foreland basin system, western U.S.A.: American Journal of Science, v. 304, p. 105–168, doi:10.2475/ajs.304.2.105.

DeCelles, P.G., and Coogan, J.C., 2006, Regional structure and kinematic history of the Sevier fold-and-thrust belt, central Utah: Geological Society of America Bulletin, v. 118, p. 841–864, doi:10.1130/B25759.1.

Dewey, J.F., 1988, Extensional collapse of orogens: Tectonics, v. 7, p. 1123–1139, doi:10.1029/TC007i006p01123.

Dickinson, W.R., 1976, Sedimentary basins developed during evolution of Mesozoic–Cenozoic arc-trench system in western North America: Canadian Journal of Earth Sciences, v. 13, p. 1268–1287, doi:10.1139/e76-129.

Dickinson, W.R., 1979, Mesozoic forearc basin in central Oregon: Geology, v. 7, p. 166–170, doi:10.1130/0091-7613(1979)7<166:MFBICO>2.0.CO;2.

Dickinson, W.R., 1981, Plate tectonic evolution of the southern Cordillera: Relations of tectonics to ore deposits in the southern Cordillera: Arizona Geological Society Digest, v. 14, p. 113–135.

Dickinson, W.R., 2004, Evolution of the North American Cordillera: Annual Review of Earth and Planetary Sciences, v. 32, p. 13–45, doi:10.1146/annurev.earth.32.101802.120257.

Dickinson, W.R., 2006, Geotectonic evolution of the Great Basin: Geosphere, v. 2, p. 353–368, doi:10.1130/GES00054.1.

Dickinson, W.R., 2008, Accretionary Mesozoic–Cenozoic expansion of the Cordilleran continental margin in California and adjacent Oregon: Geosphere, v. 4, p. 329–353, doi:10.1130/GES00105.1.

Dickinson, W.R., 2013, Phanerozoic palinspastic reconstructions of Great Basin geotectonics (Nevada-Utah, USA): Geosphere, v. 9, p. 1384–1396, doi:10.1130/GES00888.1.

Dickinson, W.R., and Gehrels, G.E., 2009, U-Pb ages of detrital zircons in Jurassic eolian and associated sandstones of the Colorado Plateau: Evidence for transcontinental dispersal and intraregional recycling of sediment: Geological Society of America Bulletin, v. 121, p. 408–433, doi:10.1130/B26406.1.

Dickinson, W.R., and Gehrels, G.E., 2010, Insights into North American paleogeography and paleotectonics from U-Pb ages of detrital zircons in Mesozoic strata of the Colorado Plateau, USA: International Journal of Earth Sciences, v. 99, p. 1247–1265, doi:10.1007/s00531-009-0462-0.

Dickinson, W.R., and Lawton, T.F., 2001, Carboniferous to Cretaceous assembly and fragmentation of Mexico: Geological Society of America Bulletin, v. 113, p. 1142–1160, doi:10.1130/0016-7606(2001)113<1142:CTCAAF>2.0.CO;2.

Dickinson, W.R., Gehrels, G.E., and Stern, R.J., 2010, Late Triassic Texas uplift preceding Jurassic opening of the Gulf of Mexico: Evidence from U-Pb ages of detrital zircons: Geosphere, v. 6, p. 641–662, doi:10.1130/GES00532.1.

du Bray, E.A., John, D.A., and Cousens, B.L., 2014, Petrologic, tectonic, and metallogenic evolution of the southern segment of the ancestral Cascades magmatic arc, California and Nevada: Geosphere, v. 10, p. 1–39, doi:10.1130/GES00944.1.

Ducea, M., 2001, The California arc: Thick granitic batholiths, eclogitic residues, lithospheric-scale thrusting, and magmatic flare-ups: GSA Today, v. 11, p. 4–10, doi:10.1130/1052-5173(2001)011<0004:TCATGB>2.0.CO;2.

Dumitru, T.A., Wakabayashi, J., Wright, J.E., and Wooden, J.L., 2010, Early Cretaceous transition from nonaccretionary behavior to strongly accretionary behavior within the Franciscan subduction complex: Tectonics, v. 29, TC5001, doi:10.1029/2009TC002542.

Duncan, R.A., and Richards, M.A., 1991, Hotspots, mantle plumes, flood basalts, and true polar wander: Reviews of Geophysics, v. 29, p. 31–50, doi:10.1029/90RG02372.

Dusel-Bacon, C., Lanphere, M.A., Sharp, W.D., Layer, P.W., and Hansen, V.L., 2002, Mesozoic thermal history and timing of structural events for the Yukon-Tanana Upland, east-central Alaska: $^{40}Ar/^{39}Ar$ data from metamorphic and plutonic rocks: Canadian Journal of Earth Sciences, v. 39, p. 1013–1051, doi:10.1139/e02-018.

Edgar, N.T., 2003, A modern analogue for tectonic, eustatic, and climatic processes in cratonic basins: Gulf of Carpenteria, northern Australia, *in* Cecil, C.B., and Edgar, N.T., eds., Climate Controls on Stratigraphy: Society for Sedimentary Geology (SEPM) Special Publication 77, http://archives.datapages.com/data/sepm_sp/SP77/A_Modern_Analogue_for_Tectonic_Eustatic_and_Climatic_Processes.pdf (accessed October 2016).

Engebretson, D.C., Cox, A., and Gordon, R.G., 1985, Relative Motions Between Oceanic and Continental Plates in the Pacific Basin: Geological Society of America. Special Paper 206, 60 p., doi:10.1130/SPE206-p1.

Enkin, R.J., 2006, Paleomagnetism and the case for Baja–British Columbia: Paleogeography of the North American Cordillera, *in* Haggart, J., Enkin, R.J., and Monger, J.W.H., eds., Paleogeography of the North American Cordillera: Evidence For and Against Large-Scale Displacements: Geological Association of Canada Special Paper 46, p. 233–253.

Ernst, W.G., 1970, Tectonic contact between the Franciscan mélange and the Great Valley sequence; crustal expression of a late Mesozoic Benioff zone: Journal of Geophysical Research, v. 75, p. 886–901, doi:10.1029/JB075i005p00886.

Ernst, W.G., 2011, Accretion of the Franciscan complex attending Jurassic–Cretaceous geotectonic development of northern and central California: Geological Society of America Bulletin, v. 123, p. 1667–1678, doi:10.1130/B30398.1.

Ernst, W.G., Saleeby, J.B., and Snow, C.A., 2009, Guadalupe Pluton–Mariposa Formation age relationships in the southern Sierran Foothills; onset of Mesozoic subduction in Northern California?: Journal of Geophysical Research, v. 114, B11204, doi:10.1029/2009JB006607.

Evenchick, C.A., and McNicoll, V.J., 2002, Stratigraphy, structure, and geochronology of the Anyox Pendant, northwest British Columbia, and implications for mineral exploration: Canadian Journal of Earth Sciences, v. 39, p. 1313–1332, doi:10.1139/e02-036.

Evenchick, C.A., McMechan, M.E., McNicoll, V.J., and Carr, S.D., 2007, A synthesis of the Jurassic–Cretaceous tectonic evolution of the central and southeastern Canadian Cordillera: Exploring links across the orogen, *in* Sears, J.W., Harms, T.A., and Evenchick, C.A., eds., Whence the Mountains? Inquiries into the Evolution of Orogenic Systems: A Volume in Honor of Raymond A. Price: Geological Society of America Special Paper 433, p. 117–145, doi:10.1130/2007.2433(06).

Evenchick, C.A., Poulton, T.P., and McNicoll, V.J., 2010, Nature and significance of the diachronous contact between the Hazelton and Bowser Lake Groups (Jurassic), north-central British Columbia: Bulletin of Canadian Petroleum Geology, v. 58, p. 235–267, doi:10.2113/gscpgbull.58.3.235.

Friedman, R.M., and Armstrong, R.L., 1995, Jurassic and Cretaceous geochronology of the Southern Coast belt, British Columbia, 49° to 51°N, *in* Miller, D.M., and Busby, C., eds., Jurassic Magmatism and Tectonics of the North American Cordillera: Geological Society of America Special Paper 299, p. 95–140, doi:10.1130/SPE299-p95.

Fukao, Y., Obayashi, M., and Nakakuki, T., 2009, Stagnant slab: A review: Annual Review of Earth and Planetary Sciences, v. 37, p. 19–46, doi:10.1146/annurev.earth.36.031207.124224.

Funiciello, F., Faccenna, C., Giardini, D., and Regenauer-Lieb, K., 2003, Dynamics of retreating slabs: 2. Insights from three-dimensional laboratory experiments: Journal of Geophysical Research–Solid Earth, v. 108, no. B4, 2207, doi:10.1029/2001JB000896.

Gardner, M.C., Bergman, S.C., Cushing, G.W., MacKevett, E.M., Plafker, G., Campbell, R.B., Dodds, C.J., McClelland, W.C., and Mueller, P.A., 1988, Pennsylvanian pluton stitching of Wrangellia and the Alexander terrane, Wrangell Mountains, Alaska: Geology, v. 16, p. 967–971, doi:10.1130/0091-7613(1988)016<0967:PPSOWA>2.3.CO;2.

Garel, F., Goes, S., Davies, D.R., Davies, J.H., Kramer, S.C., and Wilson, C.R., 2014, Interaction of subducted slabs with the mantle transition-zone: A regime diagram from 2-D thermo-mechanical models with a mobile trench and an overriding plate: Geochemistry Geophysics Geosystems, v. 15, p. 1739–1765, doi:10.1002/2014GC005257.

Garver, J.I., 1992, Provenance of Albian–Cenomanian rocks of the Methow and Tyaughton Basins, southern British Columbia; a mid-Cretaceous link between North America and the Insular terrane: Canadian Journal of Earth Sciences, v. 29, p. 1274–1295, doi:10.1139/e92-102.

Gaschnig, R.M., Vervoort, J.D., Lewis, R.S., and Tikoff, B., 2011, Isotopic evolution of the Idaho batholith and Challis intrusive province, northern US Cordillera: Journal of Petrology, v. 52, p. 2397–2429, doi:10.1093/petrology/egr050.

Gehrels, G.E., 2001, Geology of the Chatham Sound region, southeast Alaska and coastal British Columbia: Canadian Journal of Earth Sciences, v. 38, p. 1579–1599, doi:10.1139/e01-040.

Gehrels, G.E., Butler, R.F., and Bazard, D.R., 1996, Detrital zircon geochronology of the Alexander terrane, southeastern Alaska: Geological Society of America Bulletin, v. 108, p. 722–734, doi:10.1130/0016-7606(1996)108<0722:DZGOTA>2.3.CO;2.

Gehrels, G., Rusmore, M., Woodsworth, G., Crawford, M., Andronicos, C., Hollister, L., Patchett, J., Ducea, M., Butler, R., Klepeis, K., Davidson, C., Friedman, R., Haggart, J., Mahoney, B., et al., 2009, U-Th-Pb geochronology of the Coast Mountains batholith in north-coastal British Columbia: Constraints on age and tectonic evolution: Geological Society of America Bulletin, v. 121, p. 1341–1361, doi:10.1130/B26404.1.

Gibert, G., Gerbault, M., Hassani, R., and Tric, E., 2012, Dependency of slab geometry on absolute velocities and conditions for cyclicity: Insights from numerical modelling: Geophysical Journal International, v. 189, p. 747–760, doi:10.1111/j.1365-246X.2012.05426.x.

Goldhammer, R.K., and Johnson, C.A., 1999, Mesozoic sequence stratigraphy and paleogeographic evolution of northeast Mexico, *in* Bartolini, C., Wilson, J.L., and Lawton, T.F., eds., Mesozoic Sedimentary and Tectonic History of North-Central Mexico: Geological Society of America Special Paper 340, p. 1–58, doi:10.1130/0-8137-2340-X.1.

Grand, S.P., 1994, Mantle shear structure beneath the Americas and surrounding oceans: Journal of Geophysical Research, v. 99, p. 11,591–11,621, doi:10.1029/94JB00042.

Grand, S.P., van der Hilst, R.D., and Widiyantoro, S., 1997, Global seismic tomography; a snapshot of convection in the Earth: GSA Today, v. 7, no. 4, p. 1–7.

Greene, A.R., Scoates, J.S., Weis, D., Katvala, E.C., Israel, S., and Nixon, G.T., 2010, The architecture of oceanic plateaus revealed by the volcanic stratigraphy of the accreted Wrangellia oceanic plateau: Geosphere, v. 6, p. 47–73, doi:10.1130/GES00212.1.

Groome, W.G., Thorkelson, D.J., Friedman, R.M., Mortensen, J.K., Massey, N.W., Marshall, D.D., and Layer, P.W., 2003, Magmatic and tectonic history of the Leech River complex, Vancouver Island, British Columbia: Evidence for ridge-trench intersection and accretion of the Crescent terrane, *in* Sisson, V.B., Roeske, S.M., and Pavlis, T.L., eds., Geology of a Transpressional Orogen Developed During Ridge-Trench Interaction along the North Pacific Margin: Geological Society of America Special Paper 371, p. 327–353, doi:10.1130/0-8137-2371-X.327.

Grove, M., Lovera. O., and Harrison. M., 2003, Late Cretaceous cooling of the east-central Peninsular Ranges batholith (33°N): Relationship to La Posta pluton emplacement, Laramide shallow subduction, and forearc sedimentation, *in* Johnson, S.E., Paterson, S.R., Fletcher, J.M.. Girty, G.H., Kimbrough, D.L., and Martin-Barajas, A., eds., Tectonic Evolution of Northwestern Mexico and the Southwestern USA: Boulder, Colorado, Geological Society of America Special Paper 374, p. 355–379 doi:10.1130/0-8137-2374-4.355.

Guillou-Frottier, L., Buttles, J., and Olson, P., 1995, Laboratory experiments on the structure of subducted lithosphere: Earth and Planetary Science Letters, v. 133, p. 19–34, doi:10.1016/0012-821X(95)00045-E.

Haggart, J.W., Mahoney, J.B., Forgette, M., Carter, E.S., Schröder-Adams, C.J., MacLaurin, C.I., and Sweet, A.R., 2011, Paleoenvironmental and chronological constraints on the Mount Tatlow succession, British Columbia: First recognition of radiolarian and foraminiferal faunas in the Intermontane Cretaceous back-arc basins of western Canada: Canadian Journal of Earth Sciences, v. 48, p. 952–972, doi:10.1139/e11-019.

Hamilton, W.B., 1969, Mesozoic California and the underflow of Pacific mantle: Geological Society of America Bulletin, v. 80, p. 2409–2430, doi:10.1130/0016-7606(1969)80[2409:MCATUO]2.0.CO;2.

Hamilton, W.B., 1979, Tectonics of the Indonesian Region: U.S. Geological Survey Professional Paper 1078, 345 p., https://pubs.er.usgs.gov/publication/pp1078 (accessed October 2016).

Hampton, B.A., Ridgway, K.D., and Gehrels, G.E., 2007, U-Pb detrital zircon age data from Upper Triassic strata of the Chulitna terrane, south-central Alaska: A preliminary link with the western margin of North America: Geological Society of America Abstracts with Programs, v. 39, no. 4, p. 69 https://gsa.confex.com/gsa/2007CD/finalprogram/abstract_121407.htm.

Hampton, B.A., Ridgway, K.D., and Gehrels, G.E., 2010, A detrital record of Mesozoic island arc accretion and

exhumation in the North American Cordillera: U-Pb geochronology of the Kahiltna basin, southern Alaska: Tectonics, v. 29, TC4015, doi:10.1029/2009TC002544.

Harper, G.D., Saleeby, J.B., and Heizler, M., 1994, Formation and emplacement of the Josephine ophiolite and the Nevadan orogeny in the Klamath Mountains, California-Oregon: U/Pb zircon and $^{40}Ar/^{39}Ar$ geochronology: Journal of Geophysical Research–Solid Earth, v. 99, p. 4293–4321, doi:10.1029/93JB02061.

Hildebrand, R.S., 2009, Did Westward Subduction Cause Cretaceous–Tertiary Orogeny in the North American Cordillera?: Geological Society of America Special Paper 457, 71 p., doi:10.1130/2009.2457.

Hildebrand, R.S., 2012, Mesozoic Assembly of the North American Cordillera: Geological Society of America Special Paper 495, 182 p., doi:10.1130/9780813724959.

Hildebrand, R.S., 2015, Dismemberment and northward migration of the Cordilleran orogen: Baja-BC resolved: GSA Today, v. 25, no. 11, p. 4–11, http://rock.geosociety.org/gsatoday/archive/25/11/article/i1052-5173-25-11-4.htm.

Hillhouse, J.W., and Coe, R.S., 1994, Paleomagnetic data from Alaska, *in* Plafker, G., and Berg, H.C., eds., The Geology of Alaska: Boulder, Colorado, Geological Society of America, the Geology of North America, v. G-1, p. 797–812.

Himmelberg, G.R., Haeussler, P.J., and Brew, D.A., 2004, Emplacement, rapid burial, and exhumation of 90-Ma plutons in southeastern Alaska: Canadian Journal of Earth Sciences, v. 41, p. 87–102, doi:10.1139/e03-087.

Hollister, L.S., and Crawford, M.L., 1986, Melt-enhanced deformation: A major tectonic process: Geology, v. 14, p. 558–561, doi:10.1130/0091-7613(1986)14<558:MDAMTP>2.0.CO;2.

Hosseini, K., and Sigloch, K., 2015, Multifrequency measurements of core-diffracted P waves (Pdiff) for global waveform tomography: Geophysical Journal International, v. 203, p. 506–521, doi:10.1093/gji/ggv298.

Houseman, G.A., and Molnar, P., 1997, Gravitational (Rayleigh–Taylor) instability of a layer with non-linear viscosity and convective thinning of continental lithosphere: Geophysical Journal International, v. 128, p. 125–150, doi:10.1111/j.1365-246X.1997.tb04075.x.

Humphreys, E.D., Schmandt, B., Bezada, M.J., and Perry-Houts, J., 2015, Recent craton growth by slab stacking beneath Wyoming: Earth and Planetary Science Letters, v. 429, p. 170–180, doi:10.1016/j.epsl.2015.07.066.

Ingersoll, R.V., 2008, Subduction-related sedimentary basins of the USA Cordillera, *in* Miall, A.D., ed., Sedimentary Basins of the World, Volume 5: Amsterdam, Netherlands, Elsevier, p. 395–428, doi:10.1016/S1874-5997(08)00011-7.

Ingersoll, R.V., 2012, Composition of modern sand and Cretaceous sandstone derived from the Sierra Nevada, California, USA, with implications for Cenozoic and Mesozoic uplift and dissection: Sedimentary Geology, v. 280, p. 195–207, doi:10.1016/j.sedgeo.2012.03.022.

Ingersoll, R.V., and Schweickert, R.A., 1986, A plate-tectonic model for Late Jurassic ophiolite genesis, Nevadan orogeny and forearc initiation, northern California: Tectonics, v. 5, p. 901–912, doi:10.1029/TC005i006p00901.

Ingersoll, R.V., Dickinson, W.R., and Graham, S.A., 2003, Remnant-ocean submarine fans: Largest sedimentary systems on Earth, *in* Chan, M.A., and Archer, A.W., eds., Extreme Depositional Environments: Mega End Members in Geologic Time: Geological Society of America Special Paper 370, p. 191–208, doi:10.1130/0-8137-2370-1.191.

Israel, S., Murphy, D., Bennett, V., Mortensen, J., and Crowley, J., 2010, New insights into the geology and mineral potential of the Coast belt in southwestern Yukon, *in* MacFarlane, K.E., Weston, L.H., and Relf, C., eds., Yukon Exploration and Geology: Yukon Geological Survey, p. 101–123.

Jakob, J., and Johnston, S., 2015, New insights into the North American Cordillera forearc: Cretaceous to Eocene tectonic evolution of the Leech River Schist, southern Vancouver Island, Canada: European Geosciences Union General Assembly Conference Abstracts, v. 17, p. 10042, http://adsabs.harvard.edu/abs/2015EGUGA.1710042J (accessed April 2017).

Johnston, S.T., 2001, The Great Alaskan terrane wreck: Reconciliation of paleomagnetic and geological data in the northern Cordillera: Earth and Planetary Science Letters, v. 193, p. 259–272, doi:10.1016/S0012-821X(01)00516-7.

Johnston, S.T., 2008, The Cordilleran ribbon continent of North America: Annual Review of Earth and Planetary Sciences, v. 36, p. 495–530, doi:10.1146/annurev.earth.36.031207.124331.

Jones, D.L., Silberling, N.J., Gilbert, W., and Coney, P., 1982, Character, distribution, and tectonic significance of accretionary terranes in the central Alaska Range: Journal of Geophysical Research–Solid Earth, v. 87, p. 3709–3717, doi:10.1029/JB087iB05p03709.

Journeay, J.M., and Friedman, R.M., 1993, The Coast belt thrust system; evidence of Late Cretaceous shortening in southwest British Columbia: Tectonics, v. 12, p. 756–775, doi:10.1029/92TC02773.

Journeay, J.M., and Mahoney, J.B., 1994, Cayoosh assemblage: Regional correlations and implications for terrane linkages in the southern Coast belt, British Columbia: Geological Survey of Canada Current Research 1994-A, p. 165–175.

Journeay, J.M., and Northcote, B.R., 1992, Tectonic assemblages of the eastern Coast belt, southwest British Columbia: Geological Survey of Canada Current Research Paper 92-1A, p. 215–224.

Kalbas, J.L., Ridgway, K.D., and Gehrels, G.E., 2007, Stratigraphy, depositional systems, and provenance of the Lower Cretaceous Kahiltna assemblage, western Alaska Range: Basin development in response to oblique collision, *in* Ridgway, K.D., Trop, J.M., Glen, J.M.G., and O'Neill, J.M., eds., Tectonic Growth of a Collisional Continental Margin: Crustal Evolution of Southern Alaska: Geological Society of America Special Paper 431, p. 307–343, doi:10.1130/2007.2431(13).

Kennett, B.L.N., and Engdahl, E.R., 1991, Traveltimes for global earthquake location and phase identification: Geophysical Journal International, v. 105, p. 429–465, doi:10.1111/j.1365-246X.1991.tb06724.x.

Kent, D.V., and Irving, E., 2010, Influence of inclination error in sedimentary rocks on the Triassic and Jurassic apparent pole wander path for North America and implications for Cordilleran tectonics: Journal of Geophysical Research, ser. B, Solid Earth, v. 115, B10103, doi:10.1029/2009JB007205.

Kistler, R.W., and Peterman, Z.E., 1978, Reconstruction of Crustal Blocks of California on the Basis of Initial Strontium Isotopic Compositions of Mesozoic Granite Rocks: U.S. Geological Survey Professional Paper 1071, 17 p.

Kleinspehn, K.L., 1985, Cretaceous sedimentation and tectonics, Tyaughton-Methow Basin, southwestern British Columbia: Canadian Journal of Earth Sciences, v. 22, p. 154–174, doi:10.1139/e85-014.

Knight, E., Schneider, D.A., and Ryan, J., 2013, Thermochronology of the Yukon-Tanana terrane, west-central Yukon: Evidence for Jurassic extension and exhumation in the northern Canadian Cordillera: The Journal of Geology, v. 121, p. 371–400, doi:10.1086/670721.

Lambert, R.S.J., and Chamberlain, V.E., 1988, Cordilleria revisited, with a three-dimensional model for Cretaceous tectonics in British Columbia: The Journal of Geology, v. 96, p. 47–60, doi:10.1086/629192.

Laskowski, A.K., DeCelles, P.G., and Gehrels, G.E., 2013, Detrital zircon geochronology of Cordilleran retroarc foreland basin strata, western North America: Tectonics, v. 32, p. 1027–1048, doi:10.1002/tect.20065.

Lawton, T.F., and Garza, R.S.M., 2014, U-Pb geochronology of the type Nazas Formation and superjacent strata, northeastern Durango, Mexico: Implications of a Jurassic age for continental-arc magmatism in north-central Mexico: Geological Society of America Bulletin, v. 126, p. 1181–1199, doi:10.1130/B30827.1.

Li, C., van der Hilst, R.D., Engdahl, E.R., and Burdick, S., 2008, A new global model for P wave speed variations in Earth's mantle: Geochemistry Geophysics Geosystems, v. 9, Q05018, doi:10.1029/2007GC001806.

Li, S., Chung, S.-L., Wilde, S.A., Wang, T., Xiao, W.-J., and Guo, Q.-Q., 2016, Linking magmatism with collision in an accretionary orogen: Scientific Reports, v. 6, p. 1–12 http://www.ncbi.nlm.nih.gov/pmc/articles/PMC4863176/ (accessed November 2016).

Lithgow-Bertelloni, C., and Richards, M.A., 1998, The dynamics of Cenozoic and Mesozoic plate motions: Reviews of Geophysics, v. 36, p. 27–78, doi:10.1029/97RG02282.

Liu, L., 2014, Constraining Cretaceous subduction polarity in eastern Pacific from seismic tomography and geodynamic modeling: Geophysical Research Letters, v. 89, p. 221–229.

Liu, L., Spasojević, S., and Gurnis, M., 2008, Reconstructing Farallon plate subduction beneath North America back to the Late Cretaceous: Science, v. 322, p. 934–938, doi:10.1126/science.1162921.

Liu, L., Gurnis, M., Seton, M., Saleeby, J., Müller, R.D., and Jackson, J.M., 2010, The role of oceanic plateau subduction in the Laramide orogeny: Nature Geoscience, v. 3, p. 353–357, doi:10.1038/ngeo829.

Livaccari, R.F., Burke, K., and Şengör, A.M.C., 1981, Was the Laramide orogeny related to subduction of an oceanic plateau?: Nature, v. 289, p. 276–278, doi:10.1038/289276a0.

Logan, J.M., Drobe, J.R., and McClelland, W.C., 2000, Geology of the Forest Kerr–Mess Creek Area, Northwestern British Columbia: British Columbia Ministry of Energy and Mines Bulletin 104, 164 p.

López-Carmona, A., Kusky, T.M., Santosh, M., and Abati, J., 2011, *P-T* and structural constraints of lawsonite and epidote blueschists from Liberty Creek and Seldovia: Tectonic implications for early stages of subduction along the southern Alaska convergent margin: Lithos, v. 121, p. 100–116, doi:10.1016/j.lithos.2010.10.007.

MacIntyre, D.G., Villeneuve, M.E., and Schiarizza, P., 2001, Timing and tectonic setting of Stikine terrane magmatism, Babine-Takla Lakes area, central British Columbia: Canadian Journal of Earth Sciences, v. 38, p. 579–601, doi:10.1139/e00-105.

Mahoney, J.B., and Journeay, J.M., 1993, The Cayoosh assemblage, southwestern British Columbia: Last vestige of the Bridge River Ocean, *in* Current Research, Part A, Cordillera and Pacific Margin: Geological Survey of Canada Paper 93-1A, p. 235–244, doi:10.4095/134210.

Manuszak, J.D., Ridgway, K.D., Trop, J.M., and Gehrels, G.E., 2007, Sedimentary record of the tectonic growth of a collisional continental margin: Upper Jurassic–Lower Cretaceous Nutzotin Mountains sequence, eastern Alaska Range, Alaska, *in* Ridgway, K.D., Trop, J.M., Glen, J.M.G., and O'Neill, J.M., eds., Tectonic Growth of a Collisional Continental Margin: Crustal Evolution of Southern Alaska: Geological Society of America Special Paper 431, p. 345–377, doi:10.1130/2007.2431(14).

Massey, N.W.D., 1986, Metchosin Igneous Complex, southern Vancouver Island: Ophiolite stratigraphy developed in an emergent island setting: Geology, v. 14, p. 602–605, doi: 10.1130/0091-7613(1986)14<602:MICSVI>2.0.CO;2.

McClelland, W.C., Gehrels, G.E., and Saleeby, J.B., 1992, Upper Jurassic–Lower Cretaceous basinal strata along the Cordilleran margin: Implications for the accretionary history of the Alexander-Wrangellia-Peninsular terrane: Tectonics, v. 11, p. 823–835, doi:10.1029/92TC00241.

McCrory, P.A., and Wilson, D.S., 2013, A kinematic model for the formation of the Siletz-Crescent forearc terrane by capture of coherent fragments of the Farallon and Resurrection plates: Tectonics, v. 32, p. 718–736, doi:10.1002/tect.20045.

Mihalynuk, M.G., and Friedman, R.M., 2006, U-Pb isotopic ages of intrusive-related mineralization north of Terrace, BC, *in* Geological Fieldwork 2005: British Columbia Ministry of Energy, Mines and Petroleum Resources Paper 2006-1, p. 109–116.

Mihalynuk, M.G., Smith, M.T., Hancock, K.D., and Dudka, S., 1994, Regional and economic geology of the Tulsequah River and glacier areas (104K/12 & 13), *in* Geological Fieldwork 1993: British Columbia, Ministry of Energy, Mines and Petroleum Resources Paper 1994-1, p. 171–197.

Mihalynuk, M.G., Johnston, S.T., English, J.M., Cordey, F., Villeneuve, M.J., Rui, L., and Orchard, M.J., 2003, Atlin TGI Part II: Regional geology and mineralization of the Nakina area (NTS 104N/2W and 3), *in* Geological Fieldwork 2002: British Columbia Ministry of Energy and Mines Paper 2003-1, p. 9–37.

Mihalynuk, M.G., Erdmer, P., Ghent, E.D., Cordey, F., Archibald, D.A., Friedman, R.M., and Johannson, G.G., 2004, Coherent French Range blueschist: Subduction to exhumation in <2.5 m.y.?: Geological Society of America Bulletin, v. 116, p. 910–922, doi:10.1130/B25393.1.

Molnar, P., and Houseman, G.A., 2013, Rayleigh-Taylor instability, lithospheric dynamics, surface topography at convergent mountain belts, and gravity anomalies: Journal of Geophysical Research–Solid Earth, v. 118, p. 2544–2557, doi:10.1002/jgrb.50203.

Monger, J.W.H., 2014, Seeking the suture: The Coast-Cascade conundrum: Geoscience Canada, v. 41, p. 379–398, doi:10.12789/geocanj.2014.41.058.

Monger, J.W.H., and Price, R.A., 1979, Geodynamic evolution of the Canadian Cordillera; progress and problems: Canadian Journal of Earth Sciences, v. 16, p. 770–791, doi:10.1139/e79-069.

Monger, J.W.H., and Ross, C.A., 1971, Distribution of fusulinaceans in the western Canadian Cordillera: Canadian Journal of Earth Sciences, v. 8, p. 259–278, doi:10.1139/e71-026.

Monger, J.W.H., Souther, J.G., and Gabrielse, H., 1972, Evolution of the Canadian Cordillera; a plate-tectonic model: American Journal of Science, v. 272, p. 577–602, doi:10.2475/ajs.272.7.577.

Monger, J.W.H., Price, R.A., and Tempelman-Kluit, D.J., 1982, Tectonic accretion and the origin of the two major metamorphic and plutonic welts in the Canadian Cordillera: Geology, v. 10, p. 70–75, doi:10.1130/0091-7613(1982)10<70:TAATOO>2.0.CO;2.

Monger, J.W.H., Price, R.A., and Tempelman-Kluit, D.J., 1983, Comment and Reply on "Tectonic accretion and the origin of the two major metamorphic and plutonic welts in the Canadian Cordillera": Reply: Geology, v. 11, p. 428–429, doi:10.1130/0091-7613(1983)11<428:CAROTA>2.0.CO;2.

Monger, J.W.H., Van der Heyden, P., Journeay, J.M., Evenchick, C.A., and Mahoney, J.B., 1994, Jurassic–Cretaceous basins along the Canadian Coast belt: Their bearing on pre–mid-Cretaceous sinistral displacements: Geology, v. 22, p. 175–178, doi:10.1130/0091-7613(1994)022<0175:JCBATC>2.3.CO;2.

Montelli, R., Nolet, G., Dahlen, F.A., and Masters, G., 2006, A catalogue of deep mantle plumes: New results from finite-frequency tomography: Geochemistry Geophysics Geosystems, v. 7, Q11007, doi:10.1029/2006GC001248.

Moores, E.M., 1970, Ultramafics and orogeny, with models of the US Cordillera and the Tethys: Nature, v. 228, p. 837–842, doi:10.1038/228837a0.

Moores, E.M., 1998, Ophiolites, the Sierra Nevada, "Cordilleria," and orogeny along the Pacific and Caribbean margins of North and South America: International Geology Review, v. 40, p. 40–54, doi:10.1080/00206819809465197.

Morgan, W.J., 1981, Hotspot tracks and the opening of the Atlantic and Indian Oceans, *in* Emiliani, C., ed., The Oceanic Lithosphere: New York, John Wiley and Sons, v. 7, p. 443–487.

Mortensen, J.K., and Jilson, G.A., 1985, Evolution of the Yukon-Tanana terrane: Evidence from southeastern Yukon Territory: Geology, v. 13, p. 806–810, doi:10.1130/0091-7613(1985)13<806:EOTYTE>2.0.CO;2.

Müller, R.D., Sdrolias, M., Gaina, C., and Roest, W.R., 2008, Age, spreading rates, and spreading asymmetry of the world's ocean crust: Geochemistry Geophysics Geosystems, v. 9, Q04006, doi:10.1029/2007GC001743.

Murphy, D.C., van der Heyden, P., Parrish, R.R., Klepacki, D.W., McMillan, W., Struik, L.C., and Gabites, J., 1995, New geochronological constraints on Jurassic deformation of the western edge of North America, southeastern Canadian Cordillera, *in* Miller, D.M., and Busby, C., eds., Jurassic Magmatism and Tectonics of the North American Cordillera: Geological Society of America Special Paper 299, p. 159–171, doi:10.1130/SPE299-p159.

Newberry, R.J., Layer, P.W., Burleigh, R.E., and Solie, D.N., 1998, New $^{40}Ar/^{39}Ar$ dates for intrusions and mineral prospects in the eastern Yukon-Tanana terrane, Alaska; regional patterns and significance, *in* Gray, J.E., and Riehle, J.R., eds., Geologic Studies in Alaska by the U.S. Geological Survey, 1996: U.S. Geological Survey Professional Paper 1595, p. 131–159.

Nixon, G.T., and Orr, A.J., 2007, Recent revisions to the early Mesozoic stratigraphy of Vancouver Island and metallogenic implications, *in* Geological Fieldwork 2006: British Columbia Ministry of Energy Mines and Petroleum Resources Paper 2007-1, p. 163–177.

Nixon, G.T., Archibald, D.A., and Heaman, L.M., 1993, ^{40}Ar-^{39}Ar and U-Pb geochronometry of the Polaris Alaskan-type complex, British Columbia; precise timing of Quesnellia–North America interaction, *in* Geological Association of Canada–Mineralogical Association of Canada–Canadian Geophysical Union Joint Annual Meeting, Waterloo, Ontario, Canada: Geological Association of Canada Program with Abstracts, v. 1993, p. 76.

Nolet, G., and Dahlen, F.A., 2000, Wave front healing and the evolution of seismic delay times: Journal of Geophysical Research–Solid Earth, v. 105, p. 19,043–19,054, doi:10.1029/2000JB900161.

Obayashi, M., Yoshimitsu, J., Nolet, G., Fukao, Y., Shiobara, H., Sugioka, H., Miyamachi, H., and Gao, Y., 2013, Finite frequency whole mantle P wave tomography: Improvement of subducted slab images: Geophysical Research Letters, v. 40, p. 5652–5657, doi:10.1002/2013GL057401.

O'Neill, C., Mueller, D., and Steinberger, B., 2005, On the uncertainties in hot spot reconstructions and the significance of moving hot spot reference frames: Geochemistry Geophysics Geosystems, v. 6, Q04003, doi:10.1029/2004GC000784.

Orchard, M., Struik, L.C., Rui, L., Bamber, E.W., Mamet, B.L., Sano, H., and Taylor, H., 2001, Palaeontological and biogeographical constraints on the Carboniferous to Jurassic Cache Creek terrane in central British Columbia: Canadian Journal of Earth Sciences, v. 38, p. 551–578, doi:10.1139/e00-120.

Pană, D.I., and van der Pluijm, B.A., 2015, Orogenic pulses in the Alberta Rocky Mountains: Radiometric dating of major faults and comparison with the regional tectonostratigraphic record: Geological Society of America Bulletin, v. 127, p. 480–502, doi:10.1130/B31069.1.

Paterson, I.A., and Harakal, J.E., 1974, Potassium-argon dating of blueschists from Pinchi Lake, central British Columbia: Canadian Journal of Earth, v. 11, p. 1007–1011, doi:10.1139/e74-097.

Pavlis, G.L., Sigloch, K., Burdick, S., Fouch, M.J., and Vernon, F.L., 2012, Unraveling the geometry of the Farallon plate: Synthesis of three-dimensional imaging results from USArray: Tectonophysics, v. 532–535, p. 82–102, doi:10.1016/j.tecto.2012.02.008.

Phillips, W.M., Walsh, T.J., and Hagen, R.A., 1989, Eocene Transition from Oceanic to Arc Volcanism, Southwest Washington: U.S. Geological Survey Open-File Report 89-178, p. 89–178.

Poulton, T.P., Hall, R.L., and Callomon, J.H., 1994, Ammonite and bivalve assemblages in Bathonian through Oxfordian strata of northern Bowser Basin, northwestern British Columbia, Canada: Geobios, v. 27, p. 415–421, doi:10.1016/S0016-6995(94)80162-2.

Ray, G.E., 1986, The Hozameen fault system and related Coquihalla serpentine belt of southwestern British Columbia: Canadian Journal of Earth Sciences, v. 23, p. 1022–1041, doi:10.1139/e86-103.

Ren, Y., Stutzmann, E., van der Hilst, R.D., and Besse, J., 2007, Understanding seismic heterogeneities in the lower mantle beneath the Americas from seismic tomography and plate tectonic history: Journal of Geophysical Research–Solid Earth, v. 112, B01302, doi:10.1029/2005JB004154.

Ribe, N.M., 2010, Bending mechanics and mode selection in free subduction: A thin-sheet analysis: Geophysical Journal International, v. 180, p. 559–576, doi:10.1111/j.1365-246X.2009.04460.x.

Ribe, N.M., Stutzmann, E., Ren, Y., and van der Hilst, R., 2007, Buckling instabilities of subducted lithosphere beneath the transition zone: Earth and Planetary Science Letters, v. 254, p. 173–179, doi:10.1016/j.epsl.2006.11.028.

Riddell, J.M., 1991, Geology of the Mesozoic volcanic and sedimentary rocks east of Pemberton, British Columbia, *in* Current Research, Part A, p. 245–254.

Ridgway, K.D., Trop, J.M., Nokleberg, W.J., Davidson, C.M., and Eastham, K.R., 2002, Mesozoic and Cenozoic tectonics of the eastern and central Alaska Range: Progressive basin development and deformation in a suture zone: Geological Society of America Bulletin, v. 114, p. 1480–1504, doi:10.1130/0016-7606(2002)114<1480:MACTOT>2.0.CO;2.

Riggs, N.R., Reynolds, S.J., Lindner, P.J., Howell, E.R., Barth, A.P., Parker, W.G., and Walker, J.D., 2013, The early Mesozoic Cordilleran arc and Late Triassic paleotopography: The detrital record in Upper Triassic sedimentary successions on and off the Colorado Plateau: Geosphere, v. 9, p. 602–613, doi:10.1130/GES00860.1.

Rioux, M., Hacker, B., Mattinson, J., Kelemen, P., Blusztajn, J., and Gehrels, G., 2007, Magmatic development of an intra-oceanic arc: High-precision U-Pb zircon and whole-rock isotopic analyses from the accreted Talkeetna arc, south-central Alaska: Geological Society of America Bulletin, v. 119, p. 1168–1184, doi:10.1130/B25964.1.

Ritsema, J., Deuss, A., Van Heijst, H.J., and Woodhouse, J.H., 2011, S40RTS: A degree-40 shear-velocity model for the mantle from new Rayleigh wave dispersion, teleseismic traveltime and normal-mode splitting function measurements: Geophysical Journal International, v. 184, p. 1223–1236, doi:10.1111/j.1365-246X.2010.04884.x.

Roeske, S.M., Mattinson, J.M., and Armstrong, R.L., 1989, Isotopic ages of glaucophane schists on the Kodiak Islands, southern Alaska, and their implications for the Mesozoic tectonic history of the Border Ranges fault system: Geological Society of America Bulletin, v. 101, p. 1021–1037, doi:10.1130/0016-7606(1989)101<1021:IAOGSO>2.3.CO;2.

Rubin, C.M., Saleeby, J.B., Cowan, D.S., Brandon, M.T., and McGroder, M.F., 1990, Regionally extensive mid-Cretaceous west-vergent thrust system in the northwestern Cordillera; implications for continent-margin tectonism: Geology, v. 18, p. 276–280, doi:10.1130/0091-7613(1990)018<0276:REMCWV>2.3.CO;2.

Sager, W.W., Handschumacher, D.W., Hilde, T.W.C., and Bracey, D.R., 1988, Tectonic evolution of the northern Pacific plate and Pacific-Farallon-Izanagi triple junction in the Late Jurassic and Early Cretaceous (M21–M10): Tectonophysics, v. 155, p. 345–364, doi:10.1016/0040-1951(88)90274-0.

Saleeby, J.B., 1981, Ocean floor accretion and volcanoplutonic arc evolution of the Mesozoic Sierra Nevada, *in* Ernst, W.G., ed., The Geotectonic Development of California: Rubey Volume 1: Englewood Cliffs, New Jersey, Prentice-Hall, Inc., p. 132–181.

Saleeby, J.B., 1983, Accretionary tectonics of the North American Cordillera: Annual Review of Earth and Planetary Sciences, v. 11, p. 45–73, doi:10.1146/annurev.ea.11.050183.000401.

Saleeby, J.B., and Dunne, G., 2015, Temporal and tectonic relations of early Mesozoic arc magmatism, southern Sierra Nevada, California, *in* Anderson, T.H., Didenko, A.N., Johnson, C.L., Khanchuk, A.I., and MacDonald, J.H., Jr., eds., Late Jurassic Margin of Laurasia—A Record of Faulting Accommodating Plate Rotation: Geological Society of America Special Paper 513, p. 223–268, doi:10.1130/2015.2513(05).

Saleeby, J.B., Geary, E.E., Paterson, S.R., and Tobisch, O.T., 1989, Isotopic systematics of Pb/U (zircon) and $^{40}Ar/^{39}Ar$ (biotite-hornblende) from rocks of the central Foothills terrane, Sierra Nevada, California: Geological Society of America Bulletin, v. 101, p. 1481–1492, doi:10.1130/0016-7606(1989)101<1481:ISOPUZ>2.3.CO;2.

Schaeffer, A.J., and Lebedev, S., 2015, Global heterogeneity of the lithosphere and underlying mantle: A seismological appraisal based on multimode surface-wave

dispersion analysis, shear-velocity tomography, and tectonic regionalization, *in* Khan, A., and Deschamps, F., eds., The Earth's Heterogeneous Mantle: Switzerland, Springer International Publishing, p. 3–46, doi: 10.1007/978-3-319-15627-9_1.

Schellart, W.P., 2008, Kinematics and flow patterns in deep mantle and upper mantle subduction models: Influence of the mantle depth and slab to mantle viscosity ratio: Geochemistry, Geophysics, Geosystems, v. 9, Q03014, doi:10.1029/2007GC001656.

Schmandt, B., and Humphreys, E., 2010, Complex subduction and small-scale convection revealed by body-wave tomography of the western United States upper mantle: Earth and Planetary Science Letters, v. 297, p. 435–445, doi:10.1016/j.epsl.2010.06.047.

Schmandt, B., and Humphreys, E., 2011, Seismically imaged relict slab from the 55 Ma Siletzia accretion to the northwest United States: Geology, v. 39, p. 175–178, doi:10.1130/G31558.1.

Schweickert, R.A., 2015, Jurassic evolution of the western Sierra Nevada metamorphic province, *in* Anderson, T.H., Didenko, A.N., Johnson, C.L., Khanchuk, A.I., and MacDonald, J.H., Jr., eds., Late Jurassic Margin of Laurasia—A Record of Faulting Accommodating Plate Rotation: Geological Society of America Special Paper 513, p. 299–358, doi:10.1130/2015.2513(08).

Schweickert, R.A., and Cowan, D.S., 1975, Early Mesozoic tectonic evolution of the western Sierra Nevada, California: Geological Society of America Bulletin, v. 86, p. 1329–1336, doi:10.1130/0016-7606(1975)86<1329:EMTEOT>2.0.CO;2.

Schweickert, R.A., Bogen, N.L., Girty, G.H., Hanson, R.E. and Merguerian, C., 1984, Timing and structural expression of the Nevadan orogeny, Sierra Nevada, California: Geological Society of America Bulletin, v. 95, p. 967–979, doi:10.1130/0016-7606(1984)95<967:TASEOT>2.0.CO;2.

Seton, M., Müller, R.D., Zahirovic, S., Gaina, C., Torsvik, T., Shephard, G., Talsma, A., Gurnis, M., Turner, M., Maus, S., and Chandler, M., 2012, Global continental and ocean basin reconstructions since 200 Ma: Earth-Science Reviews, v. 113, p. 212–270, doi:10.1016/j.earscirev.2012.03.002.

Shephard, G.E., Mueller, R.D., and Seton, M., 2013, The tectonic evolution of the Arctic since Pangea breakup: Integrating constraints from surface geology and geophysics with mantle structure: Earth-Science Reviews, v. 124, p. 148–183, doi:10.1016/j.earscirev.2013.05.012.

Sigloch, K., 2008, Multiple-Frequency Body-Wave Tomography [Ph.D. thesis]: Princeton, New Jersey, Princeton University, 249 p.

Sigloch, K., 2011, Mantle provinces under North America from multifrequency P-wave tomography: Geochemistry Geophysics Geosystems, v. 12, Q02W08, doi:10.1029/2010GC003421.

Sigloch, K., and Mihalynuk, M.G., 2013, Intra-oceanic subduction shaped the assembly of Cordilleran North America: Nature, v. 496, p. 50–56, doi:10.1038/nature12019.

Sigloch, K., McQuarrie, N., and Nolet, G., 2008, Two-stage subduction history under North America inferred from multiple-frequency tomography: Nature Geoscience, v. 1, p. 458–462, doi:10.1038/ngeo231.

Silberling, N.J., Jones, D.L., Monger, J.W.H., and Coney, P.J., 1992, Lithotectonic Terrane Map of the North American Cordillera: U.S. Geological Survey IMAP 2176, 2 sheets.

Silver, L.T., and Chappell, B.W., 1988, The Peninsular Ranges Batholith: an insight into the evolution of the Cordilleran batholiths of southwestern North America: Earth and Environmental Science Transactions of the Royal Society of Edinburgh, v. 79, p. 105–121.

Silver, E.A., and Smith, R.B., 1983, Comparison of terrane accretion in modern Southeast Asia and the Mesozoic North American Cordillera: Geology, v. 11, p. 198–202, doi:10.1130/0091-7613(1983)11<198:COTAIM>2.0.CO;2.

Sisson, V., and Onstott, T., 1986, Dating blueschist metamorphism—A combined Ar-40/Ar-39 and electron-microprobe approach: Geochimica et Cosmochimica Acta, v. 50, p. 2111–2117, doi:10.1016/0016-7037(86)90264-4.

Smith, P.L., 2006, Paleobiogeography and Early Jurassic molluscs in the context of terrane displacement in western Canada: Paleogeography of the North American Cordillera, *in* Haggart, J., Enkin, R.J., and Monger, J.W.H., eds., Paleogeography of the North American Cordillera: Evidence For and Against Large-Scale Displacements: Geological Association of Canada Special Paper 46, p. 81–94.

Snow, C.A., and Scherer, H., 2006, Terranes of the western Sierra Nevada Foothills metamorphic belt, California: A critical review: International Geology Review, v. 48, p. 46–62, doi:10.2747/0020-6814.48.1.46.

Snow, C.A., Wakabayashi, J., Ernst, W.G., and Wooden, J.L., 2010, Detrital zircon evidence for progressive underthrusting in Franciscan metagraywackes, west-central California: Geological Society of America Bulletin, v. 122, p. 282–291, doi:10.1130/B26399.1.

Staples, R.D., Gibson, H.D., Berman, R.G., Ryan, J.J., and Colpron, M., 2013, A window into the Early to mid-Cretaceous infrastructure of the Yukon-Tanana terrane recorded in multi-stage garnet of west-central Yukon, Canada: Journal of Metamorphic Geology, v. 31, p. 729–753, doi:10.1111/jmg.12042.

Stegman, D.R., Farrington, R., Capitanio, F.A., and Schellart, W.P., 2010, A regime diagram for subduction styles from 3-D numerical models of free subduction: Tectonophysics, v. 483, p. 29–45, doi:10.1016/j.tecto.2009.08.041.

Steinberger, B., and Torsvik, T.H., 2008, Absolute plate motions and true polar wander in the absence of hotspot tracks: Nature, v. 452, p. 620–623, doi:10.1038/nature06824.

Steinberger, B., Torsvik, T.H., and Becker, T.W., 2012, Subduction to the lower mantle—A comparison between geodynamic and tomographic models: Solid Earth, v. 3, p. 415–432, doi:10.5194/se-3-415-2012.

Stewart, J.H., Anderson, T.H., Haxel, G.B., Silver, L.T., and Wright, J.E., 1986, Late Triassic paleogeography of the southern Cordillera: The problem of a source for voluminous volcanic detritus in the Chinle Formation of the Colorado Plateau region: Geology, v. 14, p. 567–570, doi:10.1130/0091-7613(1986)14<567:LTPOTS>2.0.CO;2.

Surpless, K.D., Sickmann, Z.T., and Koplitz, T.A., 2014, East-derived strata in the Methow Basin record rapid mid-Cretaceous uplift of the southern Coast Mountains batholith: Canadian Journal of Earth Sciences, v. 51, p. 339–357, doi:10.1139/cjes-2013-0144.

Tobisch, O.T., Paterson, S.R., Saleeby, J.B., and Geary, E.E., 1989, Nature and timing of deformation in the Foothills terrane, central Sierra Nevada, California: Its bearing on orogenesis: Geological Society of America Bulletin, v. 101, p. 401–413, doi:10.1130/0016-7606(1989)101<0401:NATODI>2.3.CO;2.

Umhoefer, P.J., Schiarizza, P., and Robinson, M., 2002, Relay Mountain Group, Tyaughton–Methow Basin, southwest British Columbia: A major Middle Jurassic to Early Cretaceous terrane overlap assemblage: Canadian Journal of Earth Sciences, v. 39, p. 1143–1167, doi:10.1139/e02-031.

van de Zedde, D.M.A., and Wortel, M.J.R., 2001, Shallow slab detachment as a transient source of heat at mid-lithospheric depths: Tectonics, v. 20, p. 868–882, doi:10.1029/2001TC900018.

van der Heyden, P.A.H., 1989, U-Pb and K-Ar Geochronometry of the Coast Plutonic Complex, 53°N to 54°N, British Columbia, and Implications for the Insular-Intermontane Superterrane Boundary [Ph.D. thesis]: Vancouver, Canada, University of British Columbia, 515 p.

van der Heyden, P.A.H., 1992, A Middle Jurassic to Early Tertiary Andean-Sierran arc model for the Coast belt of British Columbia: Tectonics, v. 11, p. 82–97, doi:10.1029/91TC02183.

van der Hilst, R.D., Widiyantoro, S., and Engdahl, E.R., 1997, Evidence for deep mantle circulation from global tomography: Nature, v. 386, p. 578–584, doi:10.1038/386578a0.

van der Lee, S., and Nolet, G., 1997, Seismic image of the subducted trailing fragments of the Farallon plate: Nature, v. 386, p. 266–269, doi:10.1038/386266a0.

van der Meer, D.G., Spakman, W., van Hinsbergen, D.J.J., Amaru, M.L., and Torsvik, T.H., 2010, Towards absolute plate motions constrained by lower-mantle slab remnants: Nature Geoscience, v. 3, p. 36–40, doi:10.1038/ngeo708.

van der Meer, D.G., Torsvik, T.H., Spakman, W., van Hinsbergen, D.J.J., and Amaru, M.L., 2012, Intra-Panthalassa Ocean subduction zones revealed by fossil arcs and mantle structure: Nature Geoscience, v. 5, p. 215–219, doi:10.1038/ngeo1401.

Van der Voo, R., Spakman, W., and Bijwaard, H., 1999a, Mesozoic subducted slabs under Siberia: Nature, v. 397, p. 246–249, doi:10.1038/16686.

Van der Voo, R., Spakman, W., and Bijwaard, H., 1999b, Tethyan subducted slabs under India: Earth and Planetary Science Letters, v. 171, p. 7–20, doi:10.1016/S0012-821X(99)00131-4.

Villeneuve, M., Whalen, J.B., Anderson, R.G., and Struik, L.C., 2001, The Endako batholith: Episodic plutonism culminating in formation of the Endako porphyry molybdenite deposit, north-central British Columbia: Economic Geology and the Bulletin of the Society of Economic Geologists, v. 96, p. 171–196.

Whalen, J.B., Anderson, R.G., Struik, L.C., and Villeneuve, M.E., 2001, Geochemistry and Nd isotopes of the François Lake plutonic suite, Endako batholith: Host and progenitor to the Endako molybdenum camp, central British Columbia: Canadian Journal of Earth Sciences, v. 38, p. 603–618, doi:10.1139/e00-080.

Wheeler, J.O., and McFeely, P., 1991, Tectonic Assemblage Map of the Canadian Cordillera and Adjacent Parts of the United States of America: Geological Survey of Canada Map 1712A, scale 1: 2,000,000.

Woods, M.T., and Davies, G.F., 1982, Late Cretaceous genesis of the Kula plate: Earth and Planetary Science Letters, v. 58, p. 161–166, doi:10.1016/0012-821X(82)90191-1.

Wu, J., Suppe, J., Lu, R., and Kanda, R., 2016, Philippine Sea and East Asian plate tectonics since 52 Ma constrained by new subducted slab reconstruction methods: Journal of Geophysical Research–Solid Earth, v. 121, no. 6, p. 4670–4741, doi:10.1002/2016JB012923.

Science Editor: Bradley S. Singer
Associate Editor: Clinton P. Conrad

Manuscript Received 9 March 2016
Revised Manuscript Received 4 March 2017
Manuscript Accepted 20 April 2017

Printed in the USA